# Investigating the cellular and molecular mechanisms involved in establishing and maintaining centrosome asymmetry in *Drosophila* neuroblasts

**Inauguraldissertation**
zur Erlangung der Würde eines Doktors der Philosophie
vorgelegt der
Philosophisch-Naturwissenschaftlichen Fakultät
der Universität Basel
von

**Anjana Ramdas Nair**
Kerala , India
Basel 2016

Genehmigt von der Philosophisch-
Naturwissenschaftlichen Fakultät auf Antrag von

Clemens Cabernard & Markus Affolter

Basel, 15.09.15
(Date of approval by the Faculty)

_____

Prof. Dr. C. Cabernard

_____

Dean Prof. Dr. J. Schibler

# TABLE OF CONTENTS

**Page No.**

# *Acknowledgements*

First and foremost, I would like to thank Clemens Cabernard for giving me the opportunity to work as a PhD student in his lab. I would like to thank you for the last four years of mentoring, countless critical discussions, advices and most importantly, for seeing potential in me and my work.

I would also like to thank my thesis advisory committee members, Dr. Markus Affolter and Dr. Peter Scheiffele for their valuble advice. Thanks to Erich Nigg for his input during the combined lab meetings and also agreeing to be the Committee Chair at my defence.

Similarly, I would like to thank Marianne Liechti, Jny Wittker, Andrea Thoma and Gabi Lichtenhahn for support with administrative and helping a foreigner adjust well to Switzerland.

In the same manner, I am thankful to all my labmates, old and new, for the stimulating discussions and the wonderful work environment. Thank you Emmanuel Gallaud, Tri Thanh Pham, Anna Tsankova, Niklas Iffländer, David S J Garcia, Arnaud Monnard and Marko Jukic for being so very kind and supportive through these years. I would also like to thank members of the Nigg and Reichert group for their valuable input with regard to techniques and project discussions. It has been a joy knowing and working alongside you all.

PhD is a difficult ordeal to go through if you don't have friends who are part of your support system. I would like to thank Ilaria Alborelli and Oguz Kanca for being my closest friends and helping me get through these four years. Our times together were definitely the best part of these four years. Chantal Roubinet and Michaela Roth thank you for being there for me at my good and difficult times. You both truly made

working in the lab easy.

Also, I would like to thank the imaging core facility of the Biozentrum, providing good and helpful services in imaging and image analysis. Thank you Oliver Biehlmaier, Alexia Ferrand and Niko Ehrenfeuchter.

Finally, I would like to thank my family and in laws in supporting my career choice and being patient and understanding. My parents and brother who never forgot to remind me about how proud they were and kept motivating me against odds. But most importantly, I have the deepest gratitude for my husband, Jaideep Thattamparambil who moved to Switzerland to support me through my PhD. I couldn't have managed all of this without you and this is as much your success as it is mine. Words aren't enough to describe how lucky I am to have you in my life. Thanks for everything.

# 1. SUMMARY

Centrosome asymmetry has been implicated in stem cell fate maintenance in both flies and vertebrates. *Drosophila* neuroblasts, the neural precursors of the fly's central nervous system, contain molecularly and physically asymmetric centrosomes. For instance, the apical daughter centrosome maintains a stable microtubule organizing center (MTOC) activity and remains tethered to the apical cortex throughout the cell cycle. The basal mother centrosome, however, loses MTOC activity and only regains it during prophase. This centrosome asymmetry is important for centrosome positioning, spindle orientation and centrosome segregation during asymmetric cell division.

In a gene candidate approach, we identified Bld10, fly ortholog of Cep135 and the uncharacterized gene *CG7337,* the fly ortholog of WDR62, as a regulator of centrosome asymmetry during interphase. In *bld10* mutant neuroblasts the mother centrosome does not downregulate MTOC activity resulting in two mature active centrosomes. As a consequence of perturbed centrosome asymmetry, we observed spindle misalignment during metaphase and centrosome missegregation. In contrast, we were able to show that in *CG7337/wdr62* mutant neuroblasts both centrosomes lose MTOC activity, resulting in interphase neuroblasts containing two untethered centrioles. Moreover, cold treatment of *wdr62* mutant neuroblasts displayed microtubule instability while over expression of Wdr62 had hyper stabilized microtubules. We also observed decrease in Polo levels on the apical centrosome in mutant neuroblasts. Wdr62 localizes to the microtubules during the cell cycle. Taken together, we concluded that Wdr62 plays an important role in stabilizing microtubules, which are necessary for recruitment of Polo, and hence, maintains centrosome asymmetry. In addition, *wdr62* mutants display cell cycle delay and decrease in brain size.

To gain further insight into the neuroblast centrosome cycle and centrosome asymmetry establishment, we used 3D-SIM (Structured Illumination Microscopy). We observed that centriole duplication begins soon after centriole separation and molecular markers involved in establishing centrosome asymmetry have a very precise segregation pattern based on the age of the centrioles. Using 3D-SIM, we are able to define the time points of the occurrence of these events.

# 2. INTRODUCTION

The centrosome is the microtubule-organizing center (MTOC) in a majority of eukaryotic cells with the exception of female meiotic systems and the majority of higher plants. Work from the eminent biologists Edouard van Benenden (1883) and Theodor Boveri (1887) in the 1880s have paved the way in discovering and understanding the role of centrosomes in mitosis in healthy and tumor cells. However, even after a century we have not completely understood how this organelle is structured and functions. Centrosomes have been implicated in cancer and genetic disorders such as ciliopathies, microcephaly and dwarfism (Bettencourt-Dias et al., 2011; Nigg, 2006; Nigg and Raff, 2009; Thornton and Woods, 2009). Due to its impact on human health and disease, there is a general interest in understanding the role and function of centrosomes in cell division. With the discovery and improvement of imaging techniques, such as electron microscopy and super resolution imaging, along with possibilities to genetically manipulate the genome using RNA interference and CRISPR/Cas9, there is the potential for great contributions in the field of centrosome research.

## 2.1 Structure of the centrosome

The introduction and use of electron microscopy in the 1950s to study biological structures revealed that a mammalian centrosome was composed of two cylindrical structures, known as centrioles (Figure 1A&B). The centriole is a conserved eukaryotic organelle made primarily of stabilized microtubules, approximately 200nm in diameter and 500nm in length (Azimzadeh and Marshall, 2010). The centriole's inner core is arranged in a pinwheel like structure called the cartwheel. The cartwheel consists of the central hub from which nine pinheads arise, displaying a nine-fold radial symmetry (Gönczy, 2012; Guichard et al., 2012; van Breugel et al., 2014). At

end of each pinhead, microtubule blades are arranged as triplets, which form the outer centriole wall. These microtubule blades undergo modifications such as polyglutamylation that stabilizes the microtubules against depolymerisation. The end at which the daughter centriole starts to form is known as the proximal end and the opposite end is defined as distal. The cartwheel serves as template for the newly forming centriole known as the procentriole (also called nascent centriole). The procentriole assembly is at an orthogonal position at the proximal end of the mother centriole. Interconnecting fibers link the older mother centriole and newly formed daughter centriole. A mature centriole in addition possesses distal and subdistal appendages, necessary for microtubule attachment (Paintrand et al., 1992).

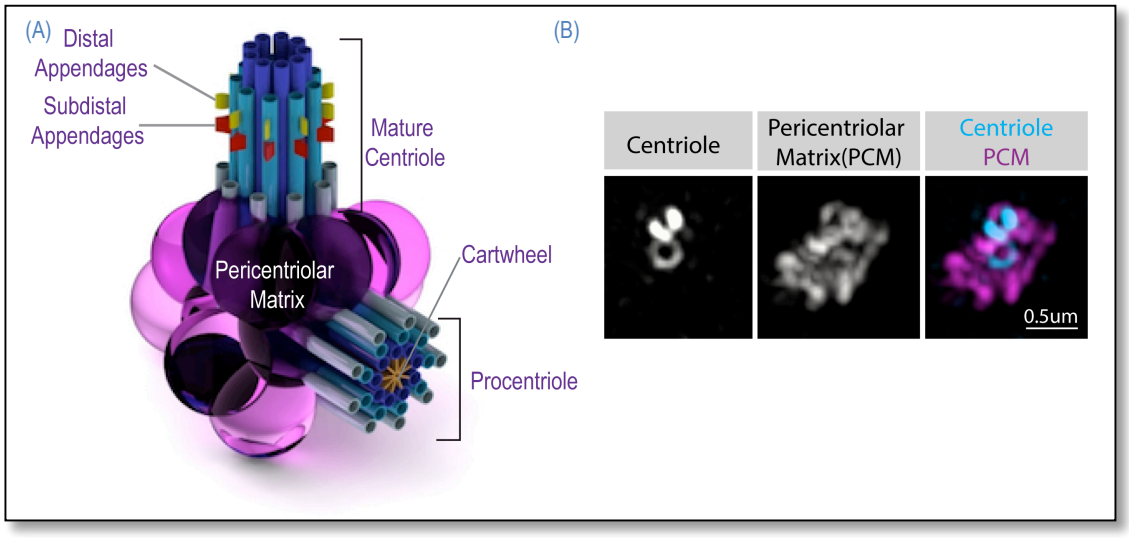


**Figure 1 : The Centrosome** (A) 3D representation of the structure of the centrosome consisting of the centriole and procentriole surrounded by pericentriolar matrix (PCM). The older mature centriole has distal and subdistal appendages necessary for cilia formation and microtubule attachment. (B) 3D-SIM images of fixed *Drosophila* neuroblasts' centrosome labeled for centrioles and centrosome.

In proliferating cells, an electron dense pericentriolar matrix (PCM) surrounds the centrioles, which serves as a lattice-like structure for microtubule nucleation and

anchoring (Bornens, 2002; Figure 1A, 1B, 2A). The molecular composition of the PCM is highly dynamic with rapid turnover of proteins during the cell cycle (Kalt and Schliwa, 1993). The centrosomes are surrounded by an array of microtubules (Figure 2A). Microtubules are nucleated from the centrioles by the subdistal appendages or by PCM protein complexes (Bornens, 2002). The key protein involved in nucleating microtubules is γ-Tubulin (γ-Tub) (Félix et al., 1994; Oakley et al., 1990; Oakley and Oakley, 1989; Stearns and Kirschner, 1994). γ-Tub along with other proteins exists as complexes known as γ -TuRCs (γ-Tubulin ring complexes) and γ -TuSCs (γ-Tubulin small complexes) that anchor and stabilize microtubules (Moritz et al., 2000; 1995). Microtubules are polar structures with fast growing plus ends and slow growing minus ends. γ-TuRCs and γ-TuSCs together organize the minus ends close to the centrosome (Stearns and Kirschner, 1994; Zheng et al., 1995; Wiese and Zheng, 2000; Moritz et al., 2000; Figure 2B).

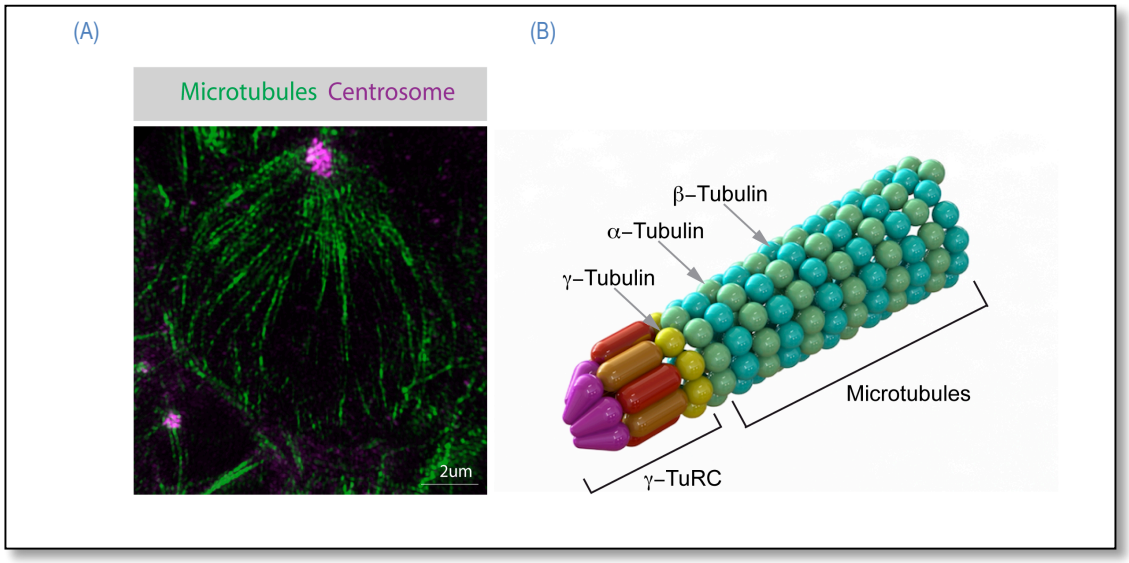


**Figure 2 : The centrosome organizes microtubule network.**(A) 3D SIM image of a fixed *Drosophila* neuroblasts labeled in green for microtubules and magenta for centrosome. As shown in the image, the microtubules arise from the centrosome and radiate outwards. (B) Model of microtubule minus end capping by γ-TuRCs

Although the centrioles' nine-fold symmetry is highly conserved, they do show structural differences among organisms. In *Drosophila melanogaster* and *Caenorhabditis elegans* embryos, centrioles fail to form microtubule triplets and form doublets or even singlets instead. Moreover, these centrioles lack appendages (Moritz et al., 1995a; Gonzalez et al., 1998; O'Toole et al., 2003). In *C.elegans*, the cartwheel structure is completely replaced by a central tube-like structure. *Chlamydomonas reinhardtii* do not seem to have any PCM although centriolar structure matches human centrioles (Dutcher, 2003). Budding yeast cells, instead of the centrosome, possess the spindle pole body, a plate-like structure embedded in the nuclear membrane with the ability to nucleate microtubules (Rout and Kilmartin, 1990; Jaspersen and Winey, 2004). Despite these structural differences, the function of a centrosome as a microtubule-organizing center remains highly conserved among various species.

## 2.2 Molecular Organization of the Centrosome

Over the recent years, the advancement in genomic and proteomics technology has brought to our knowledge multiple protein components that localize to the centrosome and centrioles. In addition, the discovery of super resolution light microscopy has helped us overcome the limitation of a conventional microscope by allowing the capture of images of higher resolution than the diffraction limit. Hence, combining the powers of electron microscopy and super resolution microscopy we have gained insight into the architecture of the centrosome. (Sillibourne et al., 2011; Fu and Glover 2012; Lau et al., 2012; Lawo et al., 2012; Menella et al., 2012; Sonnen et al., 2012 ; Figure 3).

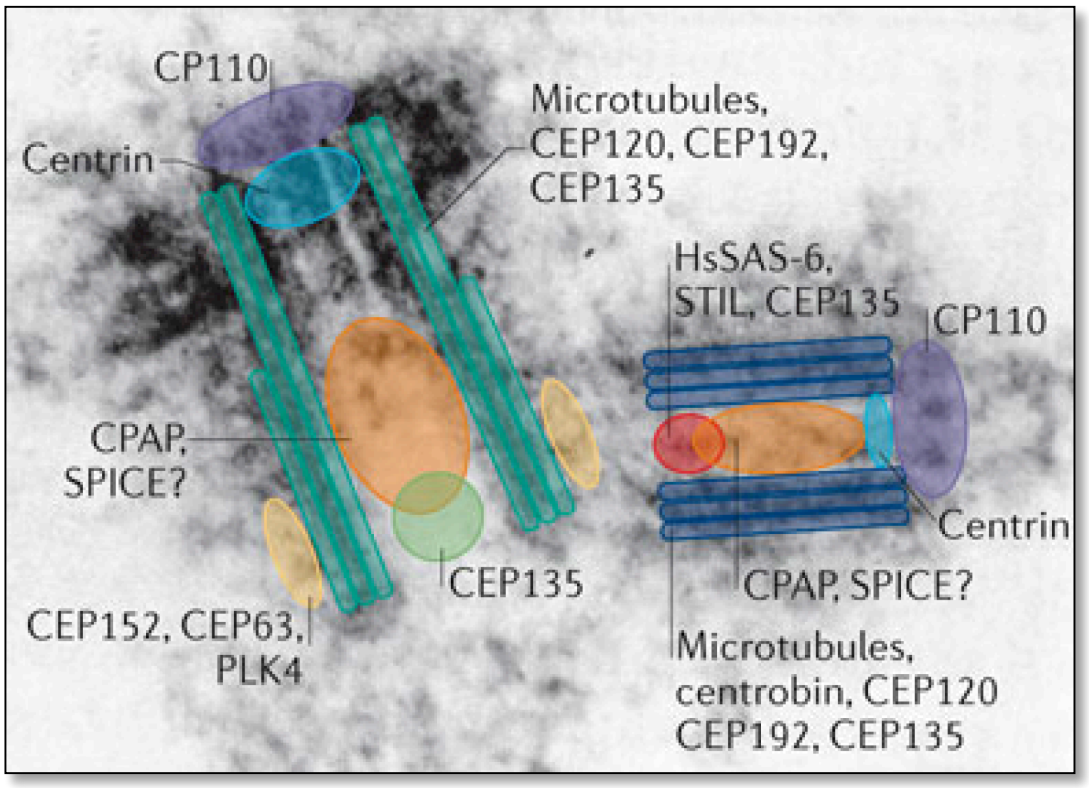


**Figure 3 : Localization of key human centriolar and centrosomal proteins (Gönczy, 2012).** HsSAS-6, STIL and CEP135 are present in the very proximal part of the procentriole. In addition, CEP135 is present in the proximal part of the centriole. CEP152 and CEP63 form a ring around the proximal part of the centriole, and PLK4, which interacts with these proteins, seems to localize in the same vicinity. CPAP is present within the procentriole and centriole and may contact microtubules, whereas SPICE has not been localized with precision (denoted with a question mark), but seems to be present below centrin in both procentriole and centriole. Centrin is found towards the distal end of both procentriole and centriole, occupying a larger domain in the centriole. CP110 (centriolar coiled-coil protein of 110 kDa) is present at the very distal tip of both centriolar cylinders. Centrobin, CEP120, CEP192 and CEP135 are found in the vicinity of microtubules in the procentriole. Similarly, CEP120, CEP192 and CEP135 are found in the vicinity of microtubules in the centriole.

### 2.2.1 The Cartwheel

The core of the centriole essentially consists of Sas-6. (Sonnen et al, 2012; Dzhindzhev et al., 2014). Studies across several species, including *Chlamydomonas*, *Drosophila* and *Paramecium*, revealed loss of Sas-6 caused severe defects or

complete loss of the cartwheel structure (Nakazawa et al., 2007; Rodriguez-Martins et al., 2007a;Jerka-Dziadosz et al., 2010). Crystallography of protein fragments from zebrafish and *Chlamydomonas*, unveiled that Sas-6 exists as homodimers . The amino part of each of the nine Sas6 homodimers undergoes head-to-head dimerization to form the central hub and the carboxy end coiled-coil dimers radiate outwards like spokes of a wheel (Cottee et al., 2011;Kitagawa et al., 2011c; Schuldt 2011; van Breugel et al., 2011;Figure 4A). In fact, Sas-6 protein could assemble into this cartwheel structure *in-vitro*. In *C.elegans*, however, Sas-6 still forms N-N homodimers and coiled-coil dimers but instead of forming a ring, they assemble into filamentous spiral oligomers giving rise to a tube-like structure (Hilbert et al., 2013). Another protein closely involved with Sas-6 during centriole duplication, is Sas-5 as has been reported in *C.elegans*. This association is conserved in human and *Drosophila* counterparts of Sas-5, STIL and Ana-2, respectively. (Stevens et al., 2010; Kitagawa et al., 2011a; Tang et al., 2011; Arquint et al., 2012; Vulprecht et al., 2012). STIL and Sas-6 colocalize to the inner core of the centriole. (Sonnen et al., 2012; Dzhindzdev et al., 2014). In *C.elegans*, Sas-5 binds to Sas-6's coiled-coil domain to prevent the dimer from forming a tetramer *in vitro* (Qiao et al., 2012;Cottee et al., 2015)(Figure 4B).

### 2.2.2 The Centriole Wall

While Sas-6 and Sas-5/STIL/Ana2 form the inner core of the centriole, Sas-4 (CenPJ/CPAP in humans) localizes to the end of the Sas-6 pinheads where the microtubule triplets form the centriolar wall. (Fu and Glover et al., 2012; Figure 4A&B). Its human ortholog CPAP causes centriole elongation when overexpressed (Kohlmaier et al., 2009; Schmidt et al., 2009; Tang et al., 2009). In Sas-4 depleted

*C.elegans* embryos, the microtubule wall fails to form even though Sas-6 is recruited indicating central tube formation (Pelletier et al.,2006). CPAP possesses a tubulin-binding domain and its localization on the centriole is dependent on γ-TuRCs and microtubules (Dammerman et al., 2010).

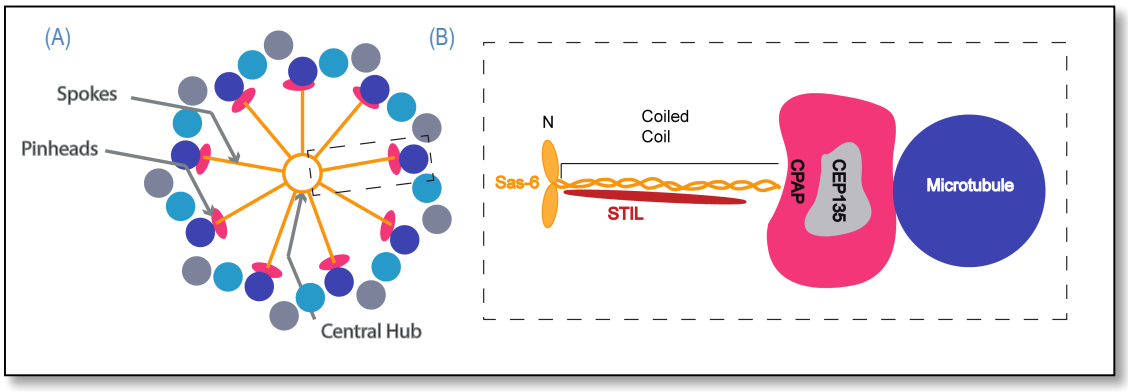


**Figure 4: Sas-6 dimerization is necessary for the nine-fold symmetry of the centriole.** Sas-6 in orange, STILin red, CPAP in pink, Cep135 in light gray (A) Top view of cross section of a mammalian centrosome displaying the nine-fold symmetry of the cartwheel structure. The dark blue, light blue and dark gray indicates the microtubule blade arranged as triplets at the end of each spoke. (B) The close-up of one spoke of the cartwheel indicated by dotted lines. Sas6 forms homodimers by dimerization of the coiled coil domains on the Carboxy Terminus. The amino end of Sas-6 undegoes a globular fold (N) and forms the central hub region with other Sas-6 homodimers. The coiled coil domains are stabilized by STIL. Sas-4 localizes at the junction between the cartwheel and centriole wall. Sas-4 is responsible for centriole wall formation by recruiting microtubules. Adapted from (Cottee et al., 2013;2015)

While the roles of Sas-6, Sas-5/STIL/Ana2 and Sas-4/CPAP are evolutionarily conserved in centriole assembly pathways, there are a variety of essential protein components contributing to the regulation of the pathway. CPAP interacts and colocalizes with Cep135 (bld10 in *Drosophila*), a protein involved in centriole assembly in some species (Cottee et al 2013; Hatzopoulos et al., 2013; Lin et al., 2013 a; Hiraki et al., 2007; Jerka-Dziadosz et al.,2010; Sonnen et al., 2012; Figure 4B). Various other proteins such as CP110 or Cep120, known to interact with CPAP/Sas-4,

localize to the centriole (Schmidt et al., 2009; Lin et al., 2013). The human centriolar proteins CP110 and POC1 appear to be involved in length control like Sas-4 (Keller et al., 2009; Kohlmaier et al., 2009; Schmidt et al., 2009). However, RNAi depletion of CP110 and Cep135 does not prevent centriole assembly in human cycling cells. Centrins are another group of centriolar proteins that's been implicated in basal body formation (Ruiz et al., 2005; Stemm-Wolf et al., 2005) but its role in centriole assembly is rather controversial (Kleylein-Sohn et al., 2007). On the other hand, depletion of coiled-coil centriolar proteins such as Spindle and centriole-associated protein (SPICE), Centrobin, and Cep120 seems to affect procentriole assembly (Figure 3).

### 2.2.3 The Pericentriolar Matrix (PCM)

With the help of super resolution imaging, we now know that the PCM is no longer just an amorphous cloud around the centriole but a structured network of proteins in layers with a clear hierarchy (Fu and Glover et al., 2012; Lawo et al 2012; Mennella et al 2012; Sonnen et al 2012). Based on this, we can divide the PCM into an inner PCM pool close to the centriole wall and an extended outer PCM.

The **Inner PCM pool** consists of vertebrate proteins Cep152 (Asterless (Asl) in *Drosophila*), NEDD1 (Dgp71WD in *Drosophila*) and Pericentrin (Pericentrin like protein (Plp) in *Drosophila*). These proteins localize as rings close to the centriole wall. Cep 152 localizes with the C-Terminus close to the centriolar wall interacting with CPAP and the N-Terminus radiating outward (Sonnen et al., 2012). NEDD1 interacts with γ-Tub as part of the γ-TuRCs and is required for microtubule nucleation. Pericentrin is necessary for PCM organization and microtubule nucleation (Dictenberg et al., 1998; Doxsey et al., 1994).

The **Outer PCM pool** predominantly consists of CDK5RAP2 (Centrosomin (Cnn) in *Drosophila*), γ-Tubulin, Transforming acidic coiled-coil (TACC; D-TACC in *Drosophila*), and Cep192 (Spindle defective-2 (Spd-2) in *Drosophila*). The boundaries of the outer PCM proteins are not well defined and they tend to localize to other parts of the centrosome. These proteins localize as scaffolds, starting close to the centriole and tend to grow and shrink through the cell cycle by constant recruitment and shedding of these proteins (Sonnen et al 2012; Mennella et al., 2012).

### 2.2.4 Appendage Proteins

Mature human centrioles have distal and subdistal appendages, which they acquire during centriole maturation (Nigg and Stearns 2011). Distal appendages proteins such as Cep164, Cep89, Cep83, SCLT1 or FBF1, form a ring and localize to the distal end of the centriole (Sonnen et al.,2012). These proteins are involved in the docking of basal bodies to the membrane during cilia formation (Tanos et al., 2013). Subdistal appendages proteins are Ninein, Cep170, ODF2 (also known as cenexin) or Centriolin, which are necessary for anchoring cytoplasmic microtubules (Sonnen et al 2012; Bornens 2002; Piel et al., 2000).

### 2.2.5 Centrosomal Regulatory Proteins

Centrosomal regulatory proteins refer to kinases, phosphatases and signaling molecules, regulating centrosome function. More than 100 of these regulatory proteins have been shown to transiently or stably associate with centrosomes (Doxsey et al.,, 2005a). They regulate centrosomal functions during duplication, maturation, separation and control microtubule nucleation capacity and they link the centrosome

to other signaling pathways. Members of four key mitotic kinase families localize to centrosomes and are further discussed below.

**Cyclin Dependent Kinases (Cdk)** are serine/threonine kinases and are known to be mitosis regulators (Morgan 2007). Cdks partner with cyclins to form a complex that phosphorylates various substrates for timely cell cycle progression (Enserink and Kolodner, 2010). Both Cdk1 and Cdk2 complexes localize to centrosomes and their activity determines transition through the different phases of cell cycle. The Cdk1/Cyclin B complex appears on the centrosome at prophase (Bailly et al., 1989) and controls centriole separation and spindle assembly (Jackman et al., 2013, Blangy et al., 1997). The Cdk2/Cyclin E complex is involved in initiating centriole duplication in Xenopus and mammalian somatic cells. (Hinchcliffe et al., 1999; Lacey et al., 1999; Matsumoto et al., 1999; Meraldi et al., 1999).

**Polo like Kinases** were named after the *Drosophila* Polo *protein* (Sunkel and Glover, 1988). They are serine/threonine kinases, which work very closely with Cdks to regulate the cell cycle (Glover et al., 1998; Van De Weerdt and Medema, 2006). At the C-terminus, they have a phosphopeptide domain, known as the Polo box domain, which is conserved across species. The Polo box domain is necessary for localizing these kinases to specific sub cellular locations for mediating phosphorylation events (Lee et al., 1998). Plk1, the vertebrate ortholog of Polo, is localizing to multiple locations during mitosis, including centrosomes, kinetochore, the central spindle and the midbody (Golsteyn et al., 1995). Plk1 is necessary for centrosome maturation by promoting recruitment of γ-Tubulin complexes, CDK5RAP2 and abnormal spindle protein (Asp) by phosphorylating them (Conduit et al., 2014; Lane and Nigg, 1996;

Lee and Rhee, 2011; Sunkel and Glover, 1988). Plk4 (SAK in *Drosophila*), is another member of the family, that is essential for centriole duplication and hence localizes to centrioles (O'Connell et al, 2001; Bettencourt-Dias et al, 2005 Habedanck et al, 2005)

**Aurora Kinases** are serine/threonine kinases that are active throughout mitosis. Aurora A localizes to centrosomes and astral microtubules. It has been shown to be required for centrosome maturation and maintenance of a bipolar spindle by mediating the recruitment of γ-Tubulin, Cnn, Minispindles (Msps) and TACC. (Berdnik and Knoblich, 2002; Barros et al., 2005). Aurora A also phosphorylates Histone H3 to initiate chromosome condensation to initiate mitosis (Crosio et al., 2002).

**NIMA** kinases (named after Aspergillus nidulans "Never in mitosis A" protein kinase) are serine/threonine kinases, necessary for cell cycle control. The most studied kinase in this family is Nek2 that localizes to centrosomes and kinetochores. Nek2 ensures proper separation of centrosomes. Other kinases from the family, such as Nek 6, Nek7 and Nek 9 are necessary for mitotic spindle organization and localize to spindle poles( O'Regan et al., 2007).

## 2.3 Centrosome Cycle and its Regulation

The centrosome cycle refers to well-orchestrated events that take place on the centrosome to modulate centrosome/centriole structure and function during the cell cycle (Figure 5A).

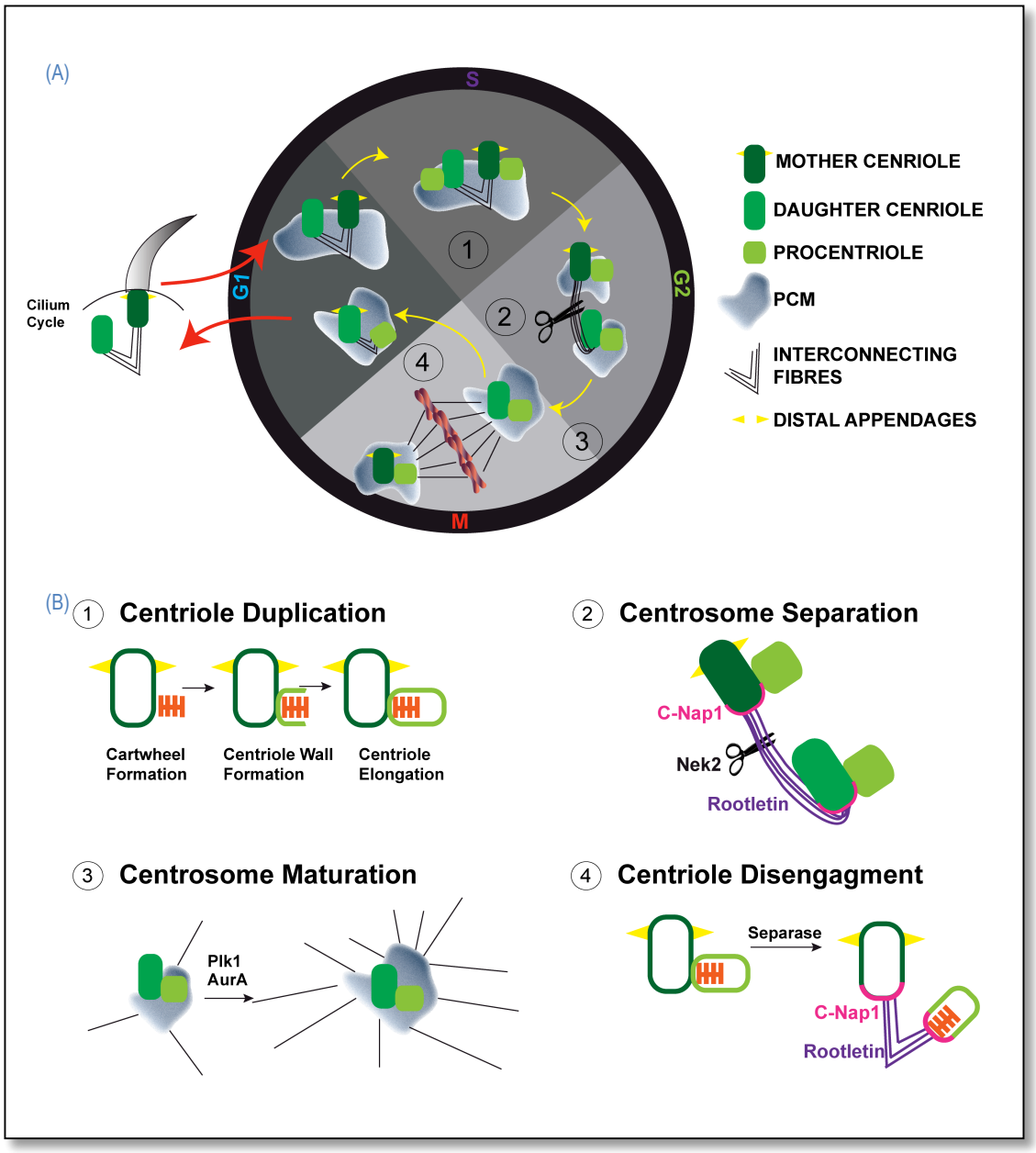


**Figure 5: The Mammalian Centrosome Cycle** (A) Illustration of events occurring on the centrosomes co-related with cell cycle phases S, G2, M and G1. (B) Centrosomal events in detail (1) Centriole Duplication (2) Centrosome Separation (3) Centrosome Maturation (4) Centriole Disengagement. For detailed description refer text below.

### 2.3.1 Centrosome Duplication and Elongation

Centrosomes at G1 consist of two centrioles connected by interconnecting fibers. One of the centriole is older and carries distal appendages, which are necessary for the formation of cilia in quiescent cells. Appendage proteins are absent on the younger daughter centriole (Tanos et al., 2013). In dividing cells, centrosomes duplicate once every cell cycle similar to DNA replication. In fact, both processes are dependent on Cdk2/Cyclin E. In *Xenopus* egg extracts and *Drosophila* embryos, treatment with DNA polymerase inhibitor caused continuous rounds of centrosome assembly (Raff and Glover 1988; Hinchcliffe et al., 1999). In contrast, treatment with Cdk inhibitors can block centrosome duplication. The G1 to S transition switches the cell from a quiescent state to a proliferative state during which centriole duplication occurs. The activation of Cdk2 initiates centriole duplication usually at the same time DNA replication starts. Existing centrioles start to form the template structure, known as the cartwheel at the proximal end of the centrioles (Azimzadeh and Bornens, 2007; Strnad and Gönczy, 2008; Gönczy, 2012; Pelletier et al.,, 2006). The centriole assembly pathway was first described for C. elegans. The protein SPD-2 (Spindle defective 2, Cep192) recruits the kinase ZYG-1 (Plk4). The kinase ensures the timely recruitment of Sas6 and Sas5 (STIL) in order to start cartwheel formation, followed by Sas-4 localization, adding the singlet microtubules to the centriole wall (O'Connell et al., 2001; Kirkham et al., 2003; Leidel and Gonczy, 2003; Dammerman et al., 2004; Delattre et al., 2004; Kemp et al., 2004; Pelletiere et al., 2004,2006; Leidel et al., 2005). All the above-mentioned duplication factors and pathways are highly conserved in vertebrate systems as well (Balestra et al., 2013; Dobbelaere et al., 2008; Kleylein-Sohn et al., 2007). It has been shown that overexpression of Plk4 or SAS-6 induces the formation of extra centrioles around a single parent centriole (Kleylein-

Sohn et al., 2007; Leidel et al., 2005; Peel et al., 2007). Therefore it is likely that the number of centrioles produced during each S-phase depends on the limited presence of these proteins at centrosomes. After template formation, centrioles start to grow by deposition of microtubules onto the template structure. CPAP/Sas4 and Cep120 promote the polymerization of centriolar wall microtubules (Mahjoub et al., 2010; Comartin et al., 2013; Lin et al., 2013b). The newly assembled procentrioles elongate throughout G2 phase and remain tightly associated with their parental centrioles until the end of the next mitosis (Figure 5B(1)).

### 2.3.2 Centrosome Separation

The two centrioles are connected by flexible protein fibers to form a single active MTOC during interphase (Bornens et al., 1987). C-Nap, a Nek2 substrate, is a centriolar protein that binds the fiber-forming protein Rootletin and thereby links the mother with daughter centriole. Phosphorylation of c-Nap by Nek2 releases this link and allows centrosomes to separate (Yang et al., 2006; Figure 5B(2)). In aid to this, PP1 (Protein Phosphatase 1) is inactivated during mitosis to ensure centrosome separation (Helps et al., 2000). The separated centrioles move away from each other with the help of various microtubule associated motor proteins such as Eg5 (Bertran et al., 2011; Blangy et al., 1995; Smith et al., 2011).

### 2.3.3 Centrosome Maturation

Once the centrosomes have separated, both centrosomes start to accumulate PCM and hence increase their MTOC activity at G2/M transition. This is enabled by kinases Plk1 (Conduit et al., 2014; Lane and Nigg, 1996; Lee and Rhee, 2011; Sunkel and Glover, 1988) and Aurora A (Berdnik and Knoblich, 2002; Hannak et al., 2001),

which recruit PCM proteins such as CDK5RAP2, Spd-2, Msps, Asp,TACC, γ-TuRC components, ensuring the nucleation of a large amount of microtubules ((Blagden and Glover, 2003; Glover, 2005; Giet et al., 2002; Barros et al., 2005; Figure 5B(3)). Apart from modification to the PCM structure and increased microtubule nucleation activity, the older centrioles acquire distal and subdistal appendage proteins (Lange and Gull, 1995; Nakagawa et al., 2001), which allow them to anchor cytoplasmic MTs (Bornens, 2002; Piel et al., 2000) or to initiate ciliogenesis (Tanos et al., 2013). Younger centrioles will undergo this modification, which is dependent on Plk1 in the next cell cycle (Wang et al 2009). The mature centrosomes proceed to orient at opposite ends and form a bipolar spindle at M phase.

### 2.3.4 Centriole Disengagement

At the M/G1 phase transitions, the mother-daughter centriole pair tend to lose its tight orthogonal orientation and centrioles are known to be disengaged (Kuriyama and Borisy, 1981; Figure 5B(4)). The orthogonal orientation of the centriole blocks the parental centriole from reduplication. This separation is necessary for the centrioles to undergo duplication in S phase (Tsou and Stearns, 2006a; Wong and Stearns, 2003; Nigg, 2007; Tsou and Stearns, 2006b). Separase is the key protease which cleaves the cohesin rings to separate sister chromatids during chromosome segregation at Anaphase (Uhlmann, 2003). It has been hypothesized that separase could be involved in disengaging the centrioles during G1 (Nakamura et al., 2009; Schöckel et al., 2011). In addition, Kendrin, a PCM component, has been reported to be a Separase substrate (Matsuo et al., 2012).

### 2.3.5 The Cilium cycle

Most vertebrate cells have cilia, which are necessary for signaling and transduction. In quiescent cells, the mother centriole associates with the ciliary vesicle at its distal end, migrates to the cell surface and docks to the plasma membrane to become the basal body (Figure 5A). Cep83 is responsible for centriole to membrane docking (Joo et al., 2013; Tanos et al 2013). The mother centriole loses CP110 and Cep97 in order to start forming cilia (Riparbelli et al., 2012; Goetz et al., 2012). Failure to lose these proteins blocks cilia formation although the basal body still docks to the membrane. The basal body acts as the site from where the cilia start to elongate. (Pederson and Rossenbaum 2008; Ishikawa and Marshall 2011; Avasthi and Marshall 2012). When the mother centriole has to regain its function as a centrosome, it loses the cilia and the basal body dissociates from the cortex. Aurora-A and Plk1 are key players in cilia disassembly in the majority of vertebrate ciliated cells (Wang et al., 2013).

## 2.4 Centrosome Functions

### 2.4.1 Microtubule dependent functions

The primary role of the centrosome is the organization and nucleation of microtubules and hence regulates all microtubule dependent functions. In mitotic cells, the main function of the centrosome is the formation of a bipolar spindle (Gadde and Heald, 2004). During mitosis, the centrosomes increase their microtubule nucleation activity and position themselves at diametrically opposite ends of the cell. Astral microtubules are formed, anchoring both centrosomes at the correct position through cortical interactions (Kotak and Gönczy, 2013). Thereafter, microtubules arising from the centrosomes connect to the kinetochores of the chromosomes. Abnormal spindle architecture, due to multiple centrosomes or centrosome separation defects, leads to

genomic instability, a common sign in cancer progression (Lingle et al., 2002; 2005; Nigg, 2002; Zyss and Gergely, 2009). Apart from faithful chromosome segregation, recent data from stem cells have also implied the role of correct spindle alignment in segregation of centrosomes into daughter cells (Yamashita et al., 2007, Wang et al., 2009; Conduit and Raff 2010; Januschke et al., 2011). It is hypothesized that the age of the centriole might influence the cell's ability to respond to niche signaling and could alter cell fate (Anderson and Stearns. 2009).

Although centrosomes are eminent in spindle assembly, female germ cells and all major plants seem to form a normal bipolar spindle even though they don't have centrosomes. This is because of an alternative pathway for spindle formation involving the RanGTP gradient, chromosomes and kinetochore fibres (Gruss and Vernos, 2004; O'Connell and Khodjakov, 2007; Wadsworth and Khodjakov, 2003). In fact, laser ablation and removal of centrosomes did not affect cell cycle progression in vertebrate cells although some cells failed to complete cytokinesis. (Hinchcliffe et al., 2001; Khodjakov and Rieder, 2001; Uetake et al., 2007). Moreover, in *Drosophila* loss of DSas4 leads to absence of centrioles and even then manages to develop into morphologically normal adult flies (Basto et al., 2006). On the other hand, Plk4 depleted mice undergo mitotic failure; implying that centrosomes are key in vertebrate development (Hudson et al., 2001).

### 2.4.2 Cell Shape, Polarity and Migration

The ability of centrosomes to maintain a microtubule network in animal cells implicates it in maintaining cell shape and establishing polarity. MTOCs are sufficient to generate cortical actin structures. It is hypothesized that centrosomes regulate cell shape because of the cross talk between the end of the microtubules and the actin

network on the cortex (Raff and Glover 1989; Vaizhel-ohayon and Schejter 1999). This has an important role in intiating furrowing and formation of the actomyosin ring by localizing kinases such as Plk1 and Rho.

Centrosomes are important in migrating cells such as in migrating nerve cells. The centrosome is positioned between the cell nucleus and the leading edge (Cooper, 2013). This polarizes the MT network and allows for stabilization of the leading edge and transport of membrane vesicles towards the site of movement.

In *C.elegans*, it has been reported that the centrosomes play an important role in initiating a break in symmetry causing the cell division axis to switch due to redistribution of cortical proteins (Gönczy and Rose, 2005). In *Drosophila* neuroblasts, loss of microtubule activity of the active centrosome causes the cell to lose memory of the existing polarity axis. Hence, reaffirming the role of the MTOC in establishing polarity in polarized cells (Januschke and Gonzalez, 2010).

### 2.4.3 Cell Signalling

Interestingly, there has been increasing evidence, implicating the MTOC as a signaling center or hub that generates and modulates cellular signaling pathways to influence cell cycle progression (Arquint et al., 2014; Doxsey et al., 2005a; Rieder et al., 2001; Sluder, 2005). For example, the entire signaling network of proteins to initiate mitosis such as Cdks, cyclins and Plk1 all localize to the centrosome, confirming the centrosome as a signaling platform (Bailly et al., 1989; Debec and Montmory 1992; Gopalan et al., 1997; Kimura et al 1997; Roghi et al 1998; Golsteyn et al., 1995; Dutertre et al., 2004). DNA damage response and cellular stress pathway proteins have also been known to reside in the centrosome (Fletcher and Muschel

2006). However, the involvement of centrosomes in signaling pathways requires further scrutiny.

## 2.5 Centrosome aberrations and Diseases

The involvement of centrosomes in cellular processes is eminent based on its functions as explained above. Hence, centrosome abnormalities byway of mutation in centrosomal genes have been implicated in various human developmental disorders; from diseases affecting brain development and supernumary centrosomes causing tumorigenesis through to global growth failure syndromes caused due to ciliary malfunctions (Chavali et al., 2014).

### 2.5.1 Neurodevelopmental disorders

Centrosomes have been known to play a role in various processes during brain developments from neurogenesis and polarity establishment to neuronal migration. A genetic neurodevelopmental disorder, known as Autosomal primary recessive microcephaly, is caused by mutations in nine genes encoding centrosome-associated proteins. Microcephaly (MCPH) is characterized by non-progressive mental retardation and reduced brain size. Depending on the gene mutated, there could be additional abnormalities including dwarfism and stertility (Mahmood et al., 2011). The nine genes implicated in MCPH are CPAP (Sas-4), Cep152 (Asl) , Cep135 (Bld10) , STIL(Ana2), CDK5RAP2(Cnn) , WDR62, ASPM/Asp, CASC5/Blinkin and Microcephalin/MCPH1 (Figure 6). The first five genes are core centrosomal proteins involved in centrosome duplication and maturation. WDR62 and ASPM are spindle pole protein necessary for accurate mitotic spindle assembly (Gilmore and Walsh. 2013). The remaining two proteins however have no known centrosomal functions.

CASC5/Blinkin is a centromere protein involved in spindle assembly checkpoint (Genin et al., 2012; Kiyomitsu et al., 2007) and MCPH1 is a nuclear and centrosomal protein that controls cell cycle checkpoint transitions, DNA damage response and repair (Lin et al., 2005; Jackson et al., 1998).

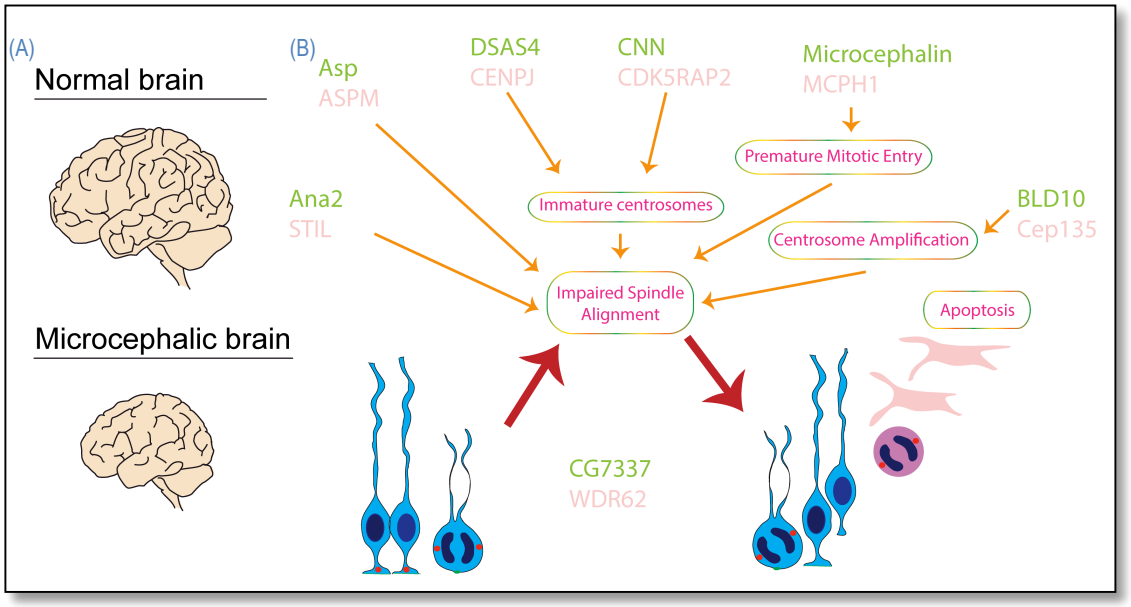


**Figure 6: Microcephaly model** (A) Microcephaly is manifested by the occurrence of reduced brain size but structurally normal brain. (B) A model depicting the role of various centrosomal proteins implicated in microcephaly. Defects in centrosomal proteins could leads to defects in centrosome maturation, centrosome amplification, premature mitotic entry and/or misaligned spindles. The neuroprogenitor cells undergo multiples rounds of symmetric divisions to generate the stem cell pool. In microcephalic brains, there are reduced numbers of progenitor cells. One of the possibilities could be that there is a premature shift in the spindle position causing it to divide asymmetrically and hence leading to reduced number of progenitor cells. Adapted from (Thornton and Woods, 2009).

Although the cell biological cause of MCPH has not been completely understood, evidence suggests that it could be due to the reduction of the neuroprogenitor stem cell pool (Thornton and Woods, 2009). This could be due to a number of reasons. Firstly, aberrant centrosomes can lead to misaligned spindles in stem cells. The orientation of the division axes determines the fate of the daughter cells. Hence, misaligned spindles could affect cell fate decisions and hence affect the balance

between the amount of progenitor and differentiated cells (Lesage et al., 2010). Secondly, during the development of the mammalian brain, changes in cell cycle length occur. As cells transition from proliferative to neurogenic, cells shorten S phase and prolong G1 phase (Takahashi et al.,1995; Calegari et al., 2005; Arai et al., 2011). Defects in cell cycle duration could also lead to a reduction in the number of cells as they divide less frequently. Lastly, the two centrosomes in a cell are very different in terms of size, age, molecular composition and function. For example, in the mouse neocortex, the mother centriole-inheriting cell maintains its stemness, while the cell undergoing differention inherits the younger daughter centriole (Spalding et al., 2013). In fact, interfering with this segregation process can deplete the progenitor pool. This is primarily because the mother centriole is necessary for forming cilia, which in turn is important for transmission of signaling proteins such as Wnt and Shh (Anderson and Stearns 2009; Wallingford and Mitchell 2011; Tasouri and Tucker 2011; Paridaen et al., 2013). Hence, missegregation of centrioles and impaired cilia formation could lead to abnormal signaling, causing premature neural differentiation.

A recent breakthrough from the Knoblich group is the generation of human cerebral organoids from induced pluripotent stem cells (Lancaster et al., 2013). These organoids recapitulate many of the features of embryonic brain development and can hence be used to study developmental disorders such as MCPH. In fact, organoids derived from CDK5RAP2 deficient patient cells show spindle misalignment defects and premature neural differentiation.

### 2.5.2 Cancer

More than a hundred years ago, Boveri made a bold prediction that centrosome amplification could lead to cancer. This hypothesis has become an area of active investigation now due to the observation that knockdown of p53, a tumour suppressor, leads to centrosome amplification in mouse fibroblasts and skin tumours (Fukasawa .2007) Cancers affecting breasts, lung, prostate, colon and brain show centrosomal abnormalities (Lingle et al., 1998; Pihan et al., 1998). These abnormalities could be structural or numerical in nature (Nigg 2006). Structural abberations commonly occur due to altered expression of centrosomal proteins causing centrosomal size enlargement or affecting the ability of the centrosome to nucleate microtubules. Numerical aberrations are however the most common characteristics of cancer (Bettencourt-Dias et al., 2011). Centrosome amplification can occur due to overexpression of centriole duplication factors such as Plk4 or due to cell cycle delay or cell cycle failure (Figure 7). It has been shown that cells with extra centrosomes can ultimately still divide in a bipolar fashion by clustering of extra centrosomes or partial inactivation of centrosomes that fail to cluster (Quintyne et al., 2005; Yang et al., 2008; Kwon et al., 2008; Basto et al., 2008). However, centrosome amplification can generate low-level chromosomal instability, even in the presence of clustering, due to simultaneous attachment of sister kinetochores to one spindle pole known as merotelic attachement (Ganem et al., 2009; Silkworth et al., 2009). However, there is very little genetic evidence of the implications of centrosome abnormalities on human tumorigenesis.

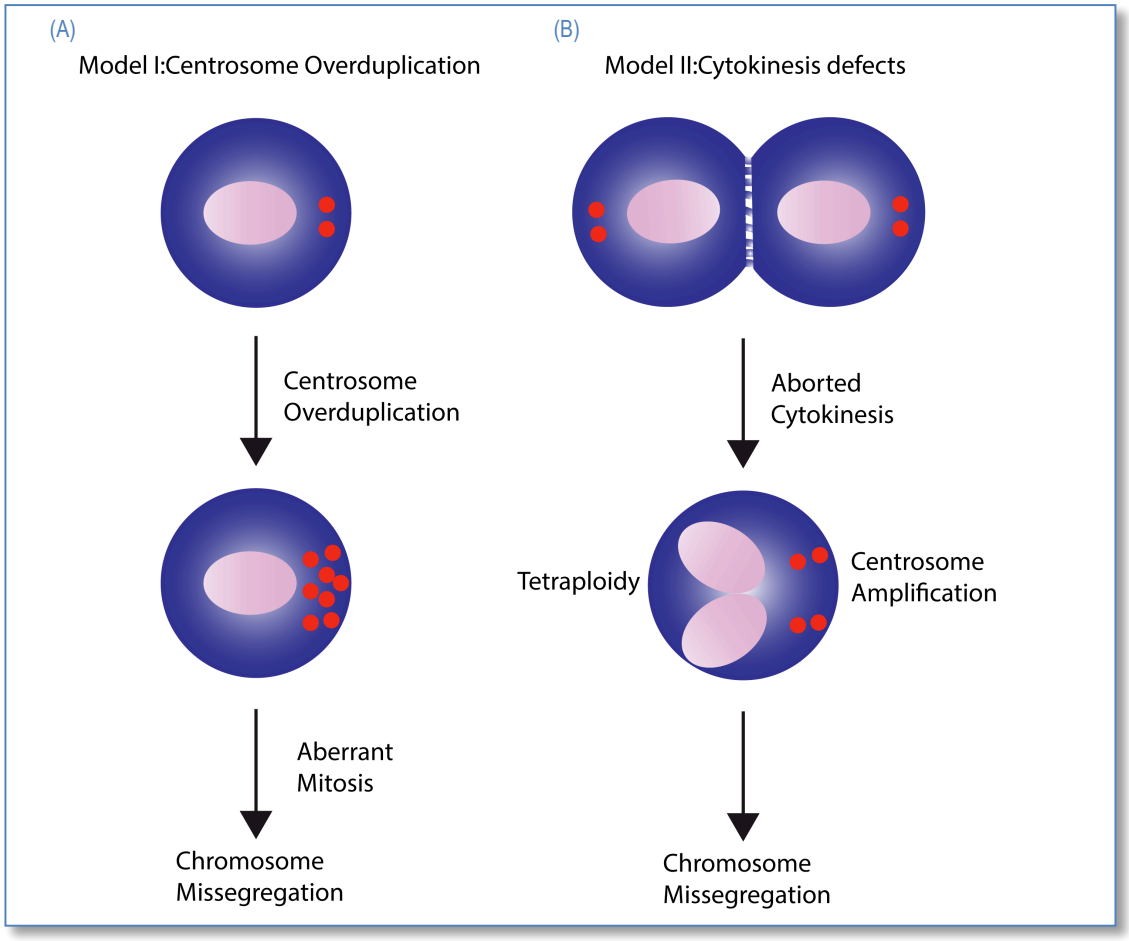


**Figure 7: Centrosome amplificiation models in Cancer cells** (A) Centrosome Overduplication model: Due to defects in centriole duplication machinery, cells undergo multiple rounds of centriole duplication during S phase. (B) Incomplete cytokinesis defects: Failure to complete cell division leads to tetraploidy and centrosome amplification due to the presence of much older centrosomes. Adapted from (Nigg, 2002)

## 2.6 *Drosophila* Neuroblasts: An ideal model to study stem cell biology

*Drosophila* melanogaster, commonly known as the fruit fly, is a widely used model organism for biological research such as genetics, cell signaling and developmental biology. Most human disease genes have orthologs in *Drosophila* with a fairly high percentage of conservation. Hence, *Drosophila* is being used as a genetic model for studying underlying mechanisms of human diseases including cancer, neurodegenerative diseases and diabetes (Reiter et al., 2001)

*Drosophila* neuroblasts are the stem cells in the developing fly brain that have over the years emerged as an important model system for studying underlying mechanisms of asymmetric stem cell division (ACD). Neuroblasts first appear from the embryonic stages 9-11 (approximately 3 hours after embryo laying) by delaminating from the neuroepithelium on the ventrolateral region of the embryo. Embryonic NBs are specified in a process called lateral inhibition in which Notch/Delta signaling refines the expression of proneural genes to individual cells (Artavanis-Tsakonas and Simpson, 1991; Skeath and Thor, 2003; Homem and Knoblich 2012). Neuroblasts undergo asymmetric cell divisions repeatedly to generate a self-renewing neuroblast and a ganglion mother cell (GMC). The GMC then undergoes division once to generate neurons or glia. Embryonic NBs generate all the neurons in the larval central nervous system (CNS) (Prokop and Technau, 1991; Green et al., 1993). While most neuroblasts from the abdominal regions of the embryo are eliminated after completing their neuronal lineages, cephalic and thoracic neuroblasts undergo cells cycle arrest and become quiescent. Around 8-10 hours after larval hatching at the end of the 1$^{st}$ instar stage, these quiescent neuroblasts enter mitosis again. This second round of asymmetric cell divisions generates 90% of the neurons in adult CNS. These neuroblasts continue to divide until early pupal stages after which they undergo cell cycle exit and disappear (White and Kankel, 1978; Truman and Bate, 1988; Maurange et al., 2008; Homem et al., 2014).

The neuroblasts in the larval brain are distinguished into different types based on their position and lineage characteristics, namely: Central brain neuroblasts and ventral nerve cord (VNC) neuroblasts (Figure 8A). The VNC neuroblasts are the abdominal and thoracic neuroblasts from embryonic stages. The central brain neuroblasts consist of type I, type II, mushroom body and optic lobe neuroblasts. While the former three

arise from embryonic cephalic neuroblasts, the optic lobe neuroblasts are formed only during larval stages (Egger et al., 2007;2010).

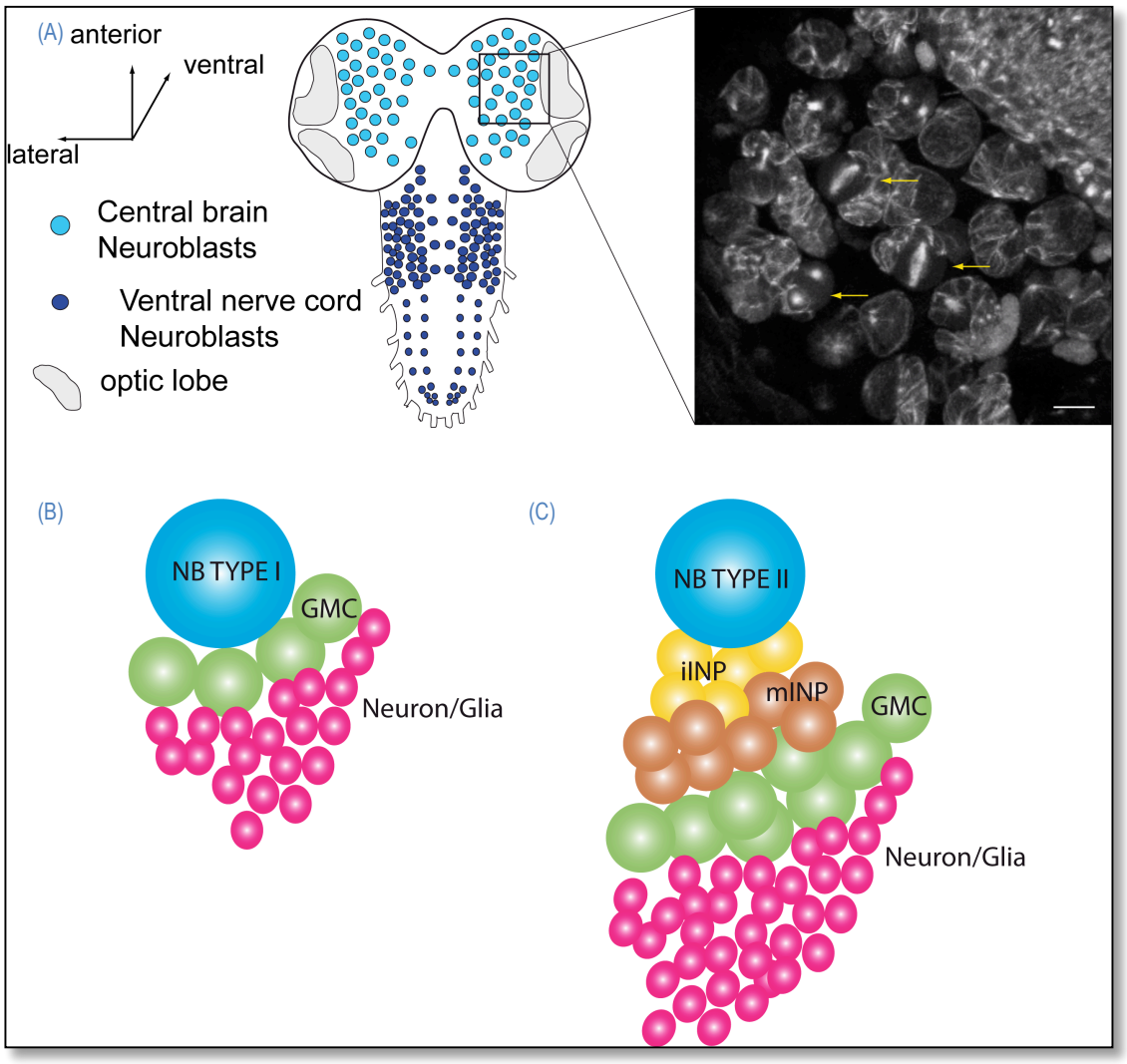


**Figure 8: Neural stem cells of the fly brain** (A) Illustration of *Drosophila* larval brain. Blue dots indicate central brain neuroblast and dark blue indicate ventral nerve cord neuroblasts. On the right is a snapshot of live larval brains expressing microtubule marker. The yellow arrows indicate central brain neuroblasts .(B) Type I neuroblasts (Blue) divide asymmetrically to generate a self renewing neuroblast and Ganglion mother cell(Green).The GMC differentiates in neuron or glia (Pink).(B) Type II neuroblasts (Blue) divide asymmetrically as well, but give rise to an immature interdiate neural progenitor cell (iINP; yellow) instead of a GMC. These cells then mature to become mature INP (mINP; brown) and under go asymmetric division to generate another INP and GMC which differentiates.

There are approximately 100 type I neuroblasts in each brain lobe and they are located on both anterior and posterior sides of the brain. They continue to divide in the same fashion as embryonic neuroblasts, generating a self-renewing neuroblast and a GMC(Figure 8B). Type II neuroblasts, on the other hand, are located on the posterior side of the brains and there are just eight of them in each brain lobe (Bello et al., 2008; Boone and Doe, 2008; Bowman et al., 2008). They divide asymmetrically to generate a self-renewing neuroblast and an immature intermediate neural progenitor (iINP). The INP eventually matures (mINP) after undergoing transcriptional changes and divides asymmetrically a few times to generate another mature INP and a GMC (Figure 8C). This mode of division amplifies the amount of neural cells produced by type II compared to type I neuroblasts. Together, type II neuroblasts generate approximately 5000 adult neural cells that form major neuropile substructures of the brain, such as the central complex (Izergina et al., 2009; Bayraktar et al., 2010; Homem and Knoblich, 2012).

Neuroblasts divide in a molecular and physically asymmetric manner to generate two cells that assume different cell fates after cytokinesis. This asymmetry is established because of four main steps during neuroblast cycle progression: establishment of a polarity axis, orientation of the spindle axis along the polarity axis, positioning the cleavage furrow in a physically asymmetric manner and asymmetric localization and segregation of cell fate determinants (Knoblich, 2008; Figure 8D). After delamination, neuroblasts inherit polarity from epithelial cells of the neuroectoderm. They then undergo multiple rounds of ACD perpendicular to the overlying epithelium in order that the neurons are on the opposite side, thus orienting initial neural tissue growth (Yoshiura et al., 2012). However, during subsequent embryonic and larval divisions the spindle is aligned dependent on the previous division axis. Hence the

cell has a memory of where polarity was established in the previous cell cycle and maintains the same orientation in future division (Yu et al., 2006).

During mitosis, neuroblasts retain apico-basal polarity due to polarized localization of the cell fate determinants and protein complexes. Known cell fate determinants are the transcription factor Prospero, the Notch regulator Numb and binding partners Miranda (Mira) and Partner of Numb (Pon), all localizing to the basal side of the neuroblast during metaphase; all these cell fate determinants segregate into the GMC after cytokinesis. The basal localization of these determinants is dependant on the apical Par complex (Wodarz, 2005). The Par complex is made up of Par6, atypical protein kinase C (aPKC) and Par3/Bazooka (Baz). aPKC directly phosphorylates Numb, leading to its release from the apical cortex. The adaptor protein Pon binds to Numb in order to localize it to the basal cortex during metaphase (Smith et al., 2007; Wirtz-Peitz et al., 2008). aPKC also phosphorylates the adaptor protein Mira which causes it to relocalize to the basal cortex (Wirtz-Peitz et al., 2008; Atwood and Prehoda, 2009). Brat and Pros localize to the basal side because they are bound to Mira. (Ikeshima-Kataoka et al., 1997; Shen et al., 1997; Matsuzaki et al., 1998; Bello et al., 2006; Betschinger et al., 2006; Lee et al., 2006c). Since Pros is bound to Mira and tethered to the cortex, it cannot regulate transcription in the neuroblast during mitosis. After cytokinesis and segregation into GMC, Mira is degraded and Pros is able to enter the nucleus to activate proneural genes while switching off cell cycle genes (Choksi et al., 2006; Southall and Brand, 2009). Numb promotes endocytosis of the Notch receptor leading to Notch inhibition in the GMC (Schweisguth, 2004; Couturier et al., 2012). Brat partners with Pros in activating differentiation in GMCs.

The apical Par complex also plays an important role in ensuring that the spindle orients itself along the polarity axis. Baz of the Par complex links the adaptor protein Inscuteable (Insc) to the Pins (Partner of Inscuteable)/GαI/Mud complex (Schaefer et al., 2000; Yu et al., 2000; Schaefer et al., 2001). Through Mud, this complex recruits the dynenin-dynactin complex, which exerts a pulling force to recruit and maintain one centrosome at the apical pole, thereby aligning the mitotic spindle along the apical/basal polarity axis (Bowman et al., 2006; Izumi et al., 2006; Siller et al., 2006;Siller and Doe, 2008). Apart from this, there is a second spindle orientation pathway involving Pins, Discs large (Dlg) and Khc73. Khc73 localizes to microtubule plus ends and is involved in inducing the formation of Dlg/Pins/GαI crescents even in absence of the Par complex (Siegrist and Doe, 2005).

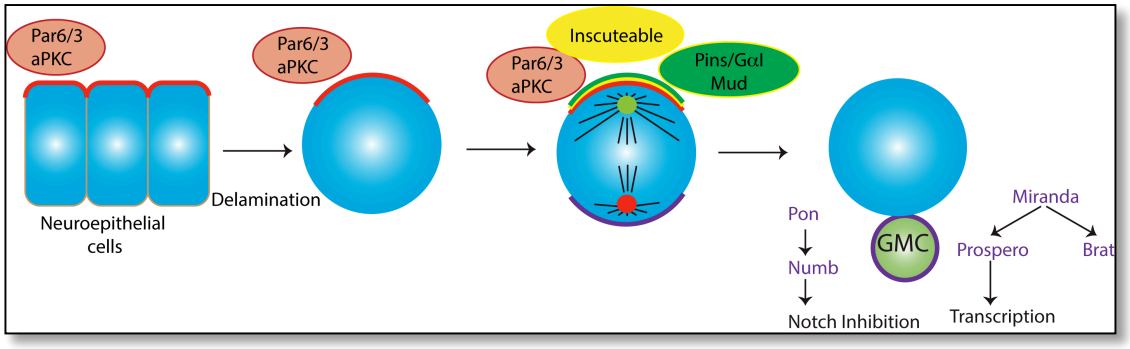


**Figure 9: *Drosophila* neuroblasts are intrinsically asymmetric**. Epithelial apical polarity (apkC-Par complex;red) is inherited by delaminated neuroblasts. During mitosis, Mud is responsible for orienting the mitotic spindle. Mud is recruited by Pins/GαI(green) , which in turn associates with Inscuteable (yellow) and the aPKC-Par complex. The asymmetric localization of cell fate determinants (Pon, Numb, Mira, Pros and Brat (in purple)) is dependent on aPKC phosphorylation. In the GMC, Numb represses Notch signaling and Pros regulates transcription. Adapted from (Knoblich, 2008)

As mentioned earlier, neuroblasts carry the memory of where the apical polarity complex was recruited in the previous cell cycle. Work from the Gonzalez group has established the importance of the interphase aster in maintenance of polarity and

spindle alignment in Drosphila neuroblasts (Januschke and Gonzalez, 2010). According to their findings, the position of the interphase MTOC is consistent with where polarity is established during mitosis. In the scenario where the aster is lost due to microtubule depolymerization by drug treatment or centrosomal protein mutations, they observed that cells lose memory of the positioning of the apical polarity proteins. On inactivation of the drug, the centrosome regains microtubule nucleating capacity and tether to the cortex serving as a reference point for accumulation of apical polarity (Januschke and Gonzalez, 2010). Although, it has to be mentioned that this was not seen in all drug treated cells that brings us to the hypothesis that there are centromal aster dependent and centrosomal independent functions that are involved in polarity maintenance. However, more research is necessary to understand what are the factors involved in this centrosome – cortical interaction. Due to this, there is an avid interest in understanding centrosome and centrosome behavior in asymmetric cell division.

## 2.7 Asymmetric centrosome behavior in stem cells

The term ‘ centrosome asymmetry’ refers to the difference in age, size and molecular composition of the two centrosomes in a cell. Centrosome asymmetry has been observed in various systems and is hypothesized to have a role in centrosome segregation and cell fate. For example, *Drosophila* male germline stem cell (GSC) divides asymmetrically into a self-renewing stem cell and a differentiating gonioblast. GSCs attach to a group of cells called the hub, which secretes signaling molecules such as Unpaired to give germ cells their stem cell identity (Kiger et al., 2001; Tulina and Matunis 2001). Pioneering work from Yamashita (2007) has established that the mother centrosome always remains in the stem cell close to the hub and the daughter

centrosome segregates to the gonioblast (Figurt 9A). The mother centrosome staying close to the hub could have a role in maintaining stemness.

A similar segregation pattern has been reported in mouse radial glia progenitors (Wang et al 2009). Removal of appendage proteins like ninein disrupts the centrosome segregation pattern leading to premature depletion of progenitors. In summary, centrosome segregation and cell fate are linked and understanding centrosome asymmetry could give insight into how cell fate is regulated.

In *Drosophila* neuroblasts, the centrosome cycle is a very intricate process involving unequal centrosomes to ensure correct spindle orientation and centrosome segregation. This was conclusively established by live imaging of neuroblasts using PCM markers like Cnn and centriolar markers like Asl which revealed that one of the centrosome remains tethered to the apical cortex throughout cell cycle (Rebello et al., 2007; Rusan and Peifer, 2007). Shortly after cytokinesis, centrioles separate; while one centriole remains on the apical side, maintaining Cnn and microtubule nucleating capacity, the separating centriole fails to maintain Cnn and microtubules. Unknown factors ensure that the separating centriole moves through the cytoplasm towards the basal part of the neuroblast. During maturation, the separating centriole becomes the second MTOC and attaches itself to the basal side of the cell before forming the bipolar spindle. The neuroblast proceeds to divide asymmetrically and the stationary centrosome always remains in the neuroblasts and the separating centriole ends up in the GMC. However, it was not known which centriole remains in the neuroblast and it was always assumed it could be the mother centrosome due to its role in maintaining stemness in mouse radial glia progenitors. Works from the Raff and Gonzalez labs a few years ago clearly showed that the daughter centrosome remains in the neuroblast and the mother centrosome segregates into the GMC (Figure 9B).

Mother and daughter centrioles were traced using live imaging and photoconversion experiment with the marker Pericentrin-AKAP450 centrosomal targeting (PACT) that accumulates more on the older centriole (Conduit and Raff, 2010; Januschke et al., 2011). Januschke also verified the same by live imaging using *Drosphila* Centrobin (Cnb; Centrobin in humans) that is a daughter centriole specific protein. Hence in the *Drosophila* brain, the daughter centriole is retained by the neuroblasts and the older mother centriole segregates into the GMC.

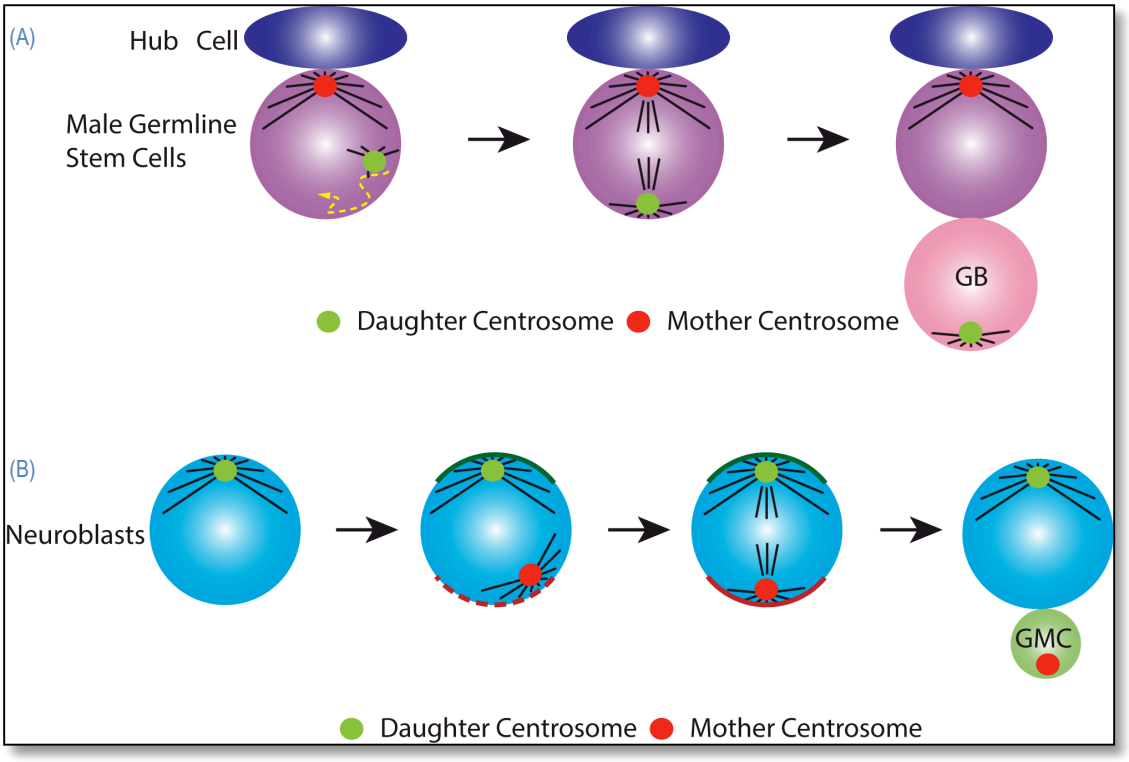


**Figure 10: Asymmetric centrosomes and cell fate.** (A) *Drosophila* male germline stem cells (Violet) are always located close to the hub cell (Indigo). The mother centrosome (Red) remains close to the side in contact with the hub cell and orients the spindle away from the hub cell. The Gonioblast (Pink) retains the daughter centrosome (Green). (B) In *Drosophila* neuroblast(blue) the daughter centrosome remains tethered to the apical side of the cell while mother centrosome matures towards the opposite side of the cell. The daughter centrosome is retained by the neuroblasts while the mother centrosome segregates into the GMC (Light Green).

Progress has since been made to identify the molecular players involved in establishing centrosome asymmetry in *Drosophila* larval neuroblasts. The key regulator of centrosome asymmetry appears to be a kinase known as Polo (Plk1 in humans). Polo phosphorylates and activates centriolar and PCM components in order to ensure accurate centrosome maturation. However, there is recent evidence of Polo playing a significant role during interphase in neuroblasts. Centrobin(Cnb) is a daughter centriole specific protein and is a target for Polo phosphorylation (Januschke et al., 2013). Loss of Cnb in neuroblasts causes both centrosomes to lose MTOC activity during interphase. However, both centrosomes mature at the same time at prophase and the cell cycle progresses normally. Moreover, ectopically localizing Cnb on the mother centriole is sufficient to generate two active MTOCs. Hence, Polo phosphorylation of Cnb triggers daughter centrosome specific PCM maintenance and microtubule nucleation during interphase.

Pericentrin like protein (Plp), the fly ortholog of Pericentrin, was discovered to be a key component in mother centrosome dematuration (Lerit and Rusan 2013). Loss of Plp in neuroblasts causes Polo to be recruited to both centrosomes during interphase apart from other defects. Plp localizes to both centrosomes but is enriched on the mother centrosome during interphase. This is because Cnb plays a role in blocking Plp accumulation on the apical centrosome. On the mother centrosome, accumulation of Plp leads to loss of Polo. In fact, ectopically localizing Cnb to the mother centriole is sufficient to make Plp symmetric on both centrosomes. Hence, the mother centrosome cannot maintain PCM and MTOC activity due to the absence of Cnb. Taken together; these papers established that Cnb is central to the establishment and maintenance of centrosome asymmetry in neuroblasts(Figure 10 A&B).

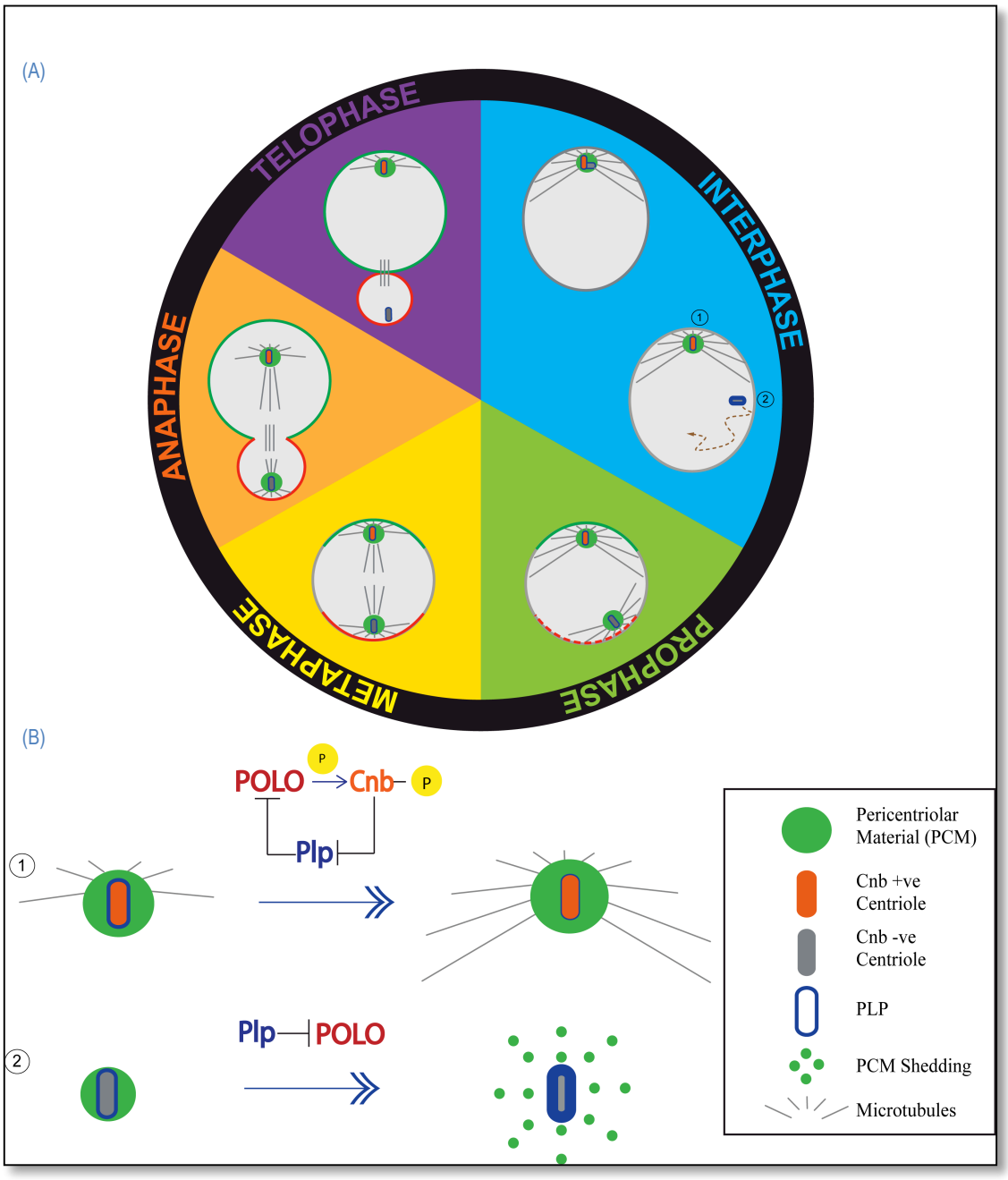


**Figure 11: Centrosome Cycle in *Drosophila* Neuroblasts** (A) Scheme of events occurring during the centrosome cycle. After cytokinesis, the apical centrosome consists of the younger Cnb+ve centriole (orange) and the older Cnb-ve centriole (gray). The older centriole separates and sheds MTOC activity. The younger centriole remains on the apical side maintaining MTOC activity. The older centriole wanders through the cytoplasm and matures only at prophase on the basal side of the cell. The centrosomes orient the spindle along the polarity axis and proceeds to divide asymmetrically. (B) 1. Polo phosphorylated Cnb blocks Plp causing PCM retention and MTOC activity 2. Plp blocks Polo recruitment on the basal centrosome causing loss of PCM and MTOC activity.

Although disturbed centrosome asymmetry does not seem to have drastic consequences in asymmetric cell divison or cell cycle progression, we are yet to exclude that this could have long-term defects in development. Centrosome asymmetry regulators have been implicated in diseases such as Polo/Plk1 in cancer and Cnn and other centrosomal proteins in Microcephaly. It would be interesting to find out if centrosome asymmetry defects could play a role in developmental disorders and other human diseases.

# 3. AIM OF THE PROJECT

Here we have analysed two centrosomal candidates Bld10 (Cep135 in humans) and CG7337 (WDR62 in humans) in *Drosophila melanogaster* neuroblasts. The human orthologs of these genes have been implicated in Microcephaly, a neurodegenerative disease that is connected to centrosomes. The precise nature of how centrosome impairment affects brain development is unknown and hence, it is the reason that prompted us to study centrosome behavior in such great detail. We also adopted higher resolution imaging using 3D-SIM to aid us in broadening our knowledge of the centrosome cycle and localization of centrosomal/centriolar proteins in *Drosophila* neuroblasts.

Recent reports have already established the importance of differential regulation of the mother and daughter centrosome during the cell cycle. We have succeeded in adding novel players into the existing pathway for establishing and maintaining the asymmetry between the centrosomes. In addition, for the first time, we now know how centrosome asymmetry is temporally regulated in neuroblasts.

# 4. RESULTS

# Manuscript I

## 4.1 The centriolar protein Bld10/Cep135 is required to establish centrosome asymmetry in *Drosophila* neuroblasts

Priyanka Singh[1,3], Anjana Ramdas Nair[1] and Clemens Cabernard[1]

[1] Biozentrum, University of Basel
Klingelbergstrasse 50-70
CH-4056 Basel, Switzerland

[2] Department of Biology, University of Fribourg
Chemin du Musée 10
CH-1700 Fribourg, Switzerland

[3] Present address:
Max-Planck Institute of Molecular Physiology
Department of Mechanistic Cell Biology
Otto-Hahn-Str. 11
D-44227 Dortmund, Germany

[#] equal author contribution

Published in Current Biology 24, 1548–1555, July 7, 2014
Submitted on: February 10, 2014
Accepted: May 21, 2014

Current Biology *24*, 1548–1555, July 7, 2014  http://dx.doi.org/10.1016/j.cub.2014.05.050

Report

# The Centriolar Protein Bld10/Cep135 Is Required to Establish Centrosome Asymmetry in *Drosophila* Neuroblasts

**Priyanka Singh,[1] Anjana Ramdas Nair,[1] and Clemens Cabernard[1,*]**
[1]Biozentrum, University of Basel, Klingelbergstrasse 50-70, 4056 Basel, Switzerland

## Summary

**Centrosome asymmetry has been implicated in stem cell fate maintenance in both flies and vertebrates [1, 2]. *Drosophila* neuroblasts, the neural precursors of the fly's central nervous system [3], contain molecularly and physically asymmetric centrosomes, established through differences in pericentriolar matrix (PCM) retention [4–7]. For instance, the daughter centriole maintains PCM and thus microtubule-organizing center (MTOC) activity through Polo-mediated phosphorylation of Centrobin (Cnb) [7, 8]. The mother centriole, however, quickly downregulates PCM and moves away from the apical cortex, randomly migrating through the cytoplasm until maturation sets in at prophase [4–6, 8]. How PCM downregulation is molecularly controlled is currently unknown, but it involves Pericentrin (PCNT)-like protein (PLP) to prevent premature Polo localization and thus MTOC activity [9]. Here, we report that the centriolar protein Bld10, the fly ortholog of Cep135, is required to establish centrosome asymmetry in *Drosophila* neuroblasts through shedding of Polo from the mother centrosome. *bld10* mutants fail to downregulate Polo and PCM, generating two active, improperly positioned MTOCs. Failure to shed Polo and PCM causes spindle alignment and centrosome segregation defects, resulting in neuroblasts incorrectly retaining the older mother centrosome. Since Cep135 is implicated in primary microcephaly, we speculate that perturbed centrosome asymmetry could contribute to this rare neurodevelopmental disease.**

## Results and Discussion

In a gene candidate approach to identify molecules required for centrosome asymmetry in *Drosophila* neuroblasts, we identified Bld10/Cep135 as a potential centrosome dematuration regulator. Bld10 is a ubiquitous centriolar protein, localizing to centrioles in *Drosophila* larval neuroblasts and other cell types ([10] and data not shown).

To investigate centrosome asymmetry, we performed live imaging experiments in intact third-instar larval brains (see the Supplemental Experimental Procedures and [11]), labeling centrosomes with the centriolar markers DSas6::GFP [12] or DSas4::GFP [13] and mCherry::Jupiter [14]. *jupiter* encodes for a microtubule binding protein, sharing properties with several structural microtubule-associated proteins (MAPs) [15], and is ideally suited to visualize microtubule dynamics and microtubule-organizing center (MTOC) activity. In agreement with previous findings [4–6], we found that wild-type (WT) interphase neuroblasts contained one apical MTOC only. The second MTOC appeared during prophase in close proximity to the basal cortex. By prometaphase, both MTOCs reached maximal activity and intensity (Figures 1A and 1B, time point 0:00). However, in *bld10* mutant interphase neuroblasts ($bld10^{c04199}$/*Df(3L)Brd15*; see the Supplemental Experimental Procedures and [10]), we observed two centrosomes of similar size and MTOC activity close together on the apical cortex. The two centrosomes progressively separated from each other until they reached their respective positions on the apical and basal cortex by prometaphase (Figures 1C and 1D, time point 0:00). Thus, in contrast to the wild-type, *bld10* mutant neuroblasts show symmetric centrosome behavior. *bld10*'s centrosome asymmetry defect could be rescued with *bld10::GFP* [12] (Figure 1E), and immunohistochemistry experiments confirmed our live imaging results (data not shown).

The $bld10^{c04199}$ allele is predicted to produce a truncated protein, retaining Bld10's N terminus [10]. We generated a new N-terminal deletion allele (*bld10ΔN*; see the Supplemental Experimental Procedures and Figures S1A and S1B) [16] that showed the same centrosome asymmetry phenotype (Figures S1C and S1D). In addition, we also found neuroblasts containing monopolar and multipolar spindles (Figures S1D–S1H), which are not observed with the $bld10^{c04199}$ allele. This suggests that $bld10^{c04199}$ is a separation-of-function allele, specifically disrupting centrosome asymmetry. Unless otherwise noted, all of the experiments described in the following sections were performed with the $bld10^{c04199}$ allele.

The lack of centrosome asymmetry in *bld10* mutant neuroblasts could be due to aberrant centriole migration. For example, the mother centriole could either fail to migrate through the cytoplasm or migrates back to the apical cortex to mature. We tested this hypothesis, measuring centriole migration as a function of time and observed that centriolar migration in wild-type and *bld10* mutant neuroblasts occur in two distinct phases: (1) centrioles steadily separated from each other, followed by (2) a sudden increase in intercentriolar distance, which peaked when centrioles reached a separation distance of ~4–6 μm in the wild-type and *bld10* mutants (Figure 1F). Centrioles in *bld10* mutants did not require more time to reach this threshold distance (Figure 1G) and did not return to the apical cortex to mature (Figure 1C). We conclude that *bld10's* centrosome asymmetry defect is not due to aberrant centriole migration.

To get mechanistic insight into *bld10*'s phenotype, we used live imaging to measure the dynamic localization of three GFP-tagged pericentriolar matrix (PCM) markers: γ-tubulin (γ-Tub), Mini spindles (Msps; CKAP5 in vertebrates) and centrosomin (Cnn; CDK5Rap2 in vertebrates) [17–19]. Wild-type neuroblasts showed robust localization of γ-Tub, Msps, and Cnn to the apical centrosome during interphase. After centrosome splitting, all three PCM markers were downregulated from the basal centrosome (shedding phase) but reaccumulated during prophase (maturation phase; Figure 2A and Movie S1). *bld10* mutant neuroblasts also correctly localized γ-Tub, Msps, and Cnn to the apical interphase centrosome. However, similar to the MTOC marker Jupiter, γ-Tub, Msps, and Cnn were not downregulated from the separating centriole (Figure 2B and

*Correspondence: clemens.cabernard@unibas.ch

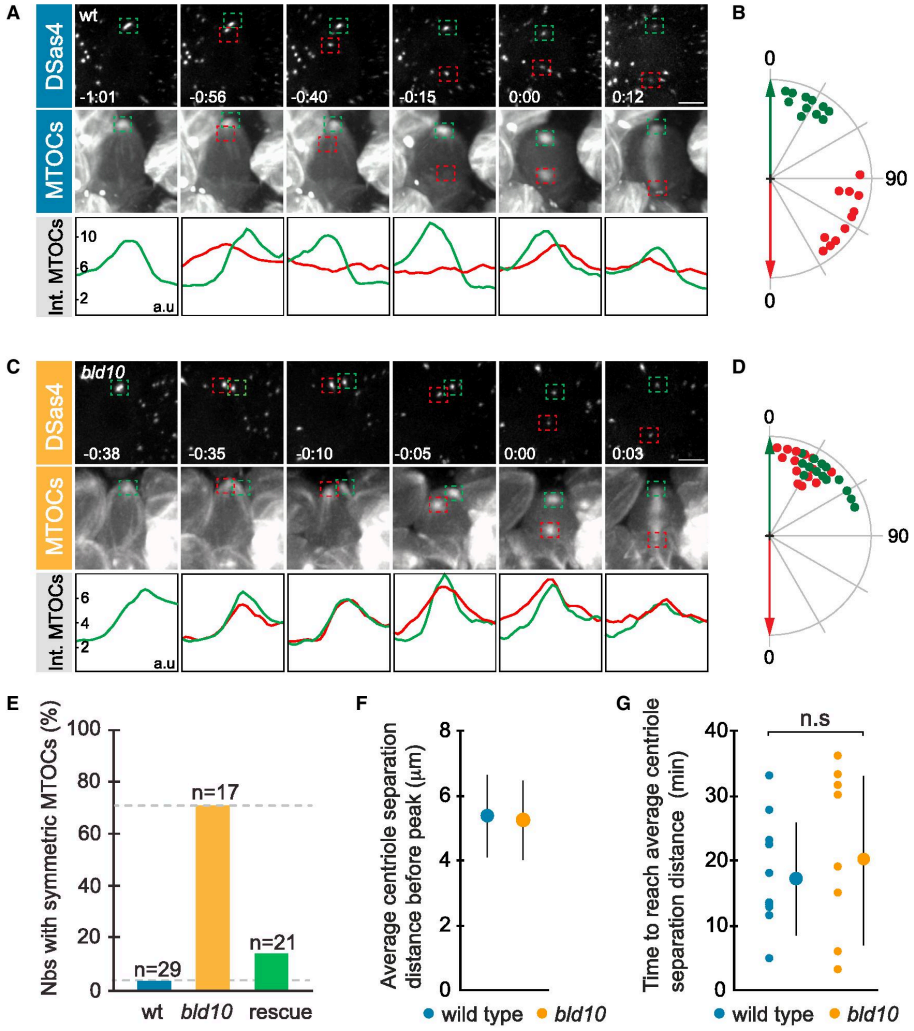


Figure 1. Bld10 Is Required for Centrosome Asymmetry

(A and C) Wild-type (A) and *bld10* mutant (C) third-instar larval neuroblasts expressing the centriolar marker DSas4::GFP (top row) and the MTOC marker Cherry::Jupiter (middle row). The green and red lines below the image sequences represent Cherry::Jupiter intensity values of the apical (green box) and basal (red box) centrosomes, respectively.

(B and D) Radial centrosome distribution plot of wild-type (B) and *bld10* mutants (D) depicting the maximal deviation of the apical (green) and basal (red) MTOC in relation to the cell division axis, denoted with the 0° line. Green and red arrows highlight the apical (green)-basal (red) polarity and division axis.

(E) Quantification of centrosome asymmetry phenotype in wild-type, *bld10* mutant, and rescued (*bld10* mutants, expressing bld10::GFP) neuroblasts expressing Cherry::Jupiter only.

(F) Average centriolar distance just before centriole separation reaches a maximum. Error bar indicate the SD.

(G) Time to reach average centriolar distance. The difference is statistically not significant (n.s.; p = 0.5748).

Int., intensity; a.u., arbitrary units; MTOC, microtubule-organizing center. Time is shown as hr:min. Scale bar, 5 µm. See also Figure S1.

Movie S2). We measured centrosome size and plotted a centrosome asymmetry index (see the Supplemental Experimental Procedures), starting at centrosome splitting until metaphase. Wild-type centrosomes developed a clear size asymmetry during the shedding phase and reduced it during the maturation phase (Figure 2C). *bld10* mutant centrosomes stayed similar in size, manifested in an asymmetry index below 1.5 (Figure 2D). Centrosome size and intensity measurements also revealed that in most wild-type neuroblasts, γ-Tub, Msps, and Cnn were removed from the basal centrosome ~15 min after centrosome splitting (Figure 2E). Basal wild-type centrosomes were essentially devoid of γ-Tub after that time,

**Current Biology** Vol 24 No 13
1550

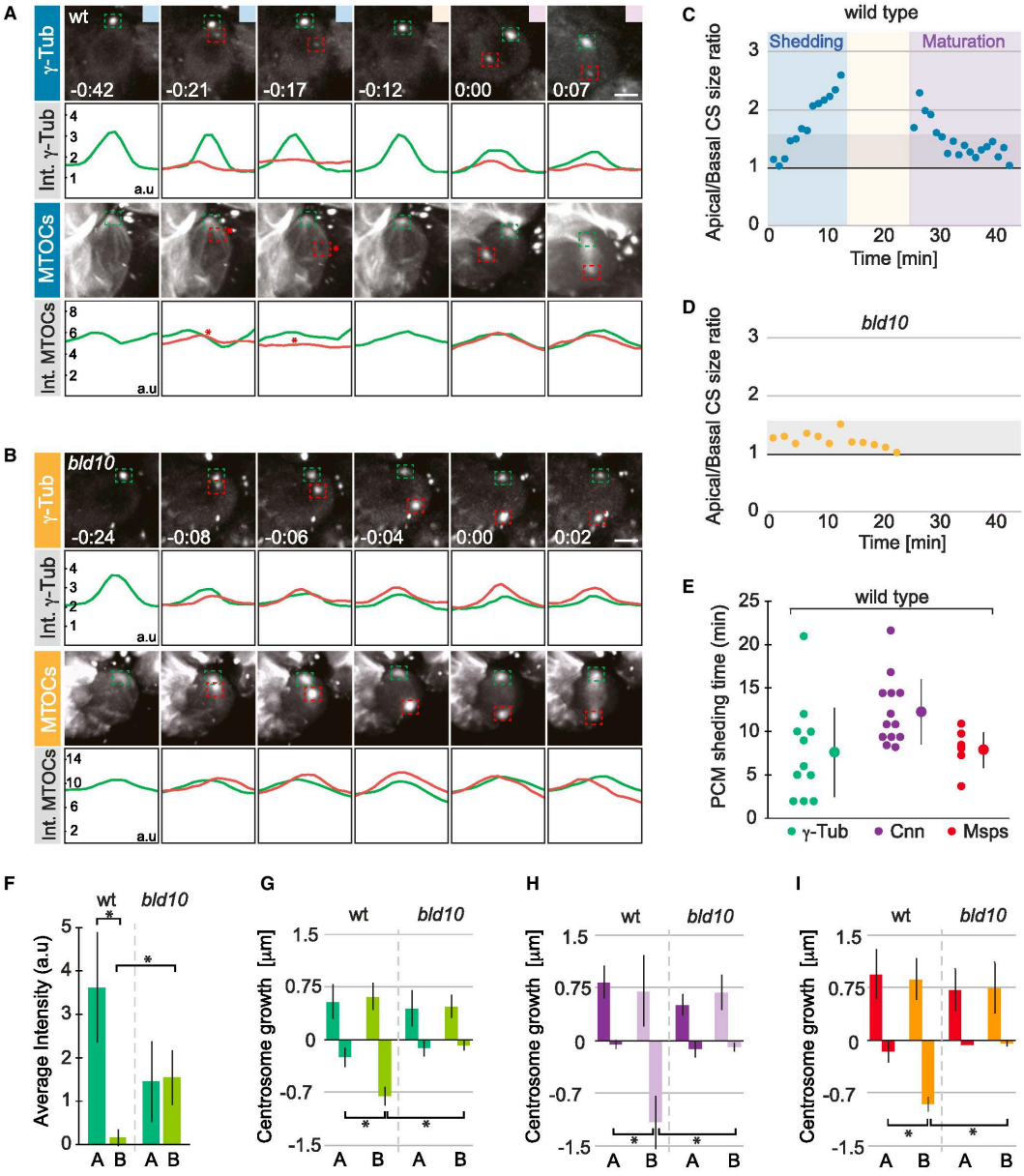


Figure 2. *bld10* Mutant Centrosomes Are Able to Mature but Fail to Downregulate PCM

(A and B) Wild-type (A) and *bld10* mutant (B) neuroblasts expressing the pericentriolar marker γ-tub::GFP and the MTOC marker Cherry::Jupiter. Colored insert boxes refer to the shedding phase (light blue), the maturation phase (light pink), and the phase in between (light yellow). Since the basal centrosome sheds almost all PCM, we cannot reliably measure its size once shedding is completed (light yellow). In all panels, the green and red dashed boxes label the apical daughter and the basal mother centrosome (CS), respectively. Asterisks denote intensity measurements with uncertainty (green line, apical CS; red line, basal CS).

(C and D) Asymmetry index graph (size of apical or bigger CS divided by the basal or smaller CS) of a representative wild-type (C) or *bld10* mutant (D) neuroblast.

(E) Measured PCM shedding time for γ-tub::GFP (green), Cnn::GFP (purple), and Msps::GFP (red) in wild-type neuroblasts. Approximately 15 min after centrosomes split, PCM markers are shed from the basal centrosome. Mean and SD are shown next to individual measurement points.

*(legend continued on next page)*

whereas *bld10* mutants contained equal amounts of this PCM marker (Figure 2F). We further compared changes in centrosome size and found that wild-type apical centrosomes predominantly grew, whereas basal centrosomes increased (maturation phase) and decreased (shedding phase) their size to almost the same extent. *bld10* mutant centrosomes were able to enlarge but showed very little size reduction, comparable to apical wild-type centrosomes (Figures 2G–2I). We conclude that *bld10* mutant centrosomes are able to mature but fail to downregulate the PCM markers γ-Tub, Msps, and Cnn.

The results above suggest two possible mechanisms for centrosome asymmetry: (1) Bld10 could prevent premature mother centrosome maturation by blocking the precocious accumulation of PCM proteins. (2) Alternatively, Bld10 could promote PCM shedding right after centrosomes separate, thereby preventing the basal mother centrosome to prematurely become an MTOC. We devised an in vivo pulse-chase labeling experiment to distinguish between these two possibilities. To this end, we tagged Cnn at its endogenous locus with the photoconvertable fluorescent protein mDendra2 [20] (see the Supplemental Experimental Procedures and [21]). If Bld10 blocks premature PCM accumulation, mother centrioles should quickly shed photoconverted Cnn and prematurely reaccumulate unconverted Cnn in *bld10* mutants. Vice versa, if PCM shedding is compromised, we should be able to follow the photoconverted centrosomes from the moment they separate until telophase. We found that apical wild-type daughter centrioles retained the majority of photoconverted Cnn::mDendra2 from early interphase until prophase (possibly longer), indicating that very little Cnn protein gets exchanged. The basal mother centriole, however, lost photoconverted Cnn::mDendra2 within approximately 10–15 min after centriole separation (n = 5), confirming that Cnn is shed quickly (Figure 3A and Movie S3). Interestingly, *bld10* centrioles retained photoconverted Cnn::mDendra2 for at least 45 min after separation (n = 7). In some cases, one of the centrioles decorated with photoconverted Cnn::mDendra2 was even inherited by the newly formed GMC (Figure 3B and Movie S4). We conclude that (1) on the apical centrosome, Cnn protein turnover is absent or significantly reduced during interphase, that (2) on the basal centrosome, Cnn is shed quickly and replaced with new Cnn when maturation sets in, and that (3) *bld10*'s centrosome asymmetry defect is not due to premature centrosome maturation. Instead, separating basal centrioles fail to shed Cnn in particular and possibly PCM proteins in general.

To elucidate the molecular mechanism underlying PCM shedding, we first analyzed the relationship between Bld10, Centrobin (Cnb), and Pericentrin (PCNT)-like protein (Plp). Recently, it was shown that Cnb is necessary and sufficient for PCM retention on the apical daughter neuroblast centrosome [8]. However, gain- and loss-of-function experiments with Cnb did not perturb Bld10's localization (Figures S2A–S2C). Similarly, as in the wild-type [7], Cnb was localized asymmetrically in *bld10* mutants (Figures 4A and 4D). *plp* mutants fail to downregulate γ-Tub on the mother centrosome [9]. We found that in *plp* mutant neuroblasts, the basal centrosome retained Cnn and MTOC activity during interphase (Figures S3A and S3B). Interestingly, photoconversion experiments showed that similar to *bld10*, Cnn shedding from the basal centrosome was compromised in *plp* mutants (n = 4) (Figure 3C). However, Plp's localization is not perturbed in *bld10* mutant neuroblasts (Figures S2D–S2G), and Bld10 was normally localized in *plp* mutants (Figures S2H–S2J). Knockdown of *plp* in *bld10* mutants (see the Supplemental Experimental Procedures) did not enhance *bld10*'s PCM shedding phenotype, but due to the occurrence of additional phenotypes (fragmented or multiple centrosomes; data not shown), the shedding phenotype could also be partially masked (Figure S3C). In sum, we conclude that Bld10 is regulating centrosome asymmetry independently of Cnb and that Plp is also required to shed Cnn.

Since the mitotic kinase Polo has been implicated in PCM retention during interphase [8, 9] we assayed Polo localization dynamics in wild-type and *bld10* mutant neuroblasts. Recently, it was reported that Polo localizes to the apical centrosome during interphase and is only detectable at the basal centrosome during prophase, when maturation sets in [9]. We used a Polo::GFP protein trap line [22] and confirmed that Polo is stably localized to the apical interphase centrosome [6, 9]. Surprisingly, we found weak Polo also on the separating mother centrosome (Figure 3D; time frame −0:47). Subsequently, Polo disappeared from the basal mother centriole within 10 min (±4 min; n = 7), comparable to Cnn, γ-Tub, and Msps shedding times (Figures 3F and 2E). With a genomic Polo::GFP transgene [23], showing lower fluorescence intensity, Polo was found to be localized on both centrosomes in *bld10* mutants (Figure 3E). These data suggest that in wild-type neuroblasts, Polo is not just recruited onto the basal mother centrosome by prophase as previously reported [6, 9], but is also subject to shedding during interphase. Polo is required for PCM retention since in *bld10* mutant neuroblasts treated with the Polo inhibitor BI2536 (see the Supplemental Experimental Procedures and [8]), both centrosomes lose MTOC activity (Figure 3G). Thus, we conclude that shedding of Polo is a requirement for the subsequent shedding of Cnn, γ-Tub, and Msps, enabling basal mother centrosome dematuration and the establishment of centrosome asymmetry.

Finally, we analyzed the consequences of disrupted centrosome asymmetry. We labeled the daughter centriole with Cnb::YFP [7] and assayed centrosome segregation. We confirmed that wild-type neuroblasts faithfully retain the $Cnb^{+}$ daughter centriole, whereas the $Cnb^{-}$ centrosome segregates into the GMC (100%, n = 10; Figures 4A–4C) [7]. *bld10* mutants showed correct asymmetric Cnb localization, but ~45% (n = 11) of *bld10* mutant neuroblasts wrongly retained the mother centriole and segregated the daughter centriole into the GMC (Figures 4C–4E). $Cnb^{+}$ centrosomes are usually bigger in wild-type and *bld10* mutant neuroblasts (Figure 4F), but centrosome segregation is independent of MTOC activity and size since *bld10* mutant neuroblasts often retained the smaller centrosome (Figure 4E). We conclude that centrosome asymmetry is required for faithful centrosome segregation.

(F) Apical and basal centrosome γ-tub::GFP (green) intensity, measured 15 min after centrosomes splitting. Mean and SD are shown next to individual measurement points.
(G–I) CS growth measurements for γ-tub::GFP (green; G), Cnn::GFP (purple; H), and Msps::GFP (red, I). Bar graphs show averaged values and standard deviation for wild-type and *bld10* mutants.
Asterisks in (F)–(I) indicate $p < 0.0001$. Int., intensity; a.u., arbitrary units; A, apical CS; B, basal CS; MTOC, microtubule-organizing center. Time is shown as hr:min. Scale bar, 5 μm. See also Movies S1 and S2.

**Current Biology** Vol 24 No 13
1552

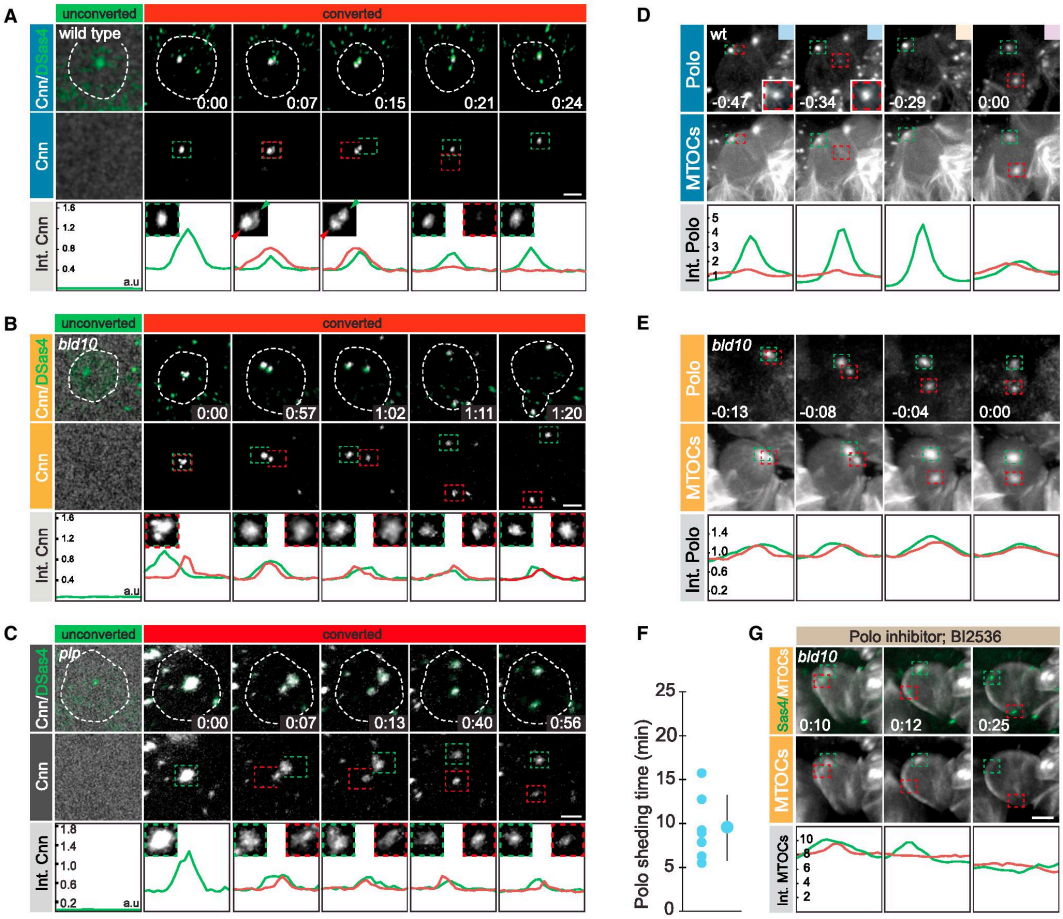


Figure 3. Neuroblasts Establish Centrosome Asymmetry through Shedding of Polo and PCM Proteins from the Mother Centrosome

The PCM marker Cnn, endogenously tagged with mDendra2 (white), was coexpressed with the centriolar marker Sas4::GFP (green) to facilitate centrosome tracking. Photoconversion was performed shortly after telophase, before centrosome separation occurred. Time point 0:00 refers to the first frame after photoconversion of Cnn::mDendra2.

(A–C) Image sequence of a wild-type (A), *bld10* mutant (B), and *plp* mutant (C) neuroblast. Wild-type basal centrosomes turn over photoconverted Cnn within 15–20 min. In *bld10* mutants, both centrosomes retain photoconverted Cnn until telophase. Basal centrosomes in *plp* mutants retain photoconverted Cnn for at least 1 hr. The white dashed line represents the cell outline. The lower panels show an intensity plot of converted Cnn::mDendra2 at apical (green dotted box) and basal (red dotted box) centrioles. Inserts show high-magnification pictures of photoconverted centrosomes.

(D) Polo::GFP (protein trap line [22]) expressed in wild-type neuroblasts. Inserts at time point −0:47 and −0:34 show higher magnifications of the basal centrosome with enhanced signal intensity. Colored insert boxes refer to the shedding phase (light blue), the maturation phase (light pink), and the phase in-between (light yellow). Polo intensity is plotted below.

(E) *bld10* mutant neuroblast expressing Polo::GFP transgene [23].

(F) Scatter plot showing the measured time to shed Polo in wild-type neuroblasts.

(G) *bld10* mutant neuroblast treated with the Polo inhibitor BI2536. Centrioles are labeled with Sas4::GFP (green). MTOCs are labeled with Cherry:Jupiter (white). MTOC intensity is plotted below.

MTOC, microtubule-organizing center; Int., intensity; a.u., arbitrary units. Time is shown as hr:min. Scale bar, 5 μm. See also Figures S2 and S3 and Movies S3 and S4.

Since *bld10* mutant neuroblasts have mispositioned MTOCs in relation to the apical-basal division axis (Figures 1B and 1D), we analyzed spindle orientation (see the Supplemental Experimental Procedures). Immunohistochemistry experiments showed that *bld10* mutant neuroblast spindles deviate from the regular orientation range, with isolated cases of extreme misalignment (Figures 4G and 4H). Metaphase spindles, aligned orthogonally to the apical-basal polarity axis, can induce symmetric neuroblast divisions, resulting in an increase of the neural stem cell pool [14]. However, neuroblast numbers were unchanged in *bld10* mutants compared to control brains (data not shown), and we did not find symmetric

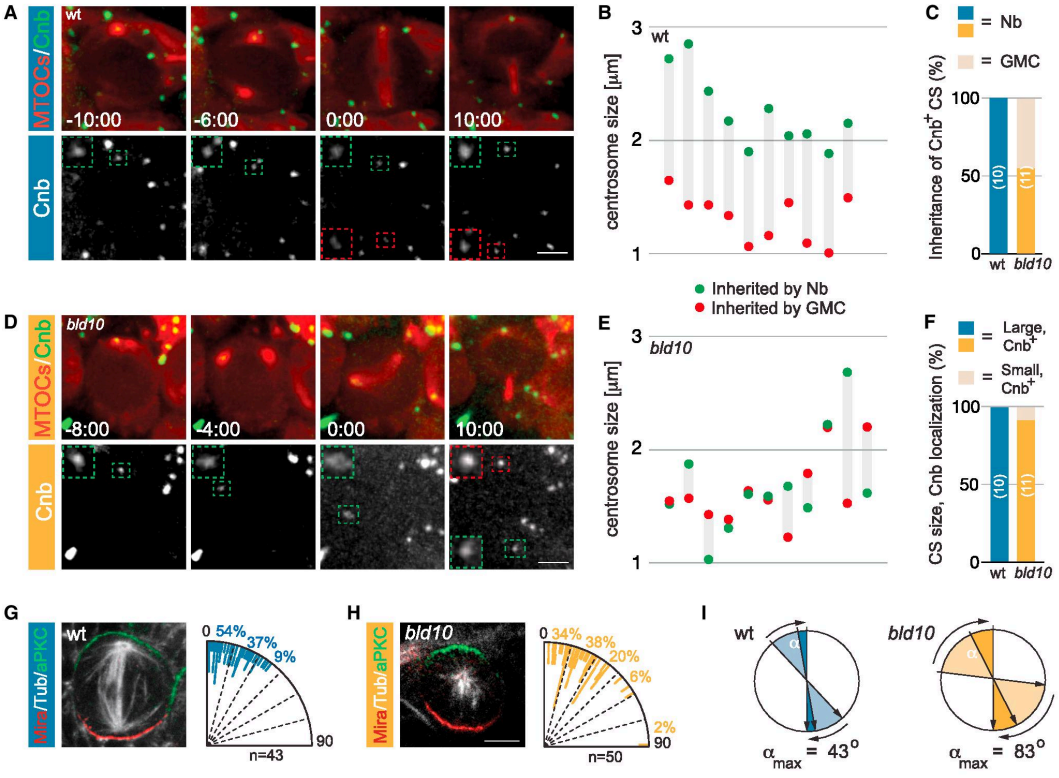


Figure 4. Centrosome Asymmetry Is Required for Correct Centrosome Segregation and Spindle Orientation

(A and D) Wild-type (A) and *bld10* mutant (D) neuroblasts expressing the daughter centriole specific marker Cnb::YFP (green) and the MTOC marker Cherry::Jupiter (red). Inserts show a high-magnification picture of the Cnb$^+$ centrioles. Note that at interphase and prophase, only the apical daughter centrosome contains a Cnb$^+$ centriole.

(B and E) Summary of wild-type (B) and *bld10* mutant (E) centrosome segregation pattern. Centrosome pairs (green and red dots, connected by gray line) of individual neuroblasts are displayed.

(C) Percentage of wild-type (blue) and *bld10* mutant (yellow) neuroblasts inheriting the Cnb$^+$ centrosome after cell division.

(F) Correlation between centrosome size and Cnb$^+$ localization.

(G and H) Representative picture of a wild-type (G) and *bld10* mutant (H) neuroblast stained with apical aPKC (green), α-tubulin (white) and basal Mira (red). Each tick mark (blue, wild-type; yellow, *bld10*) in the graph represents the orientation of the metaphase spindle with respect to the polarity axis for individual neuroblasts.

(I) Spindle correction angles are plotted for both wild-type (blue) and *bld10* (yellow). Darker shading indicates the mean correction angle (α mean). Lighter shading represents the maximal correction angle (α max). Wild-type: α max = 43°, α mean = 10° ± 8.5°; n = 26. *bld10*: α max = 83°, α-mean: 27° ± 23°; n = 22.

Nb, neuroblast; GMC, ganglion mother cell. MTOC, microtubule-organizing center. Time in min:sec; Scale bar is 5 µm.

neuroblast divisions with live imaging. Instead, our time-lapse experiments showed that *bld10* mutant centrosomes prematurely formed misaligned bipolar spindles. Spindle rotation during metaphase corrected this misalignment (Figure 4I). Apical-basal polarity is a prerequisite for correct spindle orientation (reviewed in [24]), but apical and basal polarity markers localized normally in *bld10* mutants (data not shown). Similarly, the spindle orientation regulators, Partner of Inscuteable (Pins; LGN/AGS3 in vertebrates) and the NuMA ortholog Mud, were also correctly localized (data not shown). We conclude that controlled PCM shedding and maturation is required for correct centrosome positioning but backup mechanisms exist, correcting for misaligned metaphase spindles.

Many cell types, including stem and progenitor cells, contain asymmetric centrosomes and segregate them nonrandomly, suggesting a connection between centrosome asymmetry and cell fate [25]. How centrosome asymmetry is regulated is currently not understood, but centrosome dematuration is a critical step in establishing centrosome asymmetry [4–9]. We found that the centriolar protein Bld10/Cep135, known as a centriole duplication and elongation factor [26–32], is required to establish centrosome asymmetry. On the basis of our data, we propose that Plp and Bld10 induce Polo's removal from the mother centriole, triggering the shedding of PCM proteins such as Cnn, γ-Tub, and Msps. Polo has been reported to be closely associated with centrioles [23], ideally positioned to phosphorylate both centriolar and PCM proteins [33]. Thus, we propose that Polo-mediated phosphorylation of PCM proteins maintains a stable interaction between the centriole and surrounding PCM (Figures S3D and S3E).

**Current Biology** Vol 24 No 13
1554

How Polo localization is regulated is currently not known, and we did not detect a direct molecular interaction between Bld10 and Polo (data not shown). Although we do not find centriolar markers to be mislocalized in *bld10* mutants (at the resolution level of confocal microscopy), it is possible that structural centriole defects, as detected in *bld10* mutant spermatocytes and wing disc cells [10, 31, 34], could affect PCM turnover rates. However, since Bld10 is not asymmetrically localized (data not shown), it is difficult to conceive how such defects specifically compromise the behavior of the mother but not the daughter centrosome.

Although perturbed centrosome asymmetry does not seem to undermine neuroblast polarity, the cell cycle, or physical and molecular asymmetric cell division, we cannot exclude the possibility that centrosome asymmetry could have long-term consequences currently beyond our ability to detect. Interestingly, defects in centrosome maturation or mutations in Cep135 can cause neurodevelopmental disorders such as primary microcephaly [2, 35–37]. It will be interesting to address the question whether lack of Cep135 is causing microcephaly due to compromised centrosome asymmetry and dematuration.

#### Supplemental Information

Supplemental Information includes Supplemental Experimental Procedures, three figures, and four movies and can be found with this article online at http://dx.doi.org/10.1016/j.cub.2014.05.050.

#### Author Contributions

P.S. and C.C. conceived and designed the project. P.S. performed the experiments with help from A.R.N. P.S., A.R.N., and C.C. analyzed the data. P.S. and C.C. wrote the manuscript.

#### Acknowledgments

We thank Tri Thanh Pham for custom-made MATLAB codes and Andreas Merdes, Chris Doe, and members of the C.C. and Nigg lab for helpful discussions and critical reading of the manuscript. We are grateful to Tim Megraw, Jordan Raff, Renata Basto, Juergen Knoblich, Cayetano Gonzalez, Monica Bettencourt-Dias, Tomer Avidor-Reiss, Chris Doe, Fumio Matsuzaki, and Nasser Rusan for flies and antibodies. We also thank the members of the Imaging Core Facility (IMCF) for technical support. This work was supported by the Swiss National Science Foundation (SNSF) and the Novartis Foundation for Biomedical Research. P.S. is supported by an EMBO long-term postdoctoral fellowship.

Received: February 10, 2014
Revised: May 6, 2014
Accepted: May 21, 2014
Published: June 19, 2014

#### References

1. Yamashita, Y.M., Mahowald, A.P., Perlin, J.R., and Fuller, M.T. (2007). Asymmetric inheritance of mother versus daughter centrosome in stem cell division. Science *315*, 518–521.
2. Wang, X., Tsai, J.-W., Imai, J.H., Lian, W.-N., Vallee, R.B., and Shi, S.-H. (2009). Asymmetric centrosome inheritance maintains neural progenitors in the neocortex. Nature *461*, 947–955.
3. Homem, C.C.F., and Knoblich, J.A. (2012). Drosophila neuroblasts: a model for stem cell biology. Development *139*, 4297–4310.
4. Conduit, P.T., and Raff, J.W. (2010). Cnn dynamics drive centrosome size asymmetry to ensure daughter centriole retention in Drosophila neuroblasts. Curr. Biol. *20*, 2187–2192.
5. Rebollo, E., Sampaio, P., Januschke, J., Llamazares, S., Varmark, H., and González, C. (2007). Functionally unequal centrosomes drive spindle orientation in asymmetrically dividing Drosophila neural stem cells. Dev. Cell *12*, 467–474.
6. Rusan, N.M., and Peifer, M. (2007). A role for a novel centrosome cycle in asymmetric cell division. J. Cell Biol. *177*, 13–20.
7. Januschke, J., Llamazares, S., Reina, J., and Gonzalez, C. (2011). Drosophila neuroblasts retain the daughter centrosome. Nat. Commun. *2*, 243.
8. Januschke, J., Reina, J., Llamazares, S., Bertran, T., Rossi, F., Roig, J., and Gonzalez, C. (2013). Centrobin controls mother-daughter centriole asymmetry in Drosophila neuroblasts. Nat. Cell Biol. *15*, 241–248.
9. Lerit, D.A., and Rusan, N.M. (2013). PLP inhibits the activity of interphase centrosomes to ensure their proper segregation in stem cells. J. Cell Biol. *202*, 1013–1022.
10. Mottier-Pavie, V., and Megraw, T.L. (2009). Drosophila bld10 is a centriolar protein that regulates centriole, basal body, and motile cilium assembly. Mol. Biol. Cell *20*, 2605–2614.
11. Cabernard, C., and Doe, C.Q. (2013). Live imaging of neuroblast lineages within intact larval brains in Drosophila. Cold Spring Harb. Protoc. *2013*, 970–977.
12. Blachon, S., Gopalakrishnan, J., Omori, Y., Polyanovsky, A., Church, A., Nicastro, D., Malicki, J., and Avidor-Reiss, T. (2008). Drosophila asterless and vertebrate Cep152 Are orthologs essential for centriole duplication. Genetics *180*, 2081–2094.
13. Peel, N., Stevens, N.R., Basto, R., and Raff, J.W. (2007). Overexpressing centriole-replication proteins in vivo induces centriole overduplication and de novo formation. Curr. Biol. *17*, 834–843.
14. Cabernard, C., and Doe, C.Q. (2009). Apical/basal spindle orientation is required for neuroblast homeostasis and neuronal differentiation in Drosophila. Dev. Cell *17*, 134–141.
15. Karpova, N., Bobinnec, Y., Fouix, S., Huitorel, P., and Debec, A. (2006). Jupiter, a new Drosophila protein associated with microtubules. Cell Motil. Cytoskeleton *63*, 301–312.
16. Parks, A.L., Cook, K.R., Belvin, M., Dompe, N.A., Fawcett, R., Huppert, K., Tan, L.R., Winter, C.G., Bogart, K.P., Deal, J.E., et al. (2004). Systematic generation of high-resolution deletion coverage of the Drosophila melanogaster genome. Nat. Genet. *36*, 288–292.
17. Hallen, M.A., Ho, J., Yankel, C.D., and Endow, S.A. (2008). Fluorescence recovery kinetic analysis of gamma-tubulin binding to the mitotic spindle. Biophys. J. *95*, 3048–3058.
18. Conduit, P.T., Brunk, K., Dobbelaere, J., Dix, C.I., Lucas, E.P., and Raff, J.W. (2010). Centrioles regulate centrosome size by controlling the rate of Cnn incorporation into the PCM. Curr. Biol. *20*, 2178–2186.
19. Megraw, T.L., Kilaru, S., Turner, F.R., and Kaufman, T.C. (2002). The centrosome is a dynamic structure that ejects PCM flares. J. Cell Sci. *115*, 4707–4718.
20. Gurskaya, N.G., Verkhusha, V.V., Shcheglov, A.S., Staroverov, D.B., Chepurnykh, T.V., Fradkov, A.F., Lukyanov, S., and Lukyanov, K.A. (2006). Engineering of a monomeric green-to-red photoactivatable fluorescent protein induced by blue light. Nat. Biotechnol. *24*, 461–465.
21. Venken, K.J.T., Schulze, K.L., Haelterman, N.A., Pan, H., He, Y., Evans-Holm, M., Carlson, J.W., Levis, R.W., Spradling, A.C., Hoskins, R.A., and Bellen, H.J. (2011). MiMIC: a highly versatile transposon insertion resource for engineering Drosophila melanogaster genes. Nat. Methods *8*, 737–743.
22. Buszczak, M., Paterno, S., Lighthouse, D., Bachman, J., Planck, J., Owen, S., Skora, A.D., Nystul, T.G., Ohlstein, B., Allen, A., et al. (2007). The carnegie protein trap library: a versatile tool for Drosophila developmental studies. Genetics *175*, 1505–1531.
23. Moutinho-Santos, T., Sampaio, P., Amorim, I., Costa, M., and Sunkel, C.E. (1999). In vivo localisation of the mitotic POLO kinase shows a highly dynamic association with the mitotic apparatus during early embryogenesis in Drosophila. Biol. Cell *91*, 585–596.
24. Lu, M.S., and Johnston, C.A. (2013). Molecular pathways regulating mitotic spindle orientation in animal cells. Development *140*, 1843–1856.
25. Pelletier, L., and Yamashita, Y.M. (2012). Centrosome asymmetry and inheritance during animal development. Curr. Opin. Cell Biol. *24*, 541–546.
26. Hiraki, M., Nakazawa, Y., Kamiya, R., and Hirono, M. (2007). Bld10p constitutes the cartwheel-spoke tip and stabilizes the 9-fold symmetry of the centriole. Curr. Biol. *17*, 1778–1783.
27. Matsuura, K., Lefebvre, P.A., Kamiya, R., and Hirono, M. (2004). Bld10p, a novel protein essential for basal body assembly in Chlamydomonas: localization to the cartwheel, the first ninefold symmetrical structure appearing during assembly. J. Cell Biol. *165*, 663–671.
28. Lin, Y.-C., Chang, C.-W., Hsu, W.-B., Tang, C.-J.C., Lin, Y.-N., Chou, E.-J., Wu, C.-T., and Tang, T.K. (2013). Human microcephaly protein

CEP135 binds to hSAS-6 and CPAP, and is required for centriole assembly. EMBO J. *32*, 1141–1154.

29. Dobbelaere, J., Josué, F., Suijkerbuijk, S., Baum, B., Tapon, N., and Raff, J. (2008). A genome-wide RNAi screen to dissect centriole duplication and centrosome maturation in Drosophila. PLoS Biol. *6*, e224.
30. Ohta, T., Essner, R., Ryu, J.-H., Palazzo, R.E., Uetake, Y., and Kuriyama, R. (2002). Characterization of Cep135, a novel coiled-coil centrosomal protein involved in microtubule organization in mammalian cells. J. Cell Biol. *156*, 87–99.
31. Roque, H., Wainman, A., Richens, J., Kozyrska, K., Franz, A., and Raff, J.W. (2012). Drosophila Cep135/Bld10 maintains proper centriole structure but is dispensable for cartwheel formation. J. Cell Sci. *125*, 5881–5886.
32. Kleylein-Sohn, J., Westendorf, J., Le Clech, M., Habedanck, R., Stierhof, Y.-D., and Nigg, E.A. (2007). Plk4-induced centriole biogenesis in human cells. Dev. Cell *13*, 190–202.
33. Grosstessner-Hain, K., Hegemann, B., Novatchkova, M., Rameseder, J., Joughin, B.A., Hudecz, O., Roitinger, E., Pichler, P., Kraut, N., Yaffe, M.B., et al. (2011). Quantitative phospho-proteomics to investigate the polo-like kinase 1-dependent phospho-proteome. Mol. Cell. Proteomics *10*, 008540.
34. Carvalho-Santos, Z., Machado, P., Alvarez-Martins, I., Gouveia, S.M., Jana, S.C., Duarte, P., Amado, T., Branco, P., Freitas, M.C., Silva, S.T.N., et al. (2012). BLD10/CEP135 is a microtubule-associated protein that controls the formation of the flagellum central microtubule pair. Dev. Cell *23*, 412–424.
35. Gruber, R., Zhou, Z., Sukchev, M., Joerss, T., Frappart, P.-O., and Wang, Z.-Q. (2011). MCPH1 regulates the neuroprogenitor division mode by coupling the centrosomal cycle with mitotic entry through the Chk1-Cdc25 pathway. Nat. Cell Biol. *13*, 1325–1334.
36. Hussain, M.S., Baig, S.M., Neumann, S., Nürnberg, G., Farooq, M., Ahmad, I., Alef, T., Hennies, H.C., Technau, M., Altmüller, J., et al. (2012). A truncating mutation of CEP135 causes primary microcephaly and disturbed centrosomal function. Am. J. Hum. Genet. *90*, 871–878.
37. Thornton, G.K., and Woods, C.G. (2009). Primary microcephaly: do all roads lead to Rome? Trends Genet. *25*, 501–510.

**Current Biology, Volume *24***

**Supplemental Information**

# The Centriolar Protein Bld10/Cep135 Is Required to Establish Centrosome Asymmetry in *Drosophila* Neuroblasts

**Priyanka Singh, Anjana Ramdas Nair, and Clemens Cabernard**

## Supplemental Figures

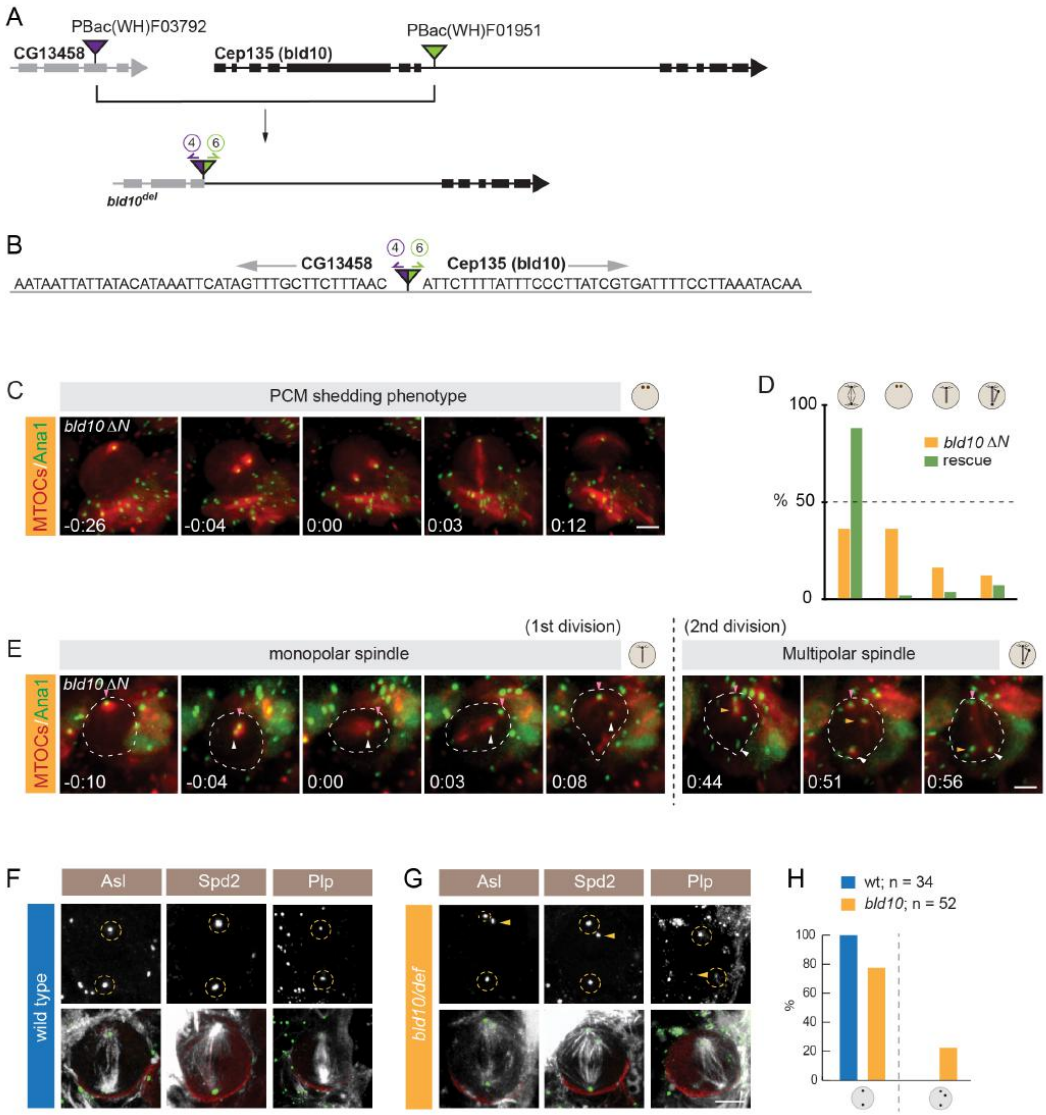


**Figure S1**

**Figure S1 (related to Figure 1): A new N-terminal *bld10* deletion allele gives rise to ectopic centrosomes.**

**(A**) Two FRT bearing PiggyBac insertions, F03792 and F01951, were used to generate a new 5`end deletion in *bld10* using site-specific recombination between the PiggyBac's FRT sites. **(B)** Sequencing with the indicated primers (4 and 6) confirmed the creation of a N-terminal Bld10 deletion (*bld10ΔN*). **(C)** Image sequence of a representative *bld10ΔN/Df* mutant neuroblast. Centrioles are labeled with Ana1::GFP and MTOCs with Cherry::Jupiter. Note that the *bld10ΔN* allele also shows the PCM shedding phenotype. **(D)** Quantification of phenotypes (orange bars; *bld10ΔN/Df.* Green bars; rescue with *bld10::GFP*). **(E)** Neuroblasts mutant for the *bld10ΔN* allele show additional mitotic spindle defects such as monopolar and tripolar spindles. Note that tripolar spindles are a consequence of monopolar spindle formation. Colored arrowheads highlight centrosomes and their origin. **(F)** Wild type neuroblasts stained with the centriolar markers Asl (green in bottom row), spindle defective-2 (Spd2; green in bottom row) or Pericentrin (PCNT)-like protein (Plp; green in bottom row) in conjunction with $\alpha$-Tub (white) and the neuroblast marker Mira (red) for wild type and **(G)** *bld10ΔN* mutant metaphase neuroblasts. Ectopic centrioles in *bld10ΔN* mutant neuroblasts are highlighted with orange arrowheads. **(H)** Quantification of centrosome number in wild type and *bld10ΔN* mutant neuroblasts from immunostainings. MTOCs; Microtubule organizing centers. MTs; microtubules. Time in h:min; Scale bar is 5 $\mu$m.

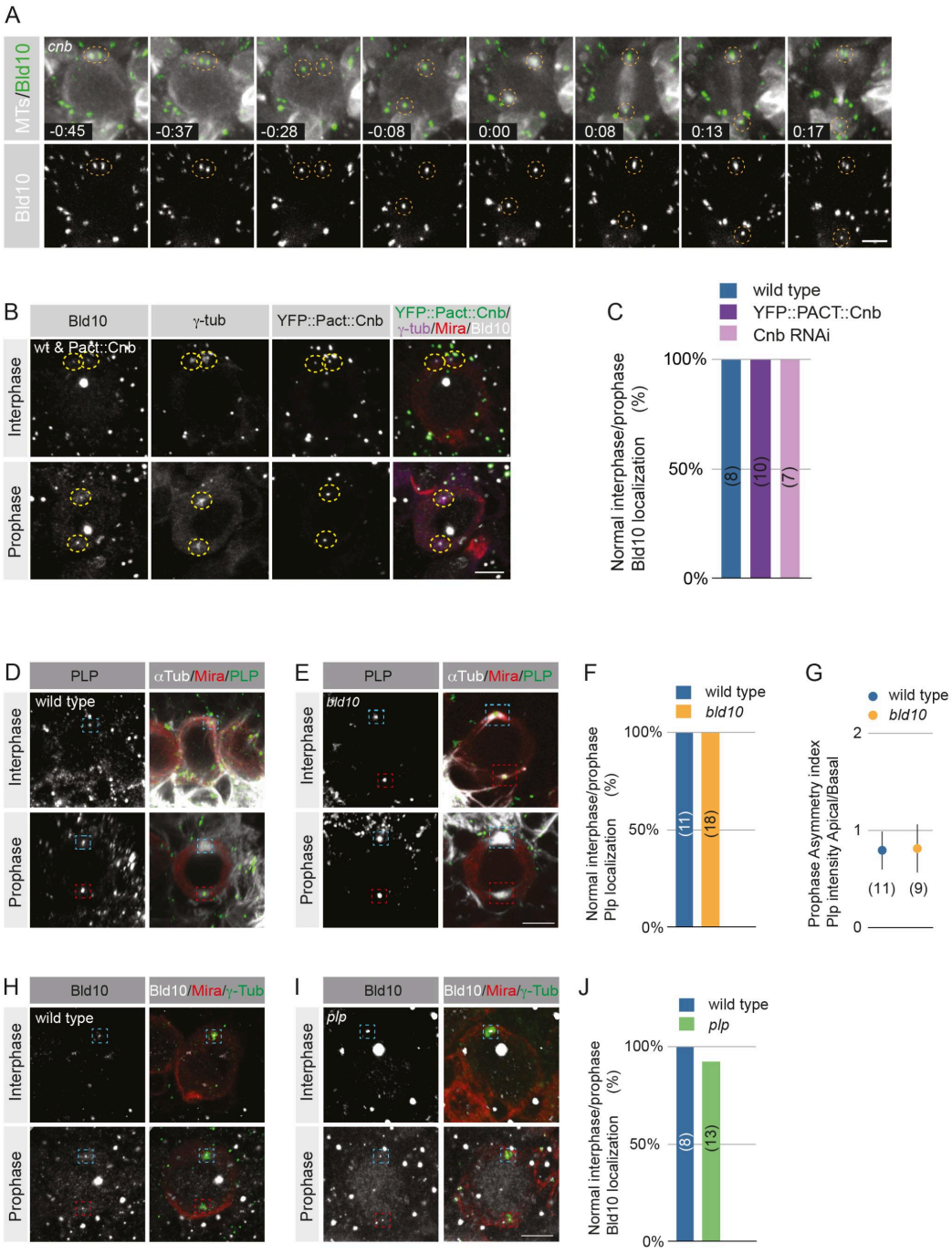
A
MT:/Bld10
Bld10
cnb
-0:45
-0:37
-0:28
-0:08
0:00
0:08
0:13
0:17
B
Bld10
γ-tub
YFP::Pact::Cnb
YFP::Pact::Cnb/
γ-tub/Mira/Bld10
wt & Pact::Cnb
Interphase
Prophase
C
wild type
YFP::PACT::Cnb
Cnb RNAi
Normal interphase/prophase
Bld10 localization (%)
100%
50%
0%
(8)
(10)
(7)
D
PLP
αTub/Mira/PLP
wild type
Interphase
Prophase
E
PLP
αTub/Mira/PLP
bld10
Interphase
Prophase
F
wild type
bld10
Normal interphase/prophase
Plp localization (%)
100%
50%
0%
(11)
(18)
G
wild type
bld10
Prophase Asymmetry index
Plp intensity Apical/Basal
2
1
0
(11)
(9)
H
Bld10
Bld10/Mira/γ-Tub
wild type
Interphase
Prophase
I
Bld10
Bld10/Mira/γ-Tub
plp
Interphase
Prophase
J
wild type
plp
Normal interphase/prophase
Bld10 localization (%)
100%
50%
0%
(8)
(13)

**Figure S2**

**Figure S2 (Related to Figure 3)**: **Bld10, Plp and Cnb localize independently of each other.**

**(A**) Image sequence of a third instar larval neuroblast expressing RNAi against Centrobin (Cnb RNAi) in conjunction with Bld10::GFP (green) and Cherry::Jupiter (white). Yellow circles highlight apical and basal centrioles. Bld10 localization is unperturbed but MTOC activity is lost on both centrosomes during interphase. **(B)** Immuno-staining of a third instar larval neuroblast expressing YFP::PACT::Cnb, localizing Cnb to both the mother and daughter centriole. Neuroblasts are co-stained with Bld10 (white in merge), γ-Tub (magenta in merge) and Mira (red in merge). This neuroblast shows symmetric centrosomes with equal amounts of γ-Tub on both centrioles. Bld10 localization is unperturbed. **(C)** Quantification of Bld10 localization in Cnb experiments. **(D)** wild type and **(E)** *bld10* mutant neuroblasts, stained for Plp (white in single channel; green in merge), α-Tub (white in merge) and Mira (red in merge). A representative interphase (top row) and prophase (bottom row) neuroblast is shown. In all panels, the blue and red dashed boxes label the apical daughter and the basal mother centrosome, respectively. **(F)** Quantification of Plp localization. **(G)** Asymmetry index based on Plp intensity for wild type and *bld10* mutant neuroblasts. Mean and standard deviation of the mean (SD) is shown. **(H)** Wild type and **(I)** *plp* mutant neuroblasts stained for Bld10 (white in single channel and merge), γ-Tub (green in merge) and Mira (red in merge). **(J)** Quantifications of Bld10 localization in *plp* mutant neuroblasts. The number on the bar graphs refers to the number of scored neuroblasts (n's). Time is in h:min. Scale bar is 5 µm

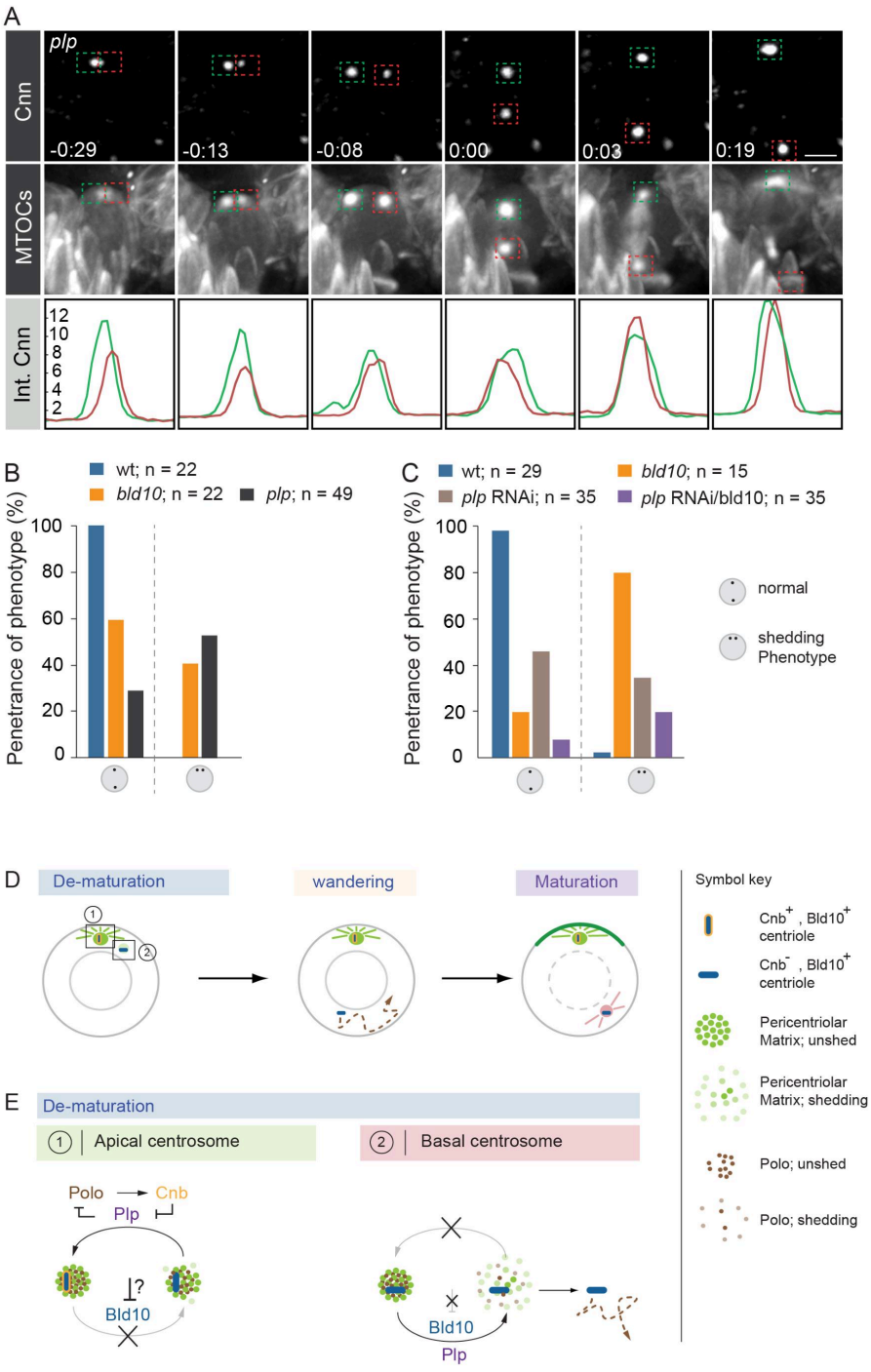
A
plp
Cnn
MTOCs
Int. Cnn
-0:29
-0:13
-0:08
0:00
0:03
0:19
12
10
8
6
4
2
B
wt; n = 22
bld10; n = 22
plp; n = 49
Penetrance of phenotype (%)
100
80
60
40
20
0
C
wt; n = 29
bld10; n = 15
plp RNAi; n = 35
plp RNAi/bld10; n = 35
normal
shedding Phenotype
D
De-maturation
wandering
Maturation
Symbol key
Cnb+ , Bld10+ centriole
Cnb- , Bld10+ centriole
Pericentriolar Matrix; unshed
Pericentriolar Matrix; shedding
Polo; unshed
Polo; shedding
E
De-maturation
1 Apical centrosome
2 Basal centrosome
Polo
Cnb
Plp
Bld10
Bld10
Plp

**Figure S3**

**Figure S3 (Related to Figure 3)**: **Plp is required to shed the PCM marker Cnn**

**(A)** *plp* mutant neuroblast, expressing Cnn::GFP and Cherry::Jupiter (MTOCs). Cnn intensity for the apical (green dashed box) and basal centrosome (red dashed box) shown below. **(B)** Quantification of *plp's* (*plp*$^{2172}$*/Df(3L)BSC441*) Cnn shedding phenotype of experiment shown in (A). **(C)** Quantification of *plp* RNAi knockdown, performed in wild type and *bld10* mutant background. Centrosome asymmetry phenotype of wild type and *bld10* mutant neuroblasts are shown as a comparison. Note that for these experiments, neuroblasts express mCherry::Jupiter only (no image sequence shown). Bar graph representing only the quantification of the PCM shedding/centrosome asymmetry phenotype. MTOC; microtubule organizing center. **(D)** Model. Centrosome asymmetry is controlled by a dynamic maturation and de-maturation cycle. The neuroblast centrosome cycle consists of three distinct phases: (1) "De-maturation phase": shortly after centriole separation, the mother centriole downregulates PCM through PCM shedding. The apical daughter centriole, however, retains PCM and remains anchored on the apical cortex. (2) "Wandering phase": The basal mother centriole wanders through the cytoplasm before prophase due to the lack of PCM and an active MTOC. (3) "Maturation phase": the basal mother centriole reaccumulates PCM from prophase onwards and matures into a MTOC. **(E)** The distinct behavior of the mother and daughter centriole is controlled by Polo, Cnb, Plp and Bld10. Based on our findings here and recent reports, we propose that on the apical, Cnb$^{+}$ daughter centriole, Polo controls the retention of PCM through phosphorylation of Cnb [S3]. Plp localization and potentially its activity is kept low through Cnb [S21]. Bld10 is localized to both centrioles, but might be inhibited apically to keep shedding at a minimum. On the basal mother centriole, Bld10 promotes shedding of Polo, possibly together with Plp. Downregulation of Polo causes the shedding of PCM proteins.

Int.; intensity. a.u; arbitrary units. Time is in h:min. Scale bar is 5 µm (overview).

**Supplemental Experimental Procedures**

**Fly strains and genetics**

All mutant chromosomes were balanced over *CyO actin::GFP* or *TM6B, Tb*. The following alleles and deficiency stocks were used: *bld10$^{c04199}$* [S1]*, Df(3L)Brd15,* (a deficiency removing the entire *bld10* locus and adjacent genes) [S1], *plp$^{2172}$* [S2], *Df(3L)BSC441*, (a deficiency removing the *plp* locus) (Bloomington stock center), *plp* RNAi (v101296*;* VDRC), cnbRNAi (v28651; VDRC). Until otherwise noted, mutants were crossed over the corresponding deficiency and analyzed in a heteroallelic combination. Transgenes and fluorescent markers: *pUASp–YFP::PACT* [S3], *pUbq-DSas4::GFP* [S4], *pUbq-DSas6::GFP* [S5], *pUbq-Cnb::YFP* [S6], *worGal4, pUAST-cherry::Jupiter* [S7], *ncd-γ-Tub::EGFP* [S8], *pUbq-Msps::GFP* [S9], *pUASp-cnn::EGFP* [S10] , *pUASp-Ana1::GFP* [S11], *polo::GFP* expressing Polo under the endogenous promoter [S12], *polo::GFP$^{CC01326}$* (protein trap line [S13]), *bld10::GFP* expressing Bld10 under the endogenous promoter [S14]. *ncd-γ-Tub::EGFP* and *pUbq-Msps::GFP* were recombined onto *bld10$^{c04199}$* using standard genetic procedures. UAS transgenes were expressed using *worGal4* [S15]. Generation of *bld10ΔN* allele: the piggyBac insertion line *PBac{WH}-CG1695(f01951)* and *PBac{WH}-CG13458(f03792)* were crossed to *hsFlp* (Bloomington Stock Center) and the resulting progeny was heat shocked at 37°C to induce Flipase activity according to previously published protocols [S16]. Generation of *cnn::mDendra2* line: the *Mi{MIC}-cnn(MI08383)* line was crossed to phiC31 integrase (expressed under the vasa promotor; Bloomington stock center) and progeny was injected with the mDendra2 exchange cassette [S17]. Positive lines were initially screened for loss of yellow body marker and the orientation of the insert was checked by PCR.

### *plp* knockdown in *bld10* mutants

Due to the proximity of the *bld10* and *plp* locus, it is not possible to recombine the two mutant alleles together. Thus, we expressed RNAi against *plp* (v101296*;* VDRC) with the worGal4 driver line to knockdown *plp* in a wild type or *bld10* mutant background. $plp^{2172}$ mutants and *plp* RNAi both show centrosome asymmetry defects with comparable penetrance.

### Antibodies

The following primary antibodies were used: rabbit anti-aPKC (1:1000; Santa Cruz Biotechnology), mouse anti-γ-tub (Sigma; 1:500), rat anti-α-Tub (Serotec; 1:1000), mouse anti-α-Tub (DM1A, Sigma; 1:2500), guinea-pig anti-Bazooka (1:1000), rat anti-Pins (1:400) [S18], mouse anti-Pros (1:1000), rat and guinea-pig anti-Mira (1:500) (gifts from Chris Doe), rabbit anti-Numb (1:100; gift from J. Knoblich), rabbit anti-Asl (1:500), rabbit anti-Spd2 (1:500), rabbit anti-Plp (1:1000), rabbit anti-Sas4 (1:250), rabbit anti-Cnn (1:1000) (gifts from J. Raff), rabbit anti-Mud (1:200; gift from Fumio Matsuzaki) [S19] and rabbit anti-Bld10 (1:200; gift from Tim Megraw) [S1]. Secondary antibodies were from Molecular Probes and the Jackson Immuno laboratory.

### Statistics and sample number

Statistical significance was calculated using the unpaired samples *t*-test. For each experiment, the data was collected from at least 3 independent brain lobes. Depending on live imaging marker expression, *bld10's* centrosome asymmetry phenotype varies in strength. In all live imaging experiments combined, we see the PCM shedding phenotype in ~50% (n = 201) of *bld10* mutant neuroblasts (wt: 5%; n=166).

**Immunostaining**

96h AEL larval brains were dissected in 1X PBS (pH 7.4) solution and fixed for 20 min in 4% paraformaldehyde in PEM (100mM PIPES pH 6.9, 1mM EGTA and 1mM $MgSO_4$). After fixing, the brains were washed with PBSBT (1X PBS, 0.1% Triton-X-100 and 1% BSA) and then blocked with 1X PBSBT for 1h. Primary antibody dilution was prepared in 1X PBSBT and brains were incubated overnight at 4 °C. Brains were washed with 1X PBSBT six times for 10 min each and then incubated with secondary antibodies diluted in 1X PBSBT at 4 °C, overnight. The next day, brains were washed with 1X PBST (1x PBS, 0.1% Triton-X-100) six times for 10 minutes each and kept in Vectashield (Vector laboratories) mounting media at 4 °C.

**Live imaging sample preparation**

5ml Schneider's insect medium (Sigma-Aldrich S0146) was mixed with 5 µL of 0.5 M ascorbic acid (Sigma-Aldrich A4034) and 50µL of HyClone bovine growth serum (Thermo Scientific SH3054102) immediately before use and warmed up to room temperature. This imaging medium was supplemented with fat bodies of ~ 10 *yw* third instar larvae. 96h (AEL; after egg laying) old mutant or wild type larval brains were dissected in imaging medium. The dissected brains, along with fat bodies, were transferred onto a gas-permeable membrane (YSI Life Sciences 5793) fitted on a metallic slide. Brains were oriented with the brain lobes facing the coverslip. Excess media was removed until the brain lobes were in contact with the coverslip. The sample was sealed with Vaseline [S20].

**Imaging**

Fixed samples were imaged using an inverted Leica TSC SPE confocal microscope. For representative images a 60X/1.40NA oil immersion objective was used. For 4X scans a z-step

size of 0.3 µm and for 1X scans a z-step size of 1.0 µm was used. Live samples were imaged with an Andor revolution spinning disc confocal system, consisting of a Yokogawa CSU-X1 spinning disk unit and two Andor iXon3 DU-897-BV EMCCD cameras. A 60X/1.4NA oil immersion objective mounted on a Nikon Eclipse Ti microscope was used for most images. Live imaging voxels sizes are 0.22 X 0.22 X 0.5µm (60x/1.4NA spinning disc).

**Photoactivation**

96h AEL larval brains expressing both *Sas4::GFP* and *cnn::mDendra2* were used. Photoconversion experiments were performed on an Andor Revolution spinning disc system containing the FRAPPA unit. Several regions of interests (ROIs) were manually chosen in the GFP channel. Cytoplasmic signal from Sas4::GFP allowed for unambiguous identification of neuroblasts. Centrioles were irradiated before splitting (late metaphase, late telophase or interphase). Before photoconversion, single Z planes containing ROIs were scanned for 10 time points with maximum speed. Subsequently, ROIs were irradiated with the 405nm laser line (~9.5%; 20 repeats; 50µs dwell time). After photoconversion, the entire neuroblast was scanned with a z-step size of 0.5 µm. Photoconverted Cnn-mDendra2 emits red fluorescence, which was detected simultaneously with Sas4::GFP emission. GFP and mDendra2 emission were merged in Andor IQ2 and converted into Imaris files using a custom-made Matlab code.

**Definition of apical and basal centrosome**

In the absence of a mother/daughter specific centriole marker (e.g. Cnb), the following nomenclature was chosen: throughout the manuscript, we refer to the centrosome segregating with the neuroblast after cytokinesis and/or localizing on the apical side as the

apical centrosome. The centrosome segregating into the GMC or residing on the basal side is referred to as the basal centrosome, respectively.

**Image processing and calculations**

Images were processed using Imaris x64 7.5.2 and Fiji. Andor IQ2 files were converted into Imaris files using a custom-made Matlab code. Radial centrosome distribution plots were generated by plotting the maximal angle between apical and/or basal MTOCs and the neuroblast polarity/division axis. To do this, we tracked centrosome positions at each time point using the spot tool in Imaris to obtain MTOC coordinates. A reference vector ("0" degree line), corresponding to the polarity/division axis was calculated, using the metaphase spindle. The position of the cell center was determined and maximum angles for the apical and basal centrosome were calculated in relation to the future division axis. Centrosome diameters were measured in Imaris using maximum intensity projections. For each centrosome and time point, the diameter was measured three times and averaged. Asymmetry indices and centrosome ratios were calculated by dividing the bigger centrosome by the smaller centrosome. To determine centrosome net growth, we calculated the difference between the largest or smallest centrosome in relation to the centrosome right after splitting. Spindle orientation in fixed samples was measured by determining the coordinates of the center of maximum intensity of apical and basal crescents, respectively. These coordinates were used to calculate a polarity axis vector. Spindle axis vectors were calculated using similar methods. Custom-made Matlab codes were used to calculate the angle between polarity and spindle vectors in 3D. The spindle orientation correction factor was determined from live imaging experiments by calculating the angle between two spindle vectors: (1) a spindle vector at the beginning of metaphase and (2) the spindle vector at the end of metaphase, respectively. Intensity measurements of centrosomes and MTs were performed in Fiji. Maximum intensity

projections were generated and a line was used to measure the intensity at the centriole position. Using a Macro, this line was duplicated onto the channel to be measured. Pictures were cropped in Adobe Photoshop CS6 and assembled in Adobe Illustrator CS6. Quantifications and graphical representations were generated in Microsoft Excel or Numbers.

**Supplemental references**


S1. Mottier-Pavie, V., and Megraw, T. L. (2009). Drosophila bld10 is a centriolar protein that regulates centriole, basal body, and motile cilium assembly. Mol. Biol. Cell *20*, 2605–2614.

S2. Lerit, D. A., and Rusan, N. M. (2013). PLP inhibits the activity of interphase centrosomes to ensure their proper segregation in stem cells. J. Cell Biol. *202*, 1013–1022.

S3. Januschke, J., Reina, J., Llamazares, S., Bertran, T., Rossi, F., Roig, J., and Gonzalez, C. (2013). Centrobin controls mother–daughter centriole asymmetry in Drosophila neuroblasts. Nat. Cell Biol. *15*, 241–248.

S4. Peel, N., Stevens, N. R., Basto, R., and Raff, J. W. (2007). Overexpressing centriole-replication proteins in vivo induces centriole overduplication and de novo formation. Curr. Biol. *17*, 834–843.

S5. Blachon, S., Cai, X., Roberts, K. A., Yang, K., Polyanovsky, A., Church, A., and Avidor-Reiss, T. (2009). A Proximal Centriole-Like Structure Is Present in Drosophila Spermatids and Can Serve as a Model to Study Centriole Duplication. Genetics *182*, 133–144.

S6. Januschke, J., Llamazares, S., Reina, J., and Gonzalez, C. (2011). Drosophila neuroblasts retain the daughter centrosome. Nat Commun *2*, 243.

S7. Cabernard, C., and Doe, C. Q. (2009). Apical/basal spindle orientation is required for neuroblast homeostasis and neuronal differentiation in Drosophila. Dev. Cell *17*, 134–141.

S8. Hallen, M. A., Ho, J., Yankel, C. D., and Endow, S. A. (2008). Fluorescence recovery kinetic analysis of gamma-tubulin binding to the mitotic spindle. Biophys. J. *95*, 3048–3058.

S9. Conduit, P. T., Brunk, K., Dobbelaere, J., Dix, C. I., Lucas, E. P., and Raff, J. W. (2010). Centrioles Regulate Centrosome Size by Controlling the Rate of Cnn Incorporation into the PCM. Current Biology *20*, 2178–2186.

S10. Megraw, T. L., Kilaru, S., Turner, F. R., and Kaufman, T. C. (2002). The centrosome is a dynamic structure that ejects PCM flares. Journal of cell science *115*, 4707–4718.

S11. Stevens, N. R., Dobbelaere, J., Brunk, K., Franz, A., and Raff, J. W. (2010). Drosophila Ana2 is a conserved centriole duplication factor. J. Cell Biol. *188*, 313–323.

S12. Moutinho Santos, T., Sampaio, P., Amorim, I., Costa, M., and Sunkel, C. E. (1999). In vivo localisation of the mitotic POLO kinase shows a highly dynamic association with the mitotic apparatus during early embryogenesis in Drosophila. Biology of the Cell *91*, 585–596.

S13. Buszczak, M., Paterno, S., Lighthouse, D., Bachman, J., Planck, J., Owen, S., Skora, A. D., Nystul, T. G., Ohlstein, B., Allen, A., et al. (2007). The carnegie protein trap library: a versatile tool for Drosophila developmental studies. Genetics *175*, 1505–1531.

S14. Blachon, S., Gopalakrishnan, J., Omori, Y., Polyanovsky, A., Church, A., Nicastro, D., Malicki, J., and Avidor-Reiss, T. (2008). Drosophila asterless and vertebrate Cep152 Are orthologs essential for centriole duplication. Genetics *180*, 2081–2094.

S15. Albertson, R., and Doe, C. Q. (2003). Dlg, Scrib and Lgl regulate neuroblast cell size and mitotic

spindle asymmetry. Nat. Cell Biol. *5*, 166–170.

S16. Parks, A. L., Cook, K. R., Belvin, M., Dompe, N. A., Fawcett, R., Huppert, K., Tan, L. R., Winter, C. G., Bogart, K. P., Deal, J. E., et al. (2004). Systematic generation of high-resolution deletion coverage of the Drosophila melanogaster genome. Nat Genet *36*, 288–292.

S17. Venken, K. J. T., Schulze, K. L., Haelterman, N. A., Pan, H., He, Y., Evans-Holm, M., Carlson, J. W., Levis, R. W., Spradling, A. C., Hoskins, R. A., et al. (2011). MiMIC: a highly versatile transposon insertion resource for engineering Drosophila melanogaster genes. Nat. Methods *8*, 737–743.

S18. Siller, K. H., and Doe, C. Q. (2009). Spindle orientation during asymmetric cell division. Nat. Cell Biol. *11*, 365–374.

S19. Izumi, Y., Ohta, N., Hisata, K., Raabe, T., and Matsuzaki, F. (2006). Drosophila Pins-binding protein Mud regulates spindle-polarity coupling and centrosome organization. Nat. Cell Biol. *8*, 586–593.

S20. Cabernard, C., and Doe, C. Q. (2013). Live Imaging of Neuroblast Lineages within Intact Larval Brains in Drosophila. Cold Spring Harbor Protocols *2013*, 970–977.

S21. Lerit, D. A., and Rusan, N. M. (2013). PLP inhibits the activity of interphase centrosomes to ensure their proper segregation in stem cells. J. Cell Biol. *202*, 1013–1022.

# Manuscript II

## 4.2 The microcephaly protein Wdr62/CG7337 is required to maintain centrosome asymmetry in *Drosophila* neuroblasts

Anjana Ramdas Nair[1], Priyanka Singh[1,3], David Salvador Garcia[1, #], David Rodriguez Crespo[2, #], Boris Egger[2] and Clemens Cabernard[1]

[1] Biozentrum, University of Basel
Klingelbergstrasse 50-70
CH-4056 Basel, Switzerland

[2] Department of Biology, University of Fribourg
Chemin du Musée 10
CH-1700 Fribourg, Switzerland

[3] Present address:
Max-Planck Institute of Molecular Physiology
Department of Mechanistic Cell Biology
Otto-Hahn-Str. 11
D-44227 Dortmund, Germany

[#] equal author contribution

Published in Cell Reports 14, 1100–1113, February 9, 2016
Submitted on: October 15, 2015
Accepted: December 21, 2015

Article

Cell Reports

# The Microcephaly-Associated Protein Wdr62/CG7337 Is Required to Maintain Centrosome Asymmetry in *Drosophila* Neuroblasts

## Graphical Abstract

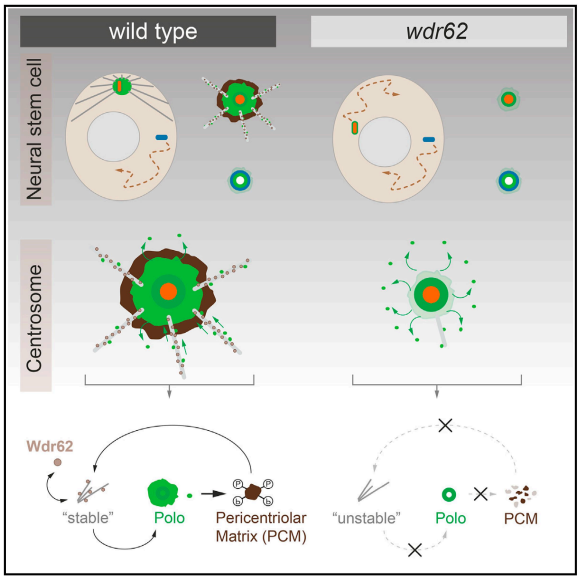


## Authors

Anjana Ramdas Nair, Priyanka Singh, David Salvador Garcia, David Rodriguez-Crespo, Boris Egger, Clemens Cabernard

## Correspondence

clemens.cabernard@unibas.ch

## In Brief

The molecular mechanisms underlying centrosome asymmetry and its function are unclear. Ramdas Nair et al. report that CG7337/Wdr62, previously implicated in the neurodevelopmental disorder microcephaly, maintains centrosome asymmetry in *Drosophila* neural stem cells by stabilizing interphase microtubules. Independently of this function, Wdr62 also regulates cell-cycle progression.

## Highlights

- CG7337/Wdr62 maintains centrosome asymmetry in *Drosophila* neural stem cells
- Wdr62 stabilizes interphase microtubules
- Interphase microtubules recruit the mitotic kinase Polo/Plk1 to the centrosome
- Centrosome asymmetry controls spindle orientation and centrosome segregation

Ramdas Nair et al., 2016, Cell Reports *14*, 1100–1113
February 9, 2016 
http://dx.doi.org/10.1016/j.celrep.2015.12.097

OPEN ACCESS
CellPress

Cell Reports
Article

# The Microcephaly-Associated Protein Wdr62/CG7337 Is Required to Maintain Centrosome Asymmetry in *Drosophila* Neuroblasts

Anjana Ramdas Nair,[1] Priyanka Singh,[1,3] David Salvador Garcia,[1] David Rodriguez-Crespo,[2] Boris Egger,[2] and Clemens Cabernard[1,*]
[1]Biozentrum, University of Basel, Klingelbergstrasse 50-70, 4056 Basel, Switzerland
[2]Department of Biology, University of Fribourg, Chemin du Musée 10, 1700 Fribourg, Switzerland
[3]Present address: Department of Mechanistic Cell Biology, Max-Planck Institute of Molecular Physiology, Otto-Hahn-Strasse 11, 44227 Dortmund, Germany
*Correspondence: clemens.cabernard@unibas.ch
http://dx.doi.org/10.1016/j.celrep.2015.12.097


## SUMMARY

**Centrosome asymmetry has been implicated in stem cell fate maintenance in both flies and vertebrates, but the underlying molecular mechanisms are incompletely understood. Here, we report that loss of CG7337, the fly ortholog of WDR62, compromises interphase centrosome asymmetry in fly neural stem cells (neuroblasts). Wdr62 maintains an active interphase microtubule-organizing center (MTOC) by stabilizing microtubules (MTs), which are necessary for sustained recruitment of Polo/Plk1 to the pericentriolar matrix (PCM) and downregulation of Pericentrin-like protein (Plp). The loss of an active MTOC in *wdr62* mutants compromises centrosome positioning, spindle orientation, and biased centrosome segregation. *wdr62* mutant flies also have an ~40% reduction in brain size as a result of cell-cycle delays. We propose that CG7337/Wdr62, a microtubule-associated protein, is required for the maintenance of interphase microtubules, thereby regulating centrosomal Polo and Plp levels. Independent of this function, Wdr62 is also required for the timely mitotic entry of neural stem cells.**

## INTRODUCTION

Centrosomes, microtubule (MT)-organizing centers (MTOCs) of metazoan cells, segregate asymmetrically in both fly and vertebrate neural stem cells and have been implicated in stem cell fate maintenance (Yamashita et al., 2007; Conduit and Raff, 2010; Januschke et al., 2011; Wang et al., 2009; Salzmann et al., 2014). The building blocks of centrosomes are centrioles, cylindrical MT-based structures ensheathed by pericentriolar matrix (PCM) proteins (Nigg and Stearns, 2011). Centrosomes are intrinsically asymmetric since centrioles replicate semi-conservatively, generating an older mother centriole and a younger daughter centriole. Centrosome asymmetry is also manifested in the localization of daughter or mother centriole-specific centrosome markers and differential MTOC activity (Januschke et al., 2011, 2013; Rusan and Peifer, 2007; Rebollo et al., 2007; Conduit and Raff, 2010; Jakobsen et al., 2011). However, the molecular mechanisms underlying centrosome asymmetry and its function are incompletely understood (reviewed in Roubinet and Cabernard, 2014).

An ideal system for studying centrosome asymmetry in vivo are *Drosophila* neuroblasts, the neural stem cells of the fly (Homem and Knoblich, 2012; Brand and Livesey, 2011). Neuroblasts establish and maintain centrosome asymmetry during interphase (Januschke et al., 2011, 2013; Conduit and Raff, 2010; Singh et al., 2014; Lerit and Rusan, 2013; Rusan and Peifer, 2007). For instance, their centrosomes separate during early interphase into two centrosomes, containing only one centriole each. These centrioles differ in age and molecular composition; the homolog of the human daughter centriole-specific protein Centrobin (Cnb) localizes to the younger daughter centriole but is absent from the older mother centriole (Januschke et al., 2011). Cnb is phosphorylated by Polo kinase (Plk1 in vertebrates), a requirement to maintain an active MTOC, tethering the daughter centriole-containing centrosome to the apical interphase cortex (Januschke et al., 2013). The mother centriole downregulates Polo and MTOC activity, mediated by Pericentrin (PCNT)-like protein (PLP) and Bld10 (Cep135 in vertebrates) (Singh et al., 2014; Lerit and Rusan, 2013). As a consequence of MTOC downregulation, the mother centriole subsequently moves away from the apical cortex and randomly migrates through the cytoplasm (Rebollo et al., 2007; Rusan and Peifer, 2007; Conduit and Raff, 2010). This centrosome asymmetry is maintained until early prophase, when centrosome maturation starts with the reaccumulation of PCM and the formation of a second MTOC on the basal cortex (Conduit and Raff, 2010; Rebollo et al., 2007; Rusan and Peifer, 2007).

Previously, we showed that Bld10/Cep135 is implicated in the establishment of centrosome asymmetry in *Drosophila* neuroblasts (Singh et al., 2014). Mutations in Cep135 have been linked to primary microcephaly (Hussain et al., 2012), an autosomal recessive neurodevelopmental disorder, manifested in small brains and mental retardation (Nigg et al., 2014). Several loci

(MCPH1–12) have been implicated in primary microcephaly, most of which encode for centrosomal proteins (Nigg et al., 2014). To test whether a causal relationship between centrosome asymmetry and microcephaly exists, we set out to study CG7337, an uncharacterized fly gene corresponding to WD40 repeat protein 62 (WDR62/MCPH2) in vertebrates (Nicholas et al., 2010; Megraw et al., 2011). Mutations in *wdr62* are the second most prevalent cause for microcephaly, but its role in this neurodevelopmental disorder is incompletely understood. WDR62 localizes to the nucleus (Bilgüvar et al., 2010) but also to the spindle poles (Nicholas et al., 2010; Yu et al., 2010; Chen et al., 2014), and it has been implicated in spindle formation and neuronal progenitor cell (NPC) proliferation (Nicholas et al., 2010; Bilgüvar et al., 2010; Yu et al., 2010). WDR62 is a c-Jun N-terminal kinase (JNK) scaffold protein (Wasserman et al., 2010; Cohen-Katsenelson et al., 2011), reported to regulate rat neurogenesis through JNK1 by controlling symmetric and asymmetric NPC divisions in the rat neocortex (Xu et al., 2014). In mice, WDR62 interacts with Aurora A kinase, necessary to regulate spindle formation, mitotic progression, and brain size (Chen et al., 2014). However, whether WDR62 is implicated in other important cellular processes is currently unclear.

Here, we report that CG7337/Wdr62 is required to maintain centrosome asymmetry in *Drosophila* neuroblasts by directly or indirectly stabilizing the interphase MTs necessary to accumulate and maintain PCM-associated Polo. Failure to maintain centrosome asymmetry in *wdr62* mutants perturbs centrosome positioning and segregation as well as spindle orientation. Additionally, and independent of this function, we found that *wdr62* mutant neuroblasts show cell-cycle defects, resulting in a developmental delay and a dramatic reduction in fly brains. We conclude that Wdr62 controls at least two distinct but important aspects of fly neurogenesis.

## RESULTS

### CG7337, the Fly Ortholog of Wdr62, Is Required to Maintain Centrosome Asymmetry during Interphase

The fly ortholog of Wdr62 is encoded by the uncharacterized gene CG7337 (Megraw et al., 2011; Nicholas et al., 2010), containing several isoforms (Figure S1A), with the longest producing a protein of predicted 2,397 amino acids. Human WDR62 shares, overall, 35% amino acid identity with this CG7337 isoform, and the N terminus alone is 48% identical. Both CG7337 and WDR62 contain three WD40-repeat-containing domains with equal numbers of WD40 repeats (Figure 1A). Due to this conservation and the similarity in domain architecture, we refer to CG7337 as Wdr62 hereinafter.

To assess the function of Wdr62 in the neuroblast centrosome cycle, we generated molecularly defined excision alleles and CRISPR/Cas9 deletions (Experimental Procedures; Figure S1A). The phenotype described in the following sections has been obtained with both the $wdr62^{\Delta 2a}$ and $wdr62^{\Delta 3-9}$ alleles ($wdr62^{\Delta 2a}$/*Df(2L)Exel8005* and $wdr62^{\Delta 3-9}$/*Df(2L)Exel8005*, respectively); both alleles show an identical phenotype, although the phenotypic penetrance is higher with the $wdr62^{\Delta 3-9}$ allele (Figures S1A–S1C). Therefore, unless otherwise noted, we collectively refer hereinafter to either allelic combination as *wdr62* mutant (see figure legends for details on allelic combinations used).

We performed live cell imaging experiments, using DSas4::GFP (Peel et al., 2007) as a centriolar marker in conjunction with the MTOC marker Cherry::Jupiter (Cabernard and Doe, 2009) (Jupiter encodes an MT-binding protein; Karpova et al., 2006). As previously reported (Januschke et al., 2011, 2013; Conduit and Raff, 2010; Singh et al., 2014; Lerit and Rusan, 2013; Rusan and Peifer, 2007), we confirmed that the apical daughter centriole-containing centrosome retained a robust MTOC throughout interphase. The basal mother centriole-containing centrosome, on the other hand, downregulated MTOC activity, preventing the inactive centriole from staying stably anchored at the apical cortex (Figure 1B; Movie S1). *wdr62* mutant centrosomes showed normal DSas4 localization and initially also contained an apical active MTOC. As in wild-type, MTOC activity is normally downregulated on the separating centriole. However, in contrast to wild-type, *wdr62* mutants downregulated MTOC activity on the apical centrosome, on average, within ~30 min, giving rise to two "naked" centrioles, devoid of MTs (Figures 1C, 1F, and 1G; Movie S2). As in wild-type, *wdr62* mutant neuroblasts initiated centrosome maturation in prophase, assembled bipolar spindles, and divided asymmetrically. Nevertheless, they displayed weaker MT intensity on maturing centrosomes and metaphase spindles (Figure 1G). The centrosome asymmetry phenotype of *wdr62* could be rescued by expressing the longest CG7337 isoform with the neuroblast-specific *worniuGal4* (*worGal4*; Albertson and Doe, 2003) driver line, suggesting that this phenotype is neuroblast intrinsic and due to loss of *wdr62* specifically (Figure S1B).

The *wdr62* mutant phenotype is very similar to both *partner of inscuteable* (*pins*; LGN/AGS3 in vertebrates) and *cnb* mutants (Rebollo et al., 2007; Januschke et al., 2013). Cnb and Pins localization was not compromised in *wdr62* mutants. However, the centrosome asymmetry phenotype of neither *pins* nor *cnb* could be rescued with our functional *wdr62* transgene (data not shown). Taken together, these results demonstrate that apical centrosomes devoid of Wdr62 behave like basal wild-type centrosomes and that Wdr62 is required to maintain centrosome asymmetry during interphase.

### Wdr62 Is Required to Maintain PCM Proteins on the Apical Interphase Centrosome

Wild-type neuroblasts downregulate basal MTOC activity by shedding PCM proteins such as γ-tubulin (γ-Tub) and centrosomin (Cnn; Cdk5rap2 in vertebrates) (Singh et al., 2014; Conduit and Raff, 2010). We imaged *wdr62* mutant neuroblasts expressing γ-Tub or Cnn in conjunction with the MTOC marker Cherry::Jupiter to test whether the loss of apical MTOC activity is due to PCM protein downregulation. Wild-type neuroblasts retained γ-Tub and Cnn on the apical centrosome throughout interphase (Figure 1D; Movie S3) but *wdr62* mutant neuroblasts lost γ-Tub and Cnn significantly from the apical, daughter centriole-containing centrosome, coincident with the loss of MTOC activity (Figures 1E, 1H, and 1I; Movie S4; data not shown). Consistent with our live-imaging results, we found that fixed *wdr62* mutant interphase neuroblasts contained centrioles with no γ-Tub, whereas all interphase wild-type neuroblast centrosomes were

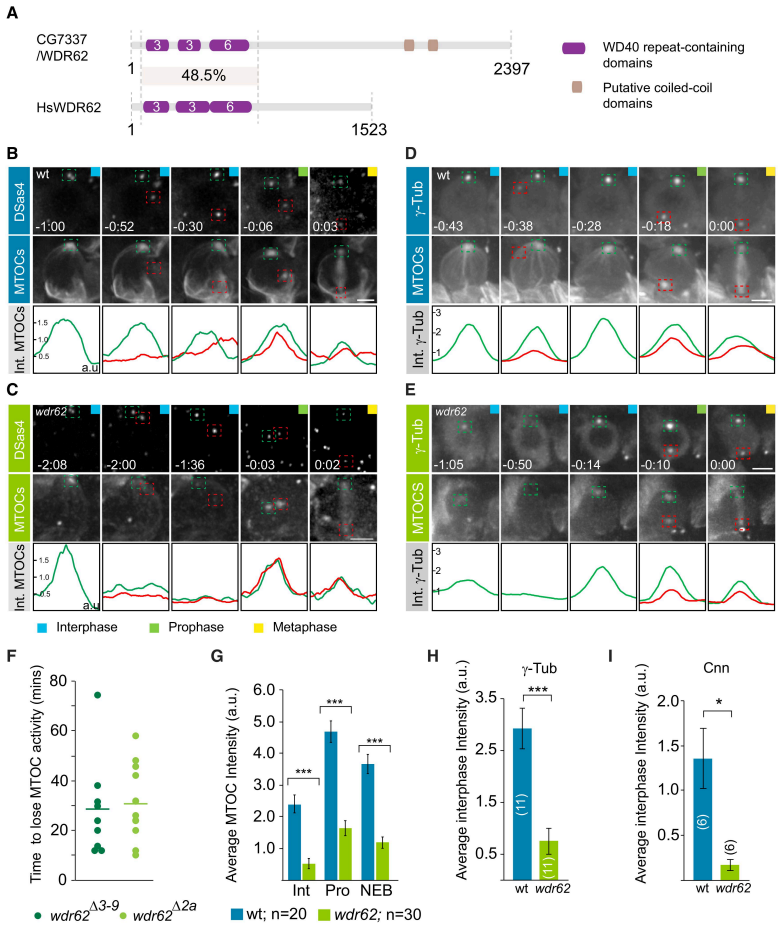


**Figure 1. CG7337, the Fly Ortholog of WDR62, Is Required to Maintain Centrosome Asymmetry during Interphase**

(A) Domain organization of CG7337 and human WDR62.

(B and C) Wild-type (wt) (B) and *wdr62* mutant (*wdr62*$^{\Delta 2a}$/*Df(2L)Exel8005*) (C) third instar larval neuroblast, expressing the centriolar marker DSas4::GFP (top row) and the MTOC marker Cherry::Jupiter (middle row). For this and subsequent panels, the green and red lines below the image sequence represent intensity (Int.) values of the indicated marker for the apical (green box) and basal (red box) centrosomes, respectively.

(D and E) Wild-type (wt) (D) and *wdr62* (*wdr62*$^{\Delta 2a}$/*Df(2L)Exel8005*) (E) mutant third instar larval neuroblast, expressing the PCM marker γ-Tub::GFP (top row) and the MTOC marker Cherry::Jupiter (middle row).

(F) Quantification of apical MTOC downregulation time in *wdr62* mutants (light green dots indicate *wdr62*$^{\Delta 2a}$/*Df(2L)Exel8005*; dark green dots indicate *wdr62*$^{\Delta 3\text{-}9}$/*Df(2L)Exel8005*). The average times are denoted with horizontal green lines.

(G) Cherry::Jupiter intensity measurements at interphase (Int), prophase (Pro), and nuclear envelope breakdown (NEB).

(H and I) Bar graphs representing average intensities for γ-Tub::GFP (H) and Cnn::mCherry (I) during interphase (20 min before NEB). Numbers in bar graphs refer to the number of scored neuroblasts ("ns"). Colored boxes refer to the corresponding cell-cycle stage.

Error bars correspond to SEM. *p < 0.05; ***p < 0.0001. Time is in hours:minutes. Scale bar, 5 μm.

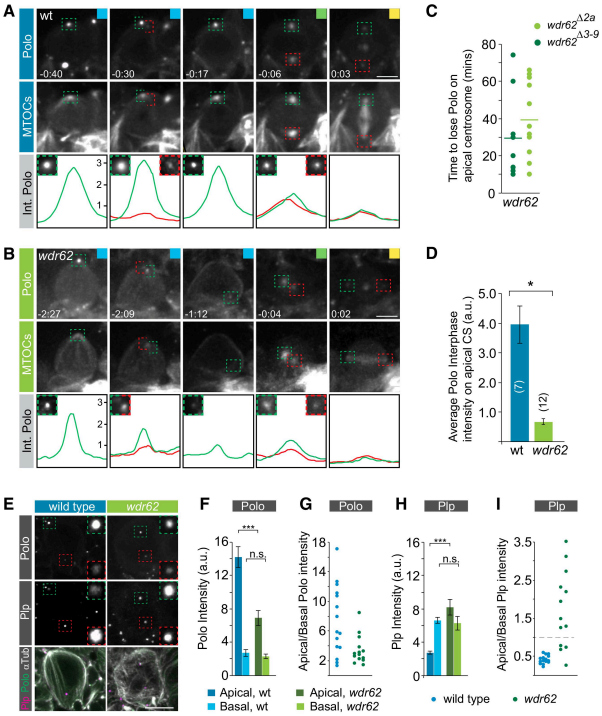


**Figure 2. Wdr62 Is Required to Maintain Polo Kinase on the Apical Interphase MTOC**

(A and B) Wild-type (wt) (A) and *wdr62* (*wdr62*$^{\Delta 2a}$/*Df(2L)Exel8005*) (B) mutant third instar larval neuroblasts, expressing Polo::GFP (top row) and the MTOC marker Cherry::Jupiter (middle row). The green and red lines below the image sequences represent Polo::GFP intensity (Int.) values of the apical (green box) and basal (red box) centrosomes, respectively.

(C) Quantification of Polo downregulation time in *wdr62* mutants (light green dots indicate *wdr62*$^{\Delta 2a}$/*Df(2L)Exel8005*; dark green dots indicate *wdr62*$^{\Delta 3\text{-}9}$/*Df(2L)Exel8005*). Average times are denoted with horizontal green lines.

(D) Average Polo::GFP intensity during interphase for wild-type (blue bar) and *wdr62* (green bar; *wdr62*$^{\Delta 2a}$/*Df(2L)Exel8005*) mutants.

(E) Representative confocal images of wild-type and *wdr62* mutant (*wdr62*$^{\Delta 3\text{-}9}$/*Df(2L)Exel8005*) neuroblasts stained for Polo (white in single channel and green in overlay), Plp (white in single channel and magenta in overlay), and α-tubulin (white in overlay). Green and red dashed boxes denote the apical and basal centrosomes, respectively, highlighted in the inserts. Contrast and brightness have been adjusted for better visibility.

(F–I) Polo (F) and Plp (H) intensity measurements performed on apical and basal centrosomes in wild-type (dark blue and light blue bars, respectively) and *wdr62* mutant (*wdr62*$^{\Delta 3\text{-}9}$/*Df(2L)Exel8005*; dark green and light green bars, respectively) neuroblasts. Polo (G) and Plp (I) asymmetry ratio for wild-type (blue dots) and *wdr62* mutants (*wdr62*$^{\Delta 3\text{-}9}$/*Df(2L)Exel8005;* green dots). Colored boxes refer to the corresponding cell-cycle stage.

Error bars correspond to the SEM. $^{*}p < 0.05$; $^{***}p < 0.0001$. Time is in hours:minutes. Scale bars, 5 μm.

asymmetric (Figures S1D and S1E). These data suggest that loss of MTOC activity in *wdr62* mutants is due to downregulation of the PCM proteins γ-Tub and Cnn on the apical centrosome.

## Wdr62 Is Required to Maintain Polo Kinase on the Apical Interphase MTOC

Maintenance of MTOC activity during interphase requires Polo kinase (Plk1 in vertebrates) (Januschke et al., 2013; Singh et al., 2014). We used a protein trap line, which endogenously labels Polo with GFP (Buszczak et al., 2007) to image Polo localization in *wdr62* mutants. Wild-type neuroblasts maintained high levels of Polo on the apical MTOC during interphase, whereas basal centrosomes downregulated Polo shortly after centrosome separation (Singh et al., 2014) (Figure 2A; Figure S4B; Movie S5). *wdr62* mutant neuroblasts downregulated Polo as early as 10 min after centrosome separation and contained significantly reduced Polo levels on both interphase centrosomes (Figures 2B–2D; Movie S6). These findings were confirmed in fixed preparations imaged with confocal microscopy (Figures 2E and 2F). The apical centrosome can still be identified because, in most cases, Polo levels are reduced, but not completely absent, resulting in a reduced asymmetry ratio between the apical and basal MTOCs (Figures 2E and 2G). Polo is required for MTOC maintenance, since neuroblasts mutant for the hypomorphic *polo1* allele failed to maintain an active apical MTOC, generating two naked centrioles shortly after centrosomes separated (Januschke and Gonzalez, 2010) (Movie S7; data not shown).

How Polo localization is controlled during interphase is currently not known, but it has been proposed that Plp is involved in the downregulation of Polo on the basal mother centriole. In interphase wild-type neuroblasts, Plp is asymmetrically localized, with the basal centrosome containing more Plp than the apical centrosome (Lerit and Rusan, 2013; Singh et al., 2014). Plp levels are roughly two times higher on the basal than on the apical wild-type centrosome, resulting in a clear asymmetry ratio. In *wdr62* mutants, this ratio was reversed because Plp levels were higher on the apical, Polo-positive centrosome compared to the basal centrosome. In comparison to wild-type apical centrosomes, Plp levels were significantly increased, whereas basal levels did not change significantly (Figures 2E, 2H, and 2I). These data suggest that Wdr62 is required

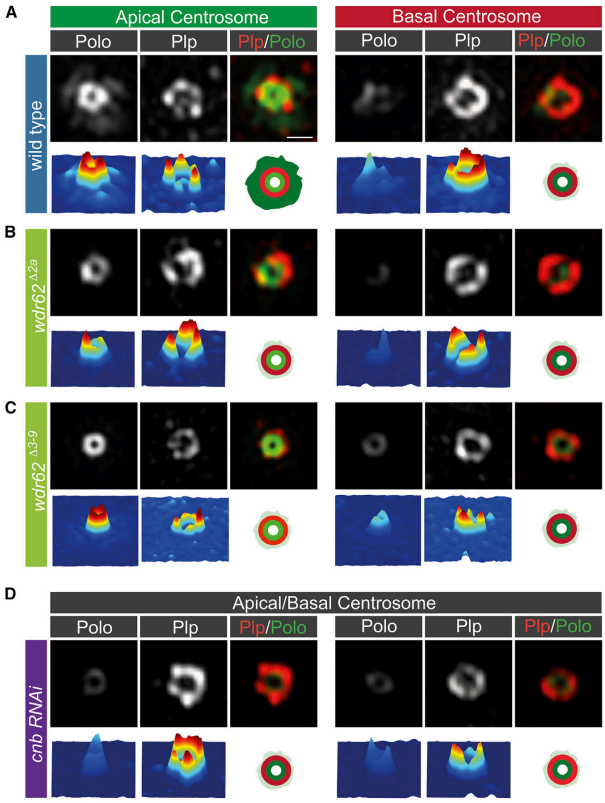


**Figure 3. Polo Is Localized to the Centriole and the PCM; Centriolar Localization Depends on Cnb, Whereas PCM Polo Requires Both Wdr62 and Cnb**

(A–D) 3D-SIM pictures of representative apical and basal interphase centrosomes in (A) wild-type, (B) *wdr62*$^{\Delta 2a}$, (C) *wdr62*$^{\Delta 3-9}$, and (D) *cnb* RNAi background, labeled with Polo (green in overlay) and Plp (red in overlay). 3D intensity plots are shown underneath the images. A schematic cartoon, summarizing the phenotype, is shown next to the intensity graphs. Since Polo levels were almost equal on both centrosomes in *cnb* RNAi-treated neuroblasts, we cannot clearly distinguish between apical and basal centrosomes. Scale bar, 0.3 μm.

to maintain Polo on the apical centrosome to retain MTOC activity during interphase. Furthermore, it shows that Wdr62 negatively regulates Plp levels on the apical centrosome.

### Interphase Centrosomes Contain Centriolar and PCM-Associated Polo

To gain better insight into the relationship of Polo and Plp, we used three-dimensional structured illumination microscopy (3D-SIM; see Experimental Procedures). Using the aforementioned Polo::GFP protein trap line (Buszczak et al., 2007), as well as a previously published Polo::GFP transgene (Moutinho-Santos et al., 1999), we found that the apical, daughter centriole-containing wild-type neuroblast centrosome showed a bright ring of centriolar Polo surrounded by Plp. A diffuse cloud of Polo was localized outside of this irregularly shaped Plp ring. This outer Polo cloud partially overlaps with the PCM marker Cnn, suggesting that Polo extends into the PCM (Figure 3A; Figures S2A and S2B). This finding is consistent with previous reports, showing that Polo also extends into the PCM space in *Drosophila* metaphase S2 cells (Fu and Glover, 2012) and *Drosophila* embryonic interphase centrosomes (Lerit et al., 2015). Basal wild-type neuroblast centrosomes contained almost no PCM-associated and also less centriolar Polo compared to the apical centrosome (Figure 3A). Apical centrosomes in *wdr62* mutants still harbored centriolar Polo surrounded by Plp, but PCM-Polo was no longer detectable. Similarly, basal centrosomes in *wdr62* mutants only contained centriolar Polo, comparable to wild-type neuroblasts (Figures 3B and 3C). In neuroblasts deficient for *cnb*, centriolar Polo was reduced and PCM-Polo was virtually absent; Plp showed a similar arrangement as in wild-type (Figure 3D).

Consistent with our confocal dataset, 3D-SIM imaging also showed that apical wild-type centrosomes contained less Plp than basal wild-type centrosomes, but this was often reversed in *wdr62* mutant neuroblasts (Figures 3A–3C). Since Polo levels are almost equal on both centrosomes in *cnb* RNAi-treated neuroblasts, it is difficult to distinguish between the apical and basal centrosomes. Nevertheless, we found neuroblasts containing both symmetric and asymmetric Plp levels (Figure 3D).

These localization data prompted us to test for molecular interactions between Wdr62, Cnb, Polo, and Plp. We performed a yeast-two hybrid assay and found an interaction between Cnb and Plp but not between Wdr62, Plp, and Polo (Figure S2C). Taken together, these results demonstrate that loss of Wdr62 or Cnb perturbs the asymmetric localization of Polo and Plp. Furthermore, it shows that the PCM-associated Polo fraction on the apical centrosome is regulated by Wdr62 and Cnb. Cnb also controls the centriolar Polo pool on the apical centrosome.

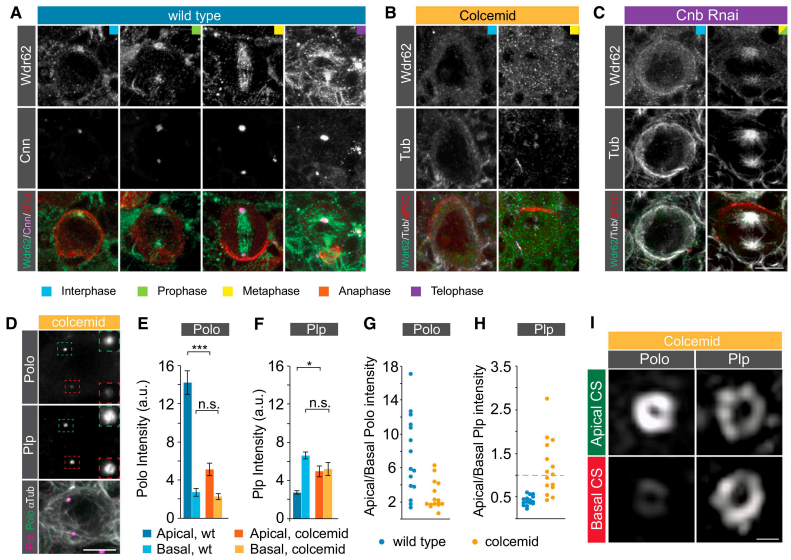


**Figure 4. Wdr62 Is a MT-Associated Protein, Controlling PCM Polo through Stabilization of MTs**

(A) Representative wild-type neuroblast stained with the Wdr62 peptide antibody (green in overlay), the PCM marker Cnn (magenta in overlay), and the neuroblast marker Miranda (Mira; red in overlay).

(B and C) Colcemid-treated wild-type (B) and *cnb* RNAi (C) neuroblasts stained for Wdr62 (green in overlay), the spindle marker α-tubulin (white in overlay), and the apical polarity marker atypical protein kinase C (aPKC) (red in overlay).

(D) Representative confocal neuroblast pictures showing Polo (white in single channel and green in overlay), Plp (white in single channel and magenta in overlay) and α-tubulin (white in overlay) after colcemid treatment. Green and red dashed boxes denote the apical and basal centrosomes, respectively, highlighted in the inserts. Contrast and brightness has been adjusted for better visibility.

(E and F) Polo (E) and Plp (F) intensity measurements performed on apical and basal centrosomes in wild-type (wt) (dark blue and light blue bars, respectively) and colcemid-treated wild-type neuroblasts (dark orange and light orange bars, respectively).

(G and H) Polo (G) and Plp (H) asymmetry ratio for wild-type (blue dots) and colcemid-treated wild-type neuroblasts (orange dots).

(I) Representative 3D-SIM centrosome pictures of Polo and Plp after colcemid treatment. Colored boxes refer to the corresponding cell-cycle stage.

Error bars correspond to SEM. *$p < 0.05$; **$p < 0.001$; ***$p < 0.0001$; n.s; not significant. Time is given in hours:minutes. Scale bars, 5 μm in (C) and (D) and 0.3 μm in (I).

## Wdr62 Is a Spindle-Associated Protein and Depends on MTs for Its Localization

To get further mechanistic insight into Wdr62's role in centrosome asymmetry, we analyzed its localization in third instar larval neuroblasts using three different reagents: (1) a functional *wdr62::mDendra2* transgene (Figures S1B and S3A); (2) a protein trap line, tagging all *wdr62* isoforms (Figures S3B and S3C); and (3) two peptide antibodies, recognizing two distinct Wdr62 antigens (Figure 4A; Figure S3D). All reagents showed comparable results; Wdr62 was localized on the apical, active MTOC during interphase. From prophase onward, Wdr62 also became enriched on the maturing basal centrosome and subsequently decorated the spindle from metaphase throughout mitosis. Wdr62 did not completely overlap with canonical PCM markers such as Cnn but suggested an association with MTs instead (Figure 4A). Indeed, chemical spindle ablation experiments using colcemid resulted in diffuse cytoplasmic Wdr62 localization when MTs were absent (Figure 4B). Similarly, removal of the interphase MTOC by knocking down *cnb* resulted in mostly cytoplasmic Wdr62 localization; Wdr62 relocalized to the spindle during prophase and metaphase (Figure 4C). These data provide evidence that Wdr62 is an MT-associated protein and is asymmetrically localized during interphase.

## PCM-Associated Polo Localization Depends on Intact MTs

Wdr62's spindle association prompted us to test whether centrosomal Polo levels could also be directly regulated through MTs. To this end, we depolymerized MTs using colcemid and analyzed the localization of Polo and Plp in interphase neuroblasts with confocal microscopy. Colcemid treatment resulted in a significant drop in apical Polo levels and close to a 2-fold

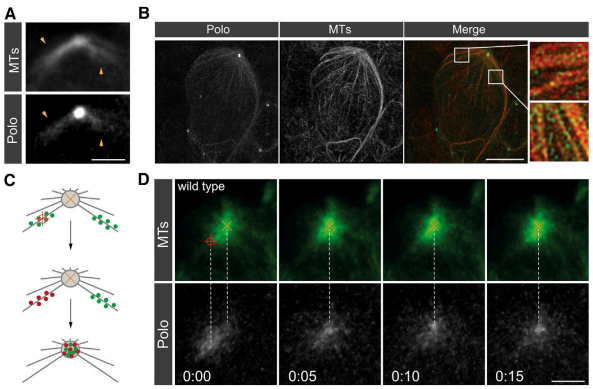


**Figure 5. Polo Is Localized on MTs and Travels to the Centrosome**

(A) Representative live-imaging snapshots of a late-telophase wild-type neuroblast expressing Cherry::Jupiter (MTs; top row) and Polo::GFP (protein trap line; bottom row). Yellow arrowheads denote MT fibers decorated with Polo.

(B) 3D-SIM pictures of an interphase wild-type neuroblast expressing Polo::GFP (protein trap line; green in overlay) and stained for α-tubulin (MTs; red in overlay). Higher magnifications of two selected regions are shown in high-magnification inserts.

(C) Cartoon illustrating photoactivation experiments for wild-type neuroblasts.

(D) Representative image sequence of a wild-type neuroblast expressing the MT marker G147 (MTs; top row; green) and Polo::mDendra2 (photoconverted in bottom row [white]). Red crosshairs represent the target area, which was photoconverted. Yellow crosses represent the center of the centrosome. Time is given in hours:minutes.

Scale bars, 5 μm.

increase of Plp on the apical interphase centrosome. Basal Polo and Plp did not change significantly upon colcemid treatment (Figures 2E and 4D–4F). As a consequence of decreased apical Polo levels, the apical/basal asymmetry ratio dropped to a level comparable to that of *wdr62* mutants (Figures 2G and 4G). Similarly, Plp asymmetry ratios were often inverted (Figures 2I and 4H).

To further asses the dynamics of Polo localization in interphase when MTs are partially depolymerized or absent, we applied low doses of colcemid to *zeste-white 10* (*zw10*) mutant neuroblasts and followed the behavior of endogenously tagged Polo (Polo::GFP) and Cnn (Cnn::mCherry), as well as MTs with live cell imaging. *zw10* mutants lack the spindle assembly checkpoint, permitting neuroblasts to enter anaphase when the mitotic spindle is missing (Basto et al., 2000). We found that a low dose of colcemid was mimicking the *wdr62* mutant phenotype; interphase MTs were depolymerized, but centrosome maturation and bipolar spindle formation were not inhibited in metaphase (Figures S4A, S5A and S5B; 100%, n = 70). In contrast to *zeste-white 10* control neuroblasts, Polo levels dropped on the apical interphase centrosome as MTs were depolymerized (100%, n = 40). The localization of Cnn was dependent on Polo; a colcemid-induced reduction in Polo was accompanied by a drop in Cnn levels (Figures S4A–S4C and S5B; 100%, n = 40). Furthermore, in *zw10* control neuroblasts, Cnn was shed on the basal centrosome shortly after Polo had been downregulated (Figure S4B; time point, −0:38) and reappeared after Polo relocalized on the maturing basal centrosome (Figure S4B; time point, −0:08). However, the apical centrosome always retained Polo, Cnn, and MTOC activity in *zw10* mutant neuroblasts that have not been exposed to colcemid (Figures S4B and S5A; 100%, n = 67).

Finally, we also confirmed with 3D-SIM that PCM-Polo was absent from the apical interphase centrosome upon colcemid treatment. Centriolar Polo was not affected, and the lack of MTs did not seem to change the localization pattern of Plp (Figure 4I).

Collectively, these results suggest that MTs are required for the recruitment and/or maintenance of Polo on the apical centrosome. It also shows that maintenance of Cnn on the active interphase centrosome and accumulation during maturation both depend on Polo. Furthermore, these data show that MTs regulate PCM-associated Polo and Plp levels. Importantly, depletion of *wdr62* and loss of MTs show very similar phenotypes.

## Astral MTs Recruit Polo to the Apical Interphase Centrosome

To test whether MTs recruit Polo to the apical centrosome, we first checked whether Polo colocalizes with MTs. Indeed, our live imaging data showed that Polo overlaps with astral MTs, predominantly during late telophase and in interphase (Figure 5A). Furthermore, 3D-SIM imaging of the Polo::GFP protein trap line (Buszczak et al., 2007) or a Polo::GFP transgene (Moutinho-Santos et al., 1999) shows Polo decorating MTs in interphase neuroblasts (Figure 5B and data not shown).

To confirm that MTs actively recruit Polo to the centrosome, we devised an in vivo pulse-chase experiment. To this end, we generated transgenic flies expressing Polo fused to the photoconvertable fluorescent protein mDendra2, expressed under the control of Polo's endogenous regulatory elements (see Experimental Procedures; Moutinho-Santos et al., 1999). We crossed Polo::mDendra2 to G147, a protein trap line labeling the MT-binding protein Jupiter with GFP endogenously (Morin et al., 2001; Karpova et al., 2006), and photoconverted Polo::mDendra2 on astral MTs ~4–7 μm away from the centrosome. If Polo travels on MTs to the centrosome, then photoconverted Polo::mDendra2 on MTs should relocalize to the center of the apical centrosome (Figure 5C). We performed this experiment in interphase wild-type neuroblasts and observed in all cases (100%; n = 10) that Polo relocalized from the periphery of the MTOC to the centrosome center (Figure 5D). Furthermore, if Polo::mDendra2 is photoconverted in the cytoplasm or colcemid-treated neuroblasts, showing a reduction, albeit not a complete lack, of astral MTs, relocalization of photoconverted

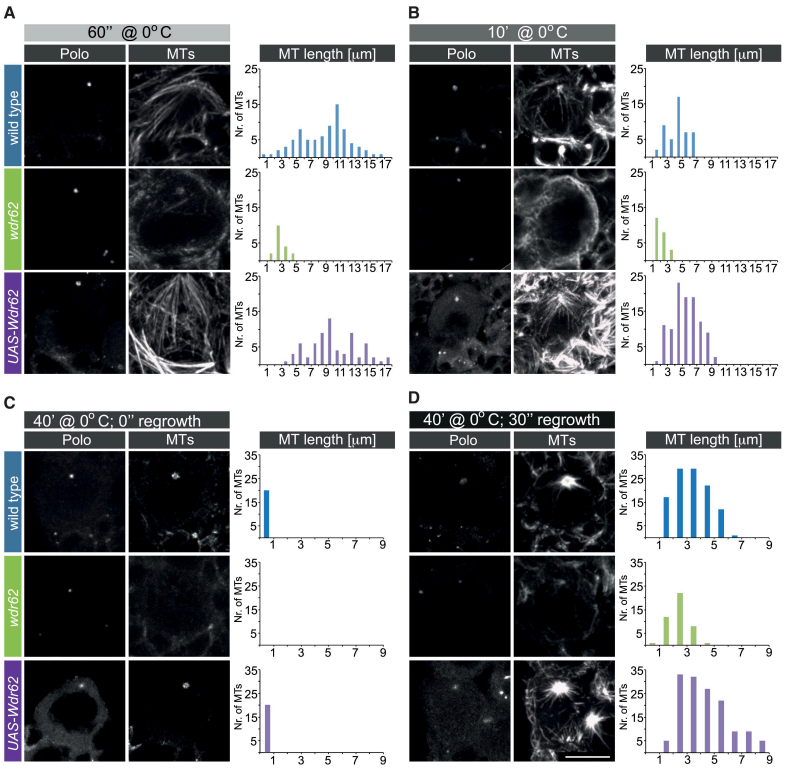


**Figure 6. Wdr62 Is Stabilizing MTs**

(A–D) Representative confocal images of wild-type (top row), *wdr62* mutant (*wdr62*$^{\Delta 3\text{-}9}$/*Df(2L)Exel8005*), or Wdr62-overexpressing (*UAS-Wdr62:mDendra2*) neuroblasts incubated at 0°C for (A) 60 s, (B) 10 min, (C) 40 min, or (D) 40 min, followed by 30 s regrowth at room temperature. In all genotypes, neuroblasts co-expressed Polo::GFP and were stained for α-tubulin. Bar graphs represent quantifications of MT bundle length for the indicated conditions. Nr, number. Scale bar, 5 µm.

Polo::mDendra2 to the centrosome was barely detectable (100%; n = 5; Figures S6A–S6D).

These results demonstrate that Polo is localized to astral MTs in interphase neuroblasts and is actively being recruited to the apical centrosome. Although, at this level of resolution, we cannot determine whether Polo will be recruited to the PCM or the centriole, the structure of the centrosome predicts that photoconverted Polo will first become enriched in the PCM. Collectively, these data provide strong evidence that MTs are required to recruit Polo to the apical interphase centrosome.

## Wdr62 Stabilizes Interphase MTs

Since *wdr62* mutants and depletion of MTs show a similar phenotype, and Wdr62 is localized to MTs, we next wanted to test the hypothesis whether Wdr62 is required to stabilize interphase MTs. MTs can dynamically switch between growth and shrinkage (catastrophe), modulated by many MT-associated proteins (MAPs) (Godek et al., 2015). We applied a cold assay to test whether the lack of, or excess of, Wdr62 would alter this dynamic instability in *Drosophila* neuroblasts. Incubating neuroblasts at 0°C will induce MTs to depolymerize. For instance, increasing the incubation time on ice from 60 s to 10 min increases the number of short interphase MTs for wild-type, *wdr62* mutants, and neuroblasts overexpressing Wdr62 (UAS-Wdr62::mDendra2). This effect was strongest in *wdr62* mutants, whereas Wdr62-overexpressing cells were affected the least (Figures 6A and 6B). If neuroblasts are incubated on ice for 40 min, MTs are almost completely

depolymerized; wild-type and Wdr62-overexpressing cells only contain a tubulin ring, surrounding Polo. However, cells lacking Wdr62 completely lost this tubulin ring but retained weak levels of Polo (centriolar Polo, most likely; Figure 6C). To measure MT regrowth, we first incubated wild-type, *wdr62* mutant, and Wdr62-overexpressing cells on ice for 40 min, followed by a temperature shift to 25°C for 30 s. Whereas wild-type neuroblasts can regrow MTs up to 7 μm (with the majority being between 2 and 6 μm in length), overexpressing Wdr62 shifted MT length toward 9 μm. *wdr62* mutant neuroblasts predominantly contained fewer and shorter MT bundles (Figure 6D). Polo intensity usually correlated with MT length and density.

These data show that MTs in *wdr62* mutant neuroblasts are more sensitive to cold than wild-type and that Wdr62-overexpressing cells are less sensitive than wild-type. Furthermore, the amount of Wdr62 protein determines MT regrowth rates, manifested in MT length. Collectively, these data suggest that Wdr62 is required to either directly or indirectly stabilize interphase MTs. Based on these results, we propose that stabilized MTs are required to recruit Polo to the apical interphase centrosome.

### Wdr62 Affects Centrosome Positioning, Spindle Orientation, and Centrosome Segregation

Defects in centrosome asymmetry have been shown to compromise centrosome positioning, spindle orientation, and centrosome segregation (Januschke et al., 2013; Januschke and Gonzalez, 2010; Lerit and Rusan, 2013; Singh et al., 2014), and we tested whether *wdr62* mutants show similar phenotypes. To this end, we first tracked centrioles during interphase until prophase in wild-type and *wdr62* mutant neuroblasts. Consistent with earlier reports (Rebollo et al., 2007; Singh et al., 2014), we found that wild-type apical centrosomes remain tethered to the apical cortex. Basal wild-type centrioles, however, lost their apical position, wandering randomly through the cytoplasm. In *wdr62* mutant neuroblasts, the apical centrosome was no longer stationary; both track length and overall centrosome displacement were similar between the apical and basal centrioles and significantly increased compared to wild-type centrioles (Figures 7A and 7B).

Centriole displacement compromises the correct positioning of centrosomes shortly before bipolar spindle formation. We measured centrosome position at prophase in relation to the metaphase spindle axis and confirmed that, in wild-type neuroblasts, the apical centrosome stayed close to the apical cortex throughout interphase. The basal centrosome, on the other hand, started maturing close to the basal cortex (Figure 7C; Singh et al., 2014). In *wdr62* mutants, apical centrosomes showed a more widespread distribution and matured close to the basal cortex in several instances (Figure 7D).

Centrosome displacement can also affect spindle orientation, and we tested this in fixed preparations by measuring the orientation of the mitotic spindle in relation to the neuroblast intrinsic polarity axis. Indeed, in contrast to wild-type, *wdr62* mutant neuroblasts contained misaligned spindles with low frequencies (Figures 7E and 7F). However, live cell imaging experiments demonstrated that misaligned spindles realigned with the neuroblast intrinsic apical-basal polarity axis (Figure 7G). This realignment often failed to correctly reposition centrosomes, which manifested in centrosome segregation defects. Wild-type neuroblasts retained the younger daughter centriole-containing centrosome and segregated the older mother centriole into the differentiating ganglion mother cell (GMC) (100%; n = 79) (Conduit and Raff, 2010; Januschke et al., 2011; Singh et al., 2014). In *wdr62* mutants, centriole segregation was mildly compromised; 16% of *wdr62* mutant neuroblasts retained the centrosome containing the older mother centriole (n = 43; Figure 7H). These results are consistent with previous findings, showing that centrosome asymmetry defects can result in centrosome missegregation (Januschke et al., 2013; Singh et al., 2014).

### Wdr62 Is Required for Normal Cell-Cycle Progression

Since *wdr62* has been implicated in primary microcephaly (Nicholas et al., 2010; Yu et al., 2010; Bilgüvar et al., 2010), we staged larval brains and performed brain size measurements, analyzing both optic lobe neuroepithelium and central brain size. Interestingly, we found that *wdr62* mutant brains are ~40% smaller compared to wild-type brains (Figures S7A and S7B). The brain size decrease is mostly attributed to a smaller central brain but not a reduction in the optic lobe (data not shown). Central brain size reduction could be a consequence of the observed centrosome asymmetry phenotype. Alternatively, cell-cycle delays, apoptosis, or a depletion of the neural stem cell pool could compromise brain development. To test this, we also knocked down *cnb* but did not find a brain size reduction (Figures S7A and S7B). Also, neuroblast number was only slightly reduced in *wdr62* but not in *cnb* RNAi brains (Figure S7C). However, our cell-cycle measurements showed that, in *wdr62* mutants, the cell cycle is significantly increased, affecting both interphase and mitosis length (Figures S7D and S7E). This neuroblast cell-cycle delay might not be specific to neuroblasts, since *wdr62* mutants are developmentally delayed (data not shown). However, the increase in neuroblast cell-cycle length is uncoupled from *wdr62*'s centrosome asymmetry phenotype since we also found ~50% of neuroblasts in $wdr62^{d3-9}$ mutants with a cell cycle comparable to that of wild-type neuroblasts, showing loss of apical MTOC activity (Figures S7F and S7G). Since lack of Cnb did not show any cell-cycle delays (Figure S7D), we conclude that the observed brain size reduction is due to an increase in cell-cycle length and an overall developmental delay.

## DISCUSSION

Here, we show that CG7337, the fly ortholog of the microcephaly protein MCPH2/WDR62, is required to maintain centrosome asymmetry in *Drosophila* neural stem cells. We demonstrate that Wdr62 is a spindle-associated protein, localizing to the active interphase MTOC and subsequently also decorating the entire mitotic spindle. In agreement with this localization, we demonstrate that Wdr62 is required to directly or indirectly stabilize MTs and to maintain MTOC activity on the apical interphase centrosome. In *wdr62* mutants, Polo, Cnn, and γ-Tub are downregulated, causing a loss in apical MTOC activity. These findings are consistent with previous reports, showing that maintenance of apical MTOC activity in interphase neuroblasts depends on

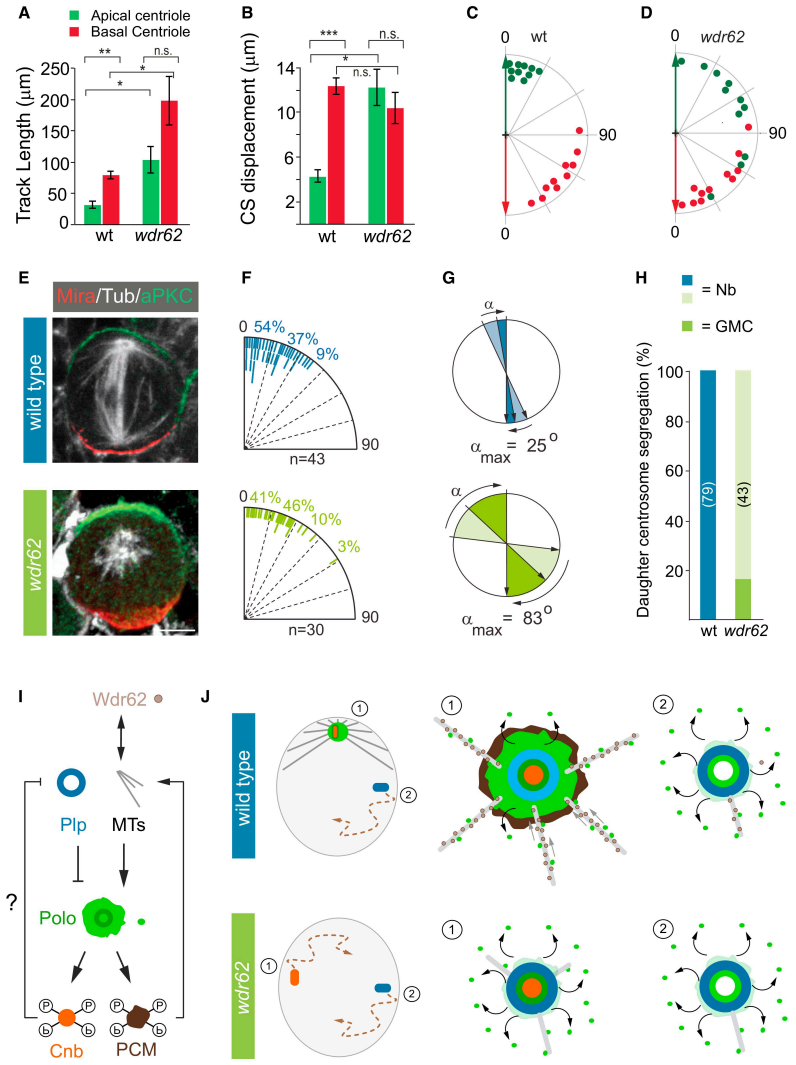


**Figure 7. Loss of Wdr62 Compromises Centrosome Positioning, Spindle Orientation, and Biased Centrosome Segregation**

(A–D) Mean track length (A) and centrosome (CS) (B) displacement for the apical (green bars) and basal (red bars) centrosomes in wild-type (wt) (n = 7) and *wdr62* mutants ($wdr62^{\Delta 28}/Df(2L)Exel8005$; n = 8). Radial centrosome distribution plot of wild-type (C) and *wdr62* ($wdr62^{\Delta 28}/Df(2L)Exel8005$) mutants (D) depicting the maximal deviation of the apical (green) and basal (red) prophase MTOC in relation to the metaphase spindle axis ("0" degree line). Green and red arrows highlight the apical (green)/basal (red) polarity and division axis.

*(legend continued on next page)*

the mitotic kinase Polo/Plk1 (Januschke et al., 2013). Polo has been shown to phosphorylate PCM components such as Cnn (Conduit et al., 2014) but also the daughter centriole-specific protein Cnb, which is necessary to maintain MTOC activity (Januschke et al., 2013). How Polo's localization is controlled is unclear, but in *Drosophila* neuroblasts, it was reported that Polo levels are partially regulated through Plp (Lerit and Rusan, 2013; Singh et al., 2014). Plp is asymmetrically localized in wild-type neuroblasts, containing higher Plp on the mother centriole-containing basal centrosome. This asymmetric localization could be controlled through a direct molecular interaction between Cnb and Plp, since ectopically localizing Cnb to both centrosomes decreases Plp levels (Singh et al., 2014; Lerit and Rusan, 2013), and our yeast-two hybrid data indicate that Cnb directly interacts with Plp. Cnb localization does not change in *wdr62* mutants, but Plp levels increase on the apical centrosome with the consequence that both centrosomes contain similar levels of Plp.

Plp and Polo could also be regulated through other mechanisms. For instance, using 3D-SIM, we further discovered that apical interphase neuroblast centrosomes contain a centriolar and a PCM-associated pool of Polo protein. PCM-associated Polo has recently been seen in metaphase centrosomes of *Drosophila* S2 cells (Fu and Glover, 2012) and embryonic interphase centrosomes (Lerit et al., 2015). *wdr62* specifically perturbed the localization of Polo associated with PCM, whereas Cnb is required to maintain both PCM and centriolar Polo.

Based on our results and previously published data, we propose the following model: neuroblasts exit mitosis with a robust array of MTs, which originates from the preceding centrosome maturation cycle. This array is used to increase the amount of Polo protein on the apical $Cnb^{+}$ centrosome through new recruitment as the neuroblast exits mitosis. Indeed, our live imaging and 3D SIM data show that interphase MTs are decorated with Polo and that colcemid treatment decreases PCM Polo levels. Furthermore, Polo levels are usually lowest at metaphase, increase after mitosis, and stay high throughout interphase. Polo recruitment to the centrosome occurs via astral MTs, which is supported by our photoconversion experiments. To allow for sustained Polo recruitment, we propose that Wdr62 stabilizes interphase MTs, which is consistent with Wdr62's localization, live imaging, and cold assay data. To maintain this cycle, Polo needs to phosphorylate not only PCM proteins (e.g., Cnn; Conduit et al., 2014) but also Cnb (Januschke et al., 2013). This is consistent with previous data, showing that increasing levels of Polo on the basal centrosome transforms the basal centrosome into an active MTOC, failing to shed the Polo target Cnn (Lerit and Rusan, 2013; Singh et al., 2014). Furthermore, *cnb* phosphomutants are unable to rescue *cnb*'s loss-of-function phenotype (Januschke et al., 2013). Our model further proposes that phosphorylated Cnb is necessary to prevent Plp protein levels from increasing on the apical interphase centrosome. Indeed, we found that Cnb directly interacts with Plp. The basal centrosome, however, also recruits Polo through MTs, but due to the lack of Cnb, Plp is upregulated, inducing the shedding of Polo and PCM and preventing the maintenance of MTs and, thus, the new recruitment of Polo (Figures 7I and 7J).

This model predicts that loss of Wdr62 and depletion of MTs should have the same phenotype. In support of this, we found that loss of MTs mimics the phenotype of *wdr62* mutants; in colcemid-treated neuroblasts, Polo and Cnn are downregulated on the apical centrosome with a concomitant increase in Plp, reaching levels similar to that of the basal centrosome. Furthermore, PCM-associated Polo is lost. Taken together, we propose that maintenance of the apical, daughter centriole-containing centrosome's MTOC activity—and, thus, neuroblast centrosome asymmetry—can be established and maintained by balancing Plp-mediated shedding of Polo and MT-dependent Polo recruitment and maintenance. Wdr62 plays a key role in this process by stabilizing MTs.

Similar to *wdr62*, *pins* mutant neuroblasts also show loss in interphase MTOC activity (Rebollo et al., 2007). However, since Pins does not co-localize with Wdr62 and Cnb during the neuroblast cell cycle, it is currently unclear how this protein affects interphase MTOC activity. Pins could compromise Polo localization in interphase in a Cnb- and Wdr62-independent manner. Alternatively, since Pins has been reported to affect spindle asymmetry (Cai et al., 2003), it could also influence centrosome architecture in mitotic neuroblasts, preventing the apical centrosome from maintaining MTOC activity in interphase. Recently, we also implicated Bld10 in Polo and PCM shedding (Singh et al., 2014), but additional work is needed to fit Bld10 and Pins into the proposed model.

MTOC asymmetry is important for proper centrosome positioning and spindle orientation (Januschke et al., 2013; Januschke and Gonzalez, 2010; Lerit and Rusan, 2013; Singh et al., 2014) (Figure 7). Whereas wild-type neuroblasts always retain the daughter centriole-containing centrosome, *wdr62* mutants show centrosome segregation defects with low frequency. Similarly, spindle orientation defects occur but are corrected in *wdr62* mutants, suggesting that backup mechanisms are in place to detect and correct spindle misalignment if centrosome mispositioning occurs (Singh et al., 2014). Our phenotypic analysis also revealed that Wdr62 is involved in normal brain

(E) Representative wild-type and *wdr62* mutant (*wdr62$^{\Delta 2a}$/Df(2L)Exel8005)* neuroblasts stained for the apical marker aPKC (green), the basal marker Miranda (Mira; red) and α-tubulin (white).
(F) Quantification of spindle orientations in fixed neuroblasts. Tick marks (wild-type; blue. *wdr62 (wdr62$^{\Delta 2a}$/Df(2L)Exel8005)*; green) represent the orientation of metaphase spindles with respect to the polarity axis.
(G) Spindle correction angles; wild-type (blue) and *wdr62* (*wdr62$^{\Delta 2a}$/Df(2L)Exel8005;* green). Mean correction angles (α-mean) are shown in darker shading and the maximal correction angle (α-max) is shown in lighter shading. Wild-type: α-max = 24.7°; α-mean = 15° ± 6.8°; n = 10. *wdr62*: α-max = 83°; α-mean: 38° ± 30°; n = 11).
(H) Quantification of centrosome segregation in wild-type (blue bar) and *wdr62* (*wdr62$^{\Delta 2a}$/Df(2L)Exel8005;* green bars) mutant neuroblasts.
(I) Model: Wdr62 (brown balls) is associated with MTs and is stabilizing interphase MTs, permitting the recruitment of Polo to the centrosome.
(J) This mechanism ensures the maintenance of an active apical MTOC in interphase neuroblasts. See Discussion for details.
Error bars indicate SEM. *p < 0.05; **p < 0.001; ***p < 0.0001; n.s., not significant. Scale bar, 5 μm.

development, in agreement with previously published vertebrate model systems (Chen et al., 2014; Xu et al., 2014). Wdr62 mutant brains are ~40% smaller compared to wild-type brains, showing only a minor decrease of neural stem cells. Based on our cell-cycle measurements, the simplest interpretation is that cell-cycle delays cause a reduction in brain size. In embryonic neural stem cells, Wdr62 controls mitotic progression through interactions with Aurora A kinase (Chen et al., 2014), and we hypothesize that the same mechanism could control neuroblast cell-cycle progression, which is consistent with the *aurA* mutant neuroblast phenotype (Lee et al., 2006). Inactivation of the apical MTOC does not seem to compromise normal brain development, since *cnb* RNAi-treated animals show normal cell-cycle length and normal brain size. However, the aforementioned backup mechanisms, correcting centrosome mispositioning and spindle misorientation, could prevent more severe developmental perturbations. This hypothesis is consistent with a recent report showing that centrosome cycle misregulation compromises spindle orientation in mouse neural progenitors, biasing the progenitor division mode toward asymmetric divisions (Gruber et al., 2011).

Although we failed to find a causal relationship between centrosome asymmetry and microcephaly, perturbed centrosome segregation could affect brain development in ways that have escaped our attention so far. For instance, recent reports suggest that biased sister chromatid and midbody segregation could be connected with centrosome asymmetry (Salzmann et al., 2014; Yadlapalli and Yamashita, 2013). Thus, the finding that centrosome positioning and biased centrosome segregation is highly stereotypic would argue for an important function of this process. However, more refined assays will be necessary to determine the consequence of compromised centrosome asymmetry. Taken together, we discovered that Wdr62 is required to stabilize MTs, ensuring MTOC activity and centrosome asymmetry, a requirement for spindle orientation and biased centrosome segregation.

## EXPERIMENTAL PROCEDURES

### Fly Strains and Genetics

A detailed list of all the generated and used fly strains and transgenes can be found in the Supplemental Experimental Procedures.

### Antibodies Used

Mouse anti-Wdr62 (1:1,000) monoclonal peptide antibodies were generated by Abmart for the following epitopes: MTPASLSASTPT (Wdr62(1–12)) and NTENGKSVAAPP (Wdr62(1154–1165)). For the representative images in Figure 5, Wdr62(1–12) was used; Wdr62(1154–1165; 1:1,000) yielded almost identical results. All the other antibodies used in this study can be found in the Supplemental Experimental Procedures.

### Immunostainings

At 96–120 hr (AEL; after egg laying), larval brains were dissected and fixed as previously described (Singh et al., 2014). Please refer to the Supplemental Experimental Procedures for details.

### Cold Assay for MT Dynamics

Brains (96-hr AEL) were dissected and transferred to 50 μl of Schneider's medium and incubated on ice for 1, 10, or 40 min and either fixed immediately or incubated at 25°C in a water bath for 30 s. Subsequently, brains were fixed and stained with mouse anti-α-Tub (Serotec; 1:1,000) and rabbit anti-Cnn (1:1,000). Complete depolymerization of long MTs was seen in all wild-type interphase neuroblasts after 40 min on ice. MT length was measured in Imaris 7.4 and higher.

### Colcemid Treatment

To inhibit MT formation, wild-type brains were dissected in Schneider's medium and incubated for 1 hr with colcemid (Sigma) at a final concentration of 20 μg/ml. Brains were fixed and stained as described earlier. For the Polo::mDendra2 photoconversion experiments, we used imaging media and 20 μg/ml colcemid (final concentration). For live-imaging colcemid experiments, larval brains (96 hr AEL) were dissected in imaging medium and incubated with 5 μg/ml of colcemid (final concentration).

### Live Imaging Sample Preparation

Live imaging experiments were performed as previously published (Cabernard and Doe, 2013) and explained in the Supplemental Experimental Procedures.

### Photoconversion

Photoconversion experiments were performed on G147 (tagging Jupiter with GFP [Morin et al., 2001; Karpova et al., 2006]) larvae (96 hr AEL), crossed to *polo::mDendra2* (this work; discussed earlier). We used an Andor Revolution spinning disc system equipped with the FRAPPA unit. A regions of interest (ROI) was manually chosen in the GFP channel. MT signal from G147 allowed for unambiguous identification of interphase neuroblast MTs. Astral MTs were irradiated at various distances away from the active centrosome. Before photoconversion, single Z planes containing ROIs were scanned for ten time points with maximum speed. Subsequently, ROIs were irradiated with the 405-nm laser line (~15%; 20 repeats; 50-μs dwell time). After photoconversion, the entire neuroblast was scanned with a z-step size of 0.65 μm. Photoconverted Polo::mDendra2 emits red fluorescence, which was detected simultaneously with G147's GFP emission GFP and mDendra2 emission were merged in Andor IQ2 and converted into Imaris files using a custom-made MATLAB code.

### Super-Resolution 3D-SIM

Super-resolution 3D-SIM was performed as published before (Roth et al., 2015). Additional details can be found in the Supplemental Experimental Procedures.

### Yeast Two-Hybrid Assay

*polo*, *cnb*, *plp*, and *wdr62* full-length cDNA were first cloned into pDONR221 using BP clonase. Gateway cloning technology was then used to subclone the cDNA from these entry vectors into pDEST32 (Gal4 DNA-binding domain containing destination vector) or pDEST22 (Gal4 activation domain containing destination vector) using LR Clonase (Life Technologies).

Yeast two-hybrid assays were performed using the ProQuest Two-Hybrid System (Life Technologies). pDEST32 and pDEST22 vectors containing the bait and prey cDNA, respectively, were co-transformed into the MaV203 yeast strain. The expression of the reporter genes *lacZ* and *URA3* was tested according to the manufacturer's manual.

### Statistics and Sample Number

Statistical significance was calculated using the unpaired-samples Student's t test. F tests were performed first to determine the equality of variance. For each experiment, the data were collected from at least three independent brain lobes. Scored neuroblasts are shown in the figures or mentioned in the legends.

## SUPPLEMENTAL INFORMATION

Supplemental Information includes Supplemental Experimental Procedures, seven figures, and seven movies and can be found with this article online at http://dx.doi.org/10.1016/j.celrep.2015.12.097.

## AUTHOR CONTRIBUTIONS

A.R.N. and C.C. conceived and designed the project. A.R.N. performed the experiments with help from P.S. D.S.G. and A.R.N. generated the *wdr62*

OPEN ACCESS
CellPress

CRISPR alleles. A.R.N., D.R.-C., and B.E. generated brain size data. A.R.N., P.S., D.R.-C., B.E., and C.C. analyzed the data. A.R.N. and C.C wrote the manuscript.

## ACKNOWLEDGMENTS

We thank Tri Thanh Pham for custom-made MATLAB codes and Emmanuel Gallaud for helping with the cold assays and insightful discussions. We also thank Emmanuel Gallaud and Fiona Doetsch for critical reading of the manuscript. We are grateful to Tim Megraw, Jordan Raff, Renata Basto, Juergen Knoblich, Cayetano Gonzalez, Monica Bettencourt-Dias, Tomer Avidor-Reiss, Chris Doe, Fumio Matsuzaki, Nasser Rusan, and the Bloomington Drosophila Stock Center (NIH P40OD018537) for flies and antibodies. We thank Alexia Isabelle Loynton-Ferrand of the Imaging Core Facility (IMCF) for technical support. This work was supported by an EMBO long-term postdoctoral fellowship to P.S. (EMBO ALTF 628-2012), the Swiss National Science Foundation (SNSF; PP00P3_133658), and the Novartis Foundation for Biomedical Research. B.E. thanks Simon Sprecher for continuous support.

Received: October 15, 2015
Revised: December 10, 2015
Accepted: December 21, 2015
Published: January 21, 2016

## REFERENCES

Albertson, R., and Doe, C.Q. (2003). Dlg, Scrib and Lgl regulate neuroblast cell size and mitotic spindle asymmetry. Nat. Cell Biol. *5*, 166–170.

Basto, R., Gomes, R., and Karess, R.E. (2000). Rough deal and Zw10 are required for the metaphase checkpoint in Drosophila. Nat. Cell Biol. *2*, 939–943.

Bilgüvar, K., Oztürk, A.K., Louvi, A., Kwan, K.Y., Choi, M., Tatli, B., Yalnizoğlu, D., Tüysüz, B., Cağlayan, A.O., Gökben, S., et al. (2010). Whole-exome sequencing identifies recessive WDR62 mutations in severe brain malformations. Nature *467*, 207–210.

Brand, A.H., and Livesey, F.J. (2011). Neural stem cell biology in vertebrates and invertebrates: more alike than different? Neuron *70*, 719–729.

Buszczak, M., Paterno, S., Lighthouse, D., Bachman, J., Planck, J., Owen, S., Skora, A.D., Nystul, T.G., Ohlstein, B., Allen, A., et al. (2007). The Carnegie protein trap library: a versatile tool for Drosophila developmental studies. Genetics *175*, 1505–1531.

Cabernard, C., and Doe, C.Q. (2009). Apical/basal spindle orientation is required for neuroblast homeostasis and neuronal differentiation in Drosophila. Dev. Cell *17*, 134–141.

Cabernard, C., and Doe, C.Q. (2013). Live imaging of neuroblast lineages within intact larval brains in Drosophila. Cold Spring Harb. Protoc. *2013*, 970–977.

Cai, Y., Yu, F., Lin, S., Chia, W., and Yang, X. (2003). Apical complex genes control mitotic spindle geometry and relative size of daughter cells in Drosophila neuroblast and pI asymmetric divisions. Cell *112*, 51–62.

Chen, J.-F., Zhang, Y., Wilde, J., Hansen, K.C., Lai, F., and Niswander, L. (2014). Microcephaly disease gene Wdr62 regulates mitotic progression of embryonic neural stem cells and brain size. Nat. Commun. *5*, 3885.

Cohen-Katsenelson, K., Wasserman, T., Khateb, S., Whitmarsh, A.J., and Aronheim, A. (2011). Docking interactions of the JNK scaffold protein WDR62. Biochem. J. *439*, 381–390.

Conduit, P.T., and Raff, J.W. (2010). Cnn dynamics drive centrosome size asymmetry to ensure daughter centriole retention in Drosophila neuroblasts. Curr. Biol. *20*, 2187–2192.

Conduit, P.T., Feng, Z., Richens, J.H., Baumbach, J., Wainman, A., Bakshi, S.D., Dobbelaere, J., Johnson, S., Lea, S.M., and Raff, J.W. (2014). The centrosome-specific phosphorylation of Cnn by Polo/Plk1 drives Cnn scaffold assembly and centrosome maturation. Dev. Cell *28*, 659–669.

Fu, J., and Glover, D.M. (2012). Structured illumination of the interface between centriole and peri-centriolar material. Open Biol. *2*, 120104.

Godek, K.M., Kabeche, L., and Compton, D.A. (2015). Regulation of kinetochore-microtubule attachments through homeostatic control during mitosis. Nat. Rev. Mol. Cell Biol. *16*, 57–64.

Gruber, R., Zhou, Z., Sukchev, M., Joerss, T., Frappart, P.O., and Wang, Z.Q. (2011). MCPH1 regulates the neuroprogenitor division mode by coupling the centrosomal cycle with mitotic entry through the Chk1-Cdc25 pathway. Nat. Cell Biol. *13*, 1325–1334.

Homem, C.C.F., and Knoblich, J.A. (2012). Drosophila neuroblasts: a model for stem cell biology. Development *139*, 4297–4310.

Hussain, M.S., Baig, S.M., Neumann, S., Nürnberg, G., Farooq, M., Ahmad, I., Alef, T., Hennies, H.C., Technau, M., Altmüller, J., et al. (2012). A truncating mutation of CEP135 causes primary microcephaly and disturbed centrosomal function. Am. J. Hum. Genet. *90*, 871–878.

Jakobsen, L., Vanselow, K., Skogs, M., Toyoda, Y., Lundberg, E., Poser, I., Falkenby, L.G., Bennetzen, M., Westendorf, J., Nigg, E.A., et al. (2011). Novel asymmetrically localizing components of human centrosomes identified by complementary proteomics methods. EMBO J. *30*, 1520–1535.

Januschke, J., and Gonzalez, C. (2010). The interphase microtubule aster is a determinant of asymmetric division orientation in Drosophila neuroblasts. J. Cell Biol. *188*, 693–706.

Januschke, J., Llamazares, S., Reina, J., and Gonzalez, C. (2011). Drosophila neuroblasts retain the daughter centrosome. Nat. Commun. *2*, 243.

Januschke, J., Reina, J., Llamazares, S., Bertran, T., Rossi, F., Roig, J., and Gonzalez, C. (2013). Centrobin controls mother-daughter centriole asymmetry in Drosophila neuroblasts. Nat. Cell Biol. *15*, 241–248.

Karpova, N., Bobinnec, Y., Fouix, S., Huitorel, P., and Debec, A. (2006). Jupiter, a new Drosophila protein associated with microtubules. Cell Motil. Cytoskeleton *63*, 301–312.

Lee, C.-Y., Andersen, R.O., Cabernard, C., Manning, L., Tran, K.D., Lanskey, M.J., Bashirullah, A., and Doe, C.Q. (2006). Drosophila Aurora-A kinase inhibits neuroblast self-renewal by regulating aPKC/Numb cortical polarity and spindle orientation. Genes Dev. *20*, 3464–3474.

Lerit, D.A., and Rusan, N.M. (2013). PLP inhibits the activity of interphase centrosomes to ensure their proper segregation in stem cells. J. Cell Biol. *202*, 1013–1022.

Lerit, D.A., Jordan, H.A., Poulton, J.S., Fagerstrom, C.J., Galletta, B.J., Peifer, M., and Rusan, N.M. (2015). Interphase centrosome organization by the PLP-Cnn scaffold is required for centrosome function. J. Cell Biol. *210*, 79–97.

Megraw, T.L., Sharkey, J.T., and Nowakowski, R.S. (2011). Cdk5rap2 exposes the centrosomal root of microcephaly syndromes. Trends Cell Biol. *21*, 470–480.

Morin, X., Daneman, R., Zavortink, M., and Chia, W. (2001). A protein trap strategy to detect GFP-tagged proteins expressed from their endogenous loci in Drosophila. Proc. Natl. Acad. Sci. USA *98*, 15050–15055.

Moutinho-Santos, T., Sampaio, P., Amorim, I., Costa, M., and Sunkel, C.E. (1999). In vivo localisation of the mitotic POLO kinase shows a highly dynamic association with the mitotic apparatus during early embryogenesis in Drosophila. Biol. Cell *91*, 585–596.

Nicholas, A.K., Khurshid, M., Désir, J., Carvalho, O.P., Cox, J.J., Thornton, G., Kausar, R., Ansar, M., Ahmad, W., Verloes, A., et al. (2010). WDR62 is associated with the spindle pole and is mutated in human microcephaly. Nat. Genet. *42*, 1010–1014.

Nigg, E.A., and Stearns, T. (2011). The centrosome cycle: Centriole biogenesis, duplication and inherent asymmetries. Nat. Cell Biol. *13*, 1154–1160.

Nigg, E.A., Čajánek, L., and Arquint, C. (2014). The centrosome duplication cycle in health and disease. FEBS Lett. *588*, 2366–2372.

Peel, N., Stevens, N.R., Basto, R., and Raff, J.W. (2007). Overexpressing centriole-replication proteins in vivo induces centriole overduplication and de novo formation. Curr. Biol. *17*, 834–843.

Rebollo, E., Sampaio, P., Januschke, J., Llamazares, S., Varmark, H., and González, C. (2007). Functionally unequal centrosomes drive spindle orientation in asymmetrically dividing Drosophila neural stem cells. Dev. Cell *12*, 467–474.

Roth, M., Roubinet, C., Iffländer, N., Ferrand, A., and Cabernard, C. (2015). Asymmetrically dividing Drosophila neuroblasts utilize two spatially and temporally independent cytokinesis pathways. Nat. Commun. *6*, 6551.

Roubinet, C., and Cabernard, C. (2014). Control of asymmetric cell division. Curr. Opin. Cell Biol. *31*, 84–91.

Rusan, N.M., and Peifer, M. (2007). A role for a novel centrosome cycle in asymmetric cell division. J. Cell Biol. *177*, 13–20.

Salzmann, V., Chen, C., Chiang, C.Y., Tiyaboonchai, A., Mayer, M., and Yamashita, Y.M. (2014). Centrosome-dependent asymmetric inheritance of the midbody ring in Drosophila germline stem cell division *25*, 267–275.

Singh, P., Ramdas Nair, A., and Cabernard, C. (2014). The centriolar protein Bld10/Cep135 is required to establish centrosome asymmetry in Drosophila neuroblasts. Curr. Biol. *24*, 1548–1555.

Wang, X., Tsai, J.W., Imai, J.H., Lian, W.N., Vallee, R.B., and Shi, S.H. (2009). Asymmetric centrosome inheritance maintains neural progenitors in the neocortex. Nature *461*, 947–955.

Wasserman, T. et al., 2010. A novel c-Jun N-terminal kinase (JNK)-binding protein WDR62 is recruited to stress granules and mediates a nonclassical JNK activation. 21, 117–130.

Xu, D., Zhang, F., Wang, Y., Sun, Y., and Xu, Z. (2014). Microcephaly-associated protein WDR62 regulates neurogenesis through JNK1 in the developing neocortex. Cell Rep. *6*, 104–116.

Yadlapalli, S., and Yamashita, Y.M. (2013). Chromosome-specific nonrandom sister chromatid segregation during stem-cell division. Nature *498*, 251–254.

Yamashita, Y.M., Mahowald, A.P., Perlin, J.R., and Fuller, M.T. (2007). Asymmetric inheritance of mother versus daughter centrosome in stem cell division. Science *315*, 518–521.

Yu, T.W., Mochida, G.H., Tischfield, D.J., Sgaier, S.K., Flores-Sarnat, L., Sergi, C.M., Topçu, M., McDonald, M.T., Barry, B.J., Felie, J.M., et al. (2010). Mutations in WDR62, encoding a centrosome-associated protein, cause microcephaly with simplified gyri and abnormal cortical architecture. Nat. Genet. *42*, 1015–1020.

**Cell Reports, Volume *14***

**Supplemental Information**

# The Microcephaly-Associated Protein Wdr62/CG7337 Is Required to Maintain Centrosome Asymmetry in *Drosophila* Neuroblasts

**Anjana Ramdas Nair, Priyanka Singh, David Salvador Garcia, David Rodriguez-Crespo, Boris Egger, and Clemens Cabernard**

# Supplemental Information

## Supplemental Data

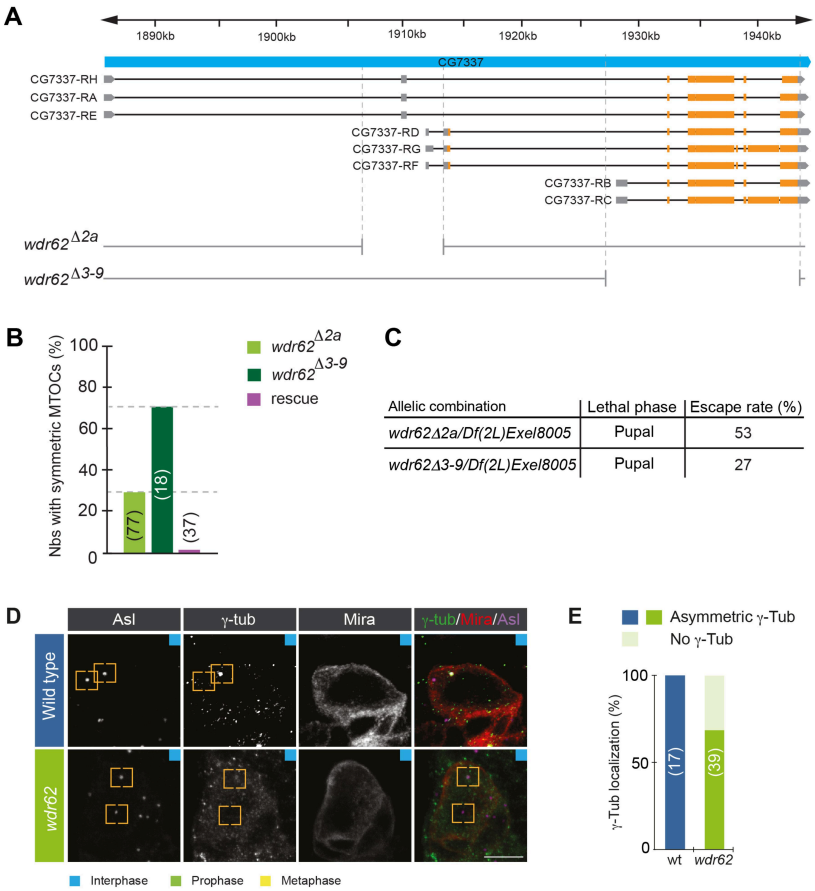


**Figure S1: *wdr62* locus and alleles, related to Figure 1**
**(A)** Locus map of *CG7337/wdr62*. Orange bars represent the predicted coding region. *wdr62* alleles are indicated below; molecularly defined breakpoints are highlighted with vertical dashed lines. **(B)** Phenotypic penetrance of the generated *wdr62* alleles. The centrosome asymmetry phenotype of *wdr62*$^{\Delta 2a}$ was fully rescued by expressing *UAS-CG7337::mDendra2*. **(C)** Table indicating lethal phase and number of escapers for *wdr62*$^{\Delta 2a}$ and *wdr62*$^{\Delta 3-9}$ crossed over the deficiency *Df(2L)Exel8005*. This deficiency removes the entire CG7337 locus plus adjacent genes (not shown in (a)). **(D)** Representing confocal images of wild type and *wdr62* mutant (*wdr62*$^{\Delta 2a}$*/Df(2L)Exel8005*) neuroblasts stained for the centriolar marker Asterless (Asl; magenta in overlay), γ-tubulin (γ-tub; green in overlay) and the neuroblast marker Miranda (Mira; red in overlay). Yellow brackets highlight neuroblast centrosomes. **(E)** Quantification of the centrosome asymmetry phenotype in the immunohistochemistry experiment. Number of scored neuroblasts (n's) is indicated on the bar graphs. Colored boxes refer to the corresponding cell cycle stage. Scale bar is 5 μm.

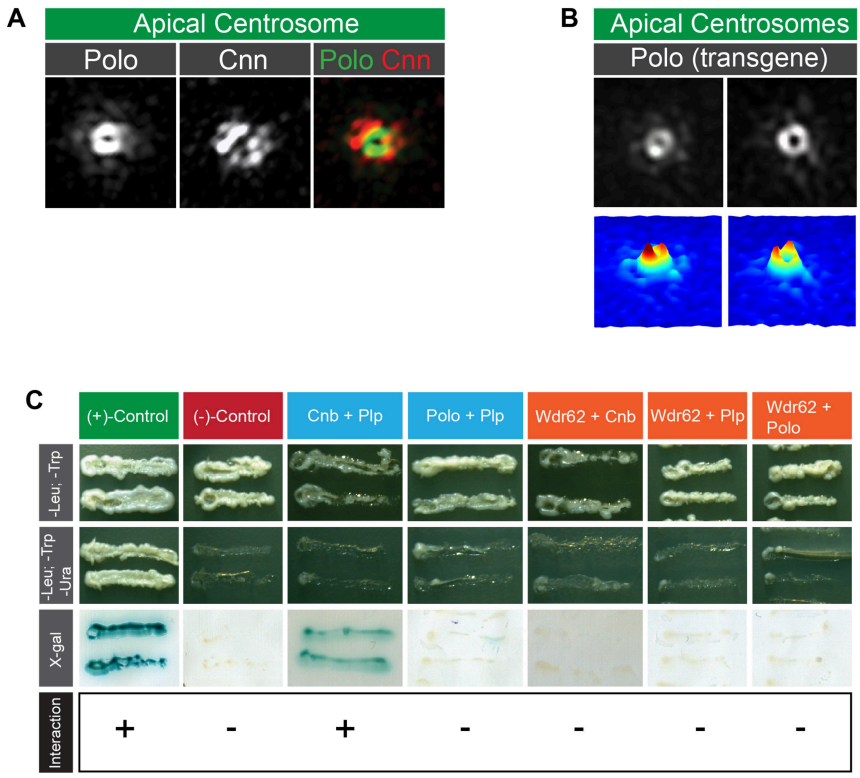


**Figure S2: Wdr62 is required for Polo's association with the PCM, related to Figure 2&3**
**(A)** Representative image of an apical wild type interphase centrosome expressing Polo fused to GFP. In this line, the GFP cassette is inserted into Polo's coding region, resulting in an in-frame fusion between Polo's exons and GFP (Protein trap line). The neuroblast was stained for Cnn (white in single channel and red in overlay). **(B)** Representative image of an apical wild type centrosome expressing Polo::GFP, encoded by a transgene. In this line, Polo's cDNA has been fused to GFP and combined with its own regulatory elements. Note that both Polo::GFP lines (protein trap in (a) and transgenic line in (b)) show the pool of Polo associated with the PCM. **(C)** Yeast-two Hybrid experiments, testing for direct molecular interactions between Cnb, Polo and Wdr62. Positive and negative controls are on the left. Positive interactions are denoted with a (+), negative interactions with a (-). See Experimental procedures for details.

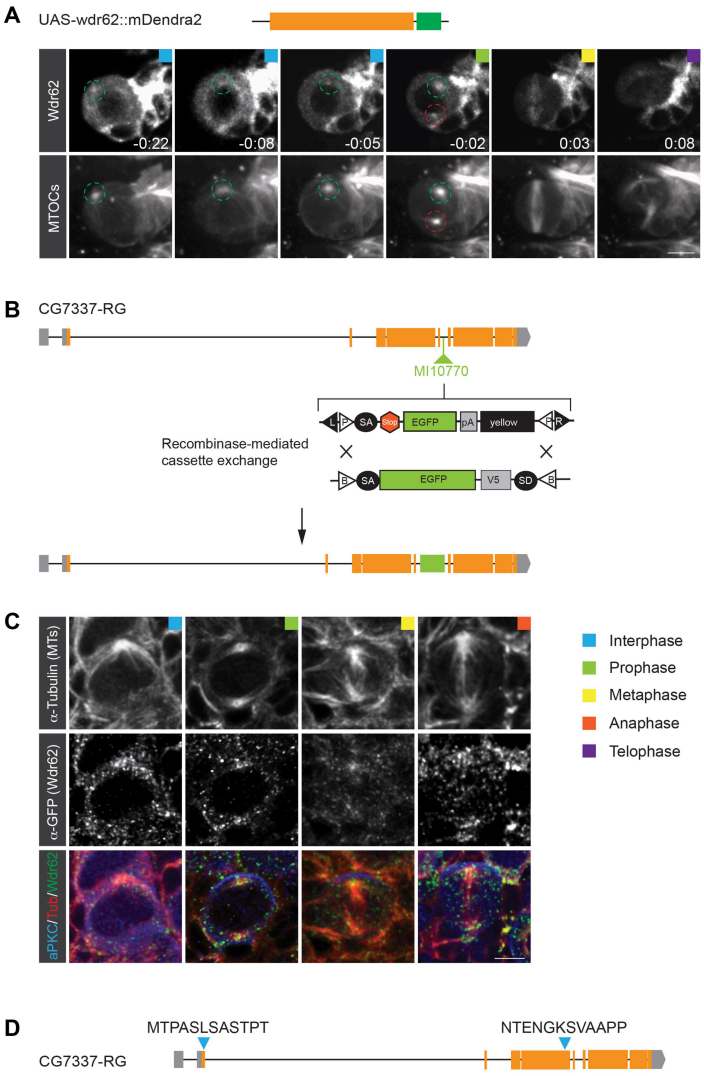


**Figure S3: Wdr62 is a MT-associated protein, related to Figure 4**
**(A)** Image sequence of a wild type neuroblast, expressing *UAS-CG7337::mDendra2*, driven by the neuroblast specific *worGal4* driver line. **(B)** The coding region of the longest *CG7337/wdr62* isoform, highlighting the location of the MiMIC cassette (green triangle), amenable for recombination mediated cassette exchange (RMCE). **(C)** Representative wild type neuroblast, expressing *wdr62::EGFP* (MiMIC line; in-frame fusion of GFP inserted into intron as shown in (b)), stained for a-GFP (green in overlay), alpha-Tubulin (red in overlay) and aPKC (blue in overlay). **(D)** The coding region of the longest *CG7337/wdr62* isoform, highlighting the locations (blue triangles) and sequence of the epitopes used to generate peptide antibodies. Colored boxes refer to cell cycle stages. Time in h:min; Scale bar is 5 μm.

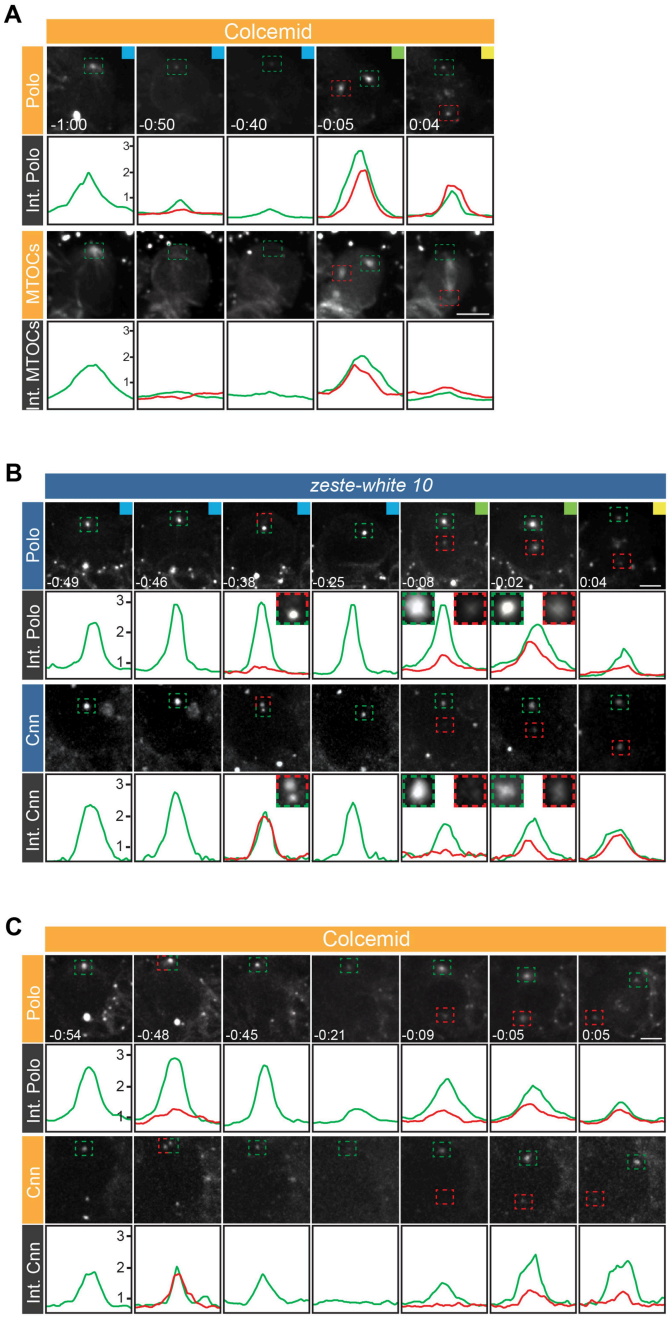
A
Colcemid
Polo
-1:00
-0:50
-0:40
-0:05
0:04
Int. Polo
MTOCs
Int. MTOCs
B
zeste-white 10
Polo
-0:49
-0:46
-0:38
-0:25
-0:08
-0:02
0:04
Int. Polo
Cnn
Int. Cnn
C
Colcemid
Polo
-0:54
-0:48
-0:45
-0:21
-0:09
-0:05
0:05
Int. Polo
Cnn
Int. Cnn

**Figure S4: microtubules are required to maintain Polo and Cnn on the apical interphase centrosome, related to Figure 4**

**(A)** Representative *zeste-white 10* mutant neuroblasts expressing Polo::GFP and the MTOC marker Jupiter::mCherry or **(C)** Cnn::mCherry exposed to low doses of colcemid. **(B)** Representative control image sequence of a *zeste-white 10* mutant neuroblast expressing Polo::GFP (top row) and the PCM marker Cnn::mCherry (bottom row). In all panels, the green and red lines below the image sequences represent Cnn, Polo or MT intensity values of the apical (green box) and basal (red box) centrosomes, respectively. Inserts show high magnification of the apical and basal centrosome for selected time points. Contrast and brightness has been adjusted for better visibility. Time in h:min; Scale bar is 5 μm.

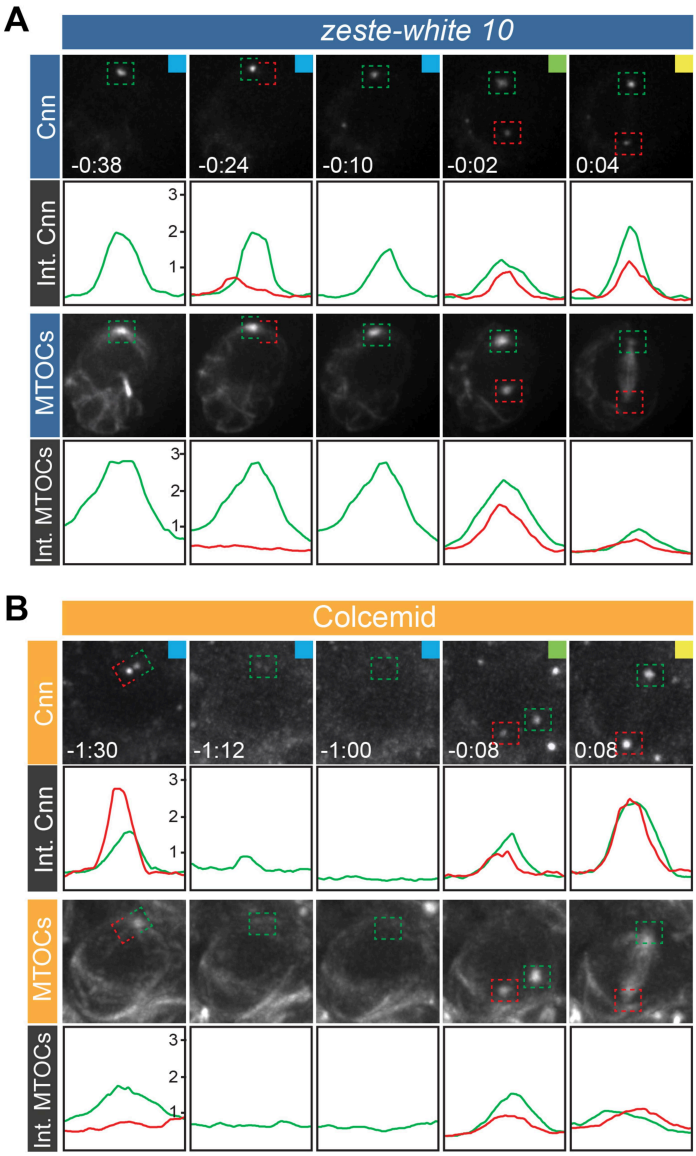


**Figure S5: Loss or gain of Cnn correlates with Polo localization, related to Figure 4**
**(A)** Representative *zeste-white 10* mutant control neuroblast expressing Polo::GFP and the MTOC marker Jupiter::mCherry. **(B)** *zeste-white 10* mutant neuroblast expressing Polo::GFP and the MTOC marker Jupiter::mCherry exposed to low doses of colcemid. The green and red lines below the image sequences represent Polo and MTOC intensity values of the apical (green box) and basal (red box) centrosomes, respectively. Time in h:min; Scale bar is 5 μm.

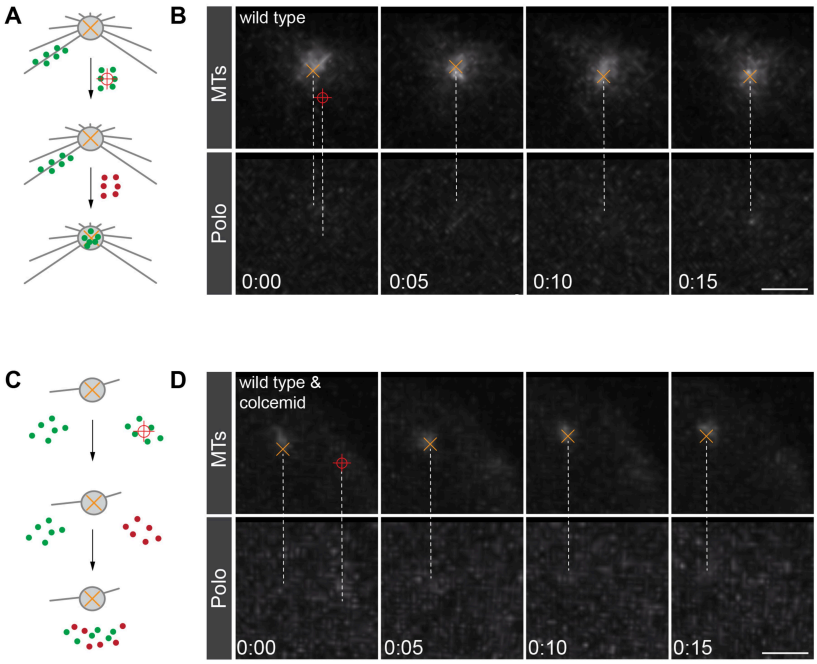


**Figure S6: Polo is traveling on MTs to the centrosome center, related to Figure 5**
**(A)** Cartoon illustrating a control photoactivation experiment in wild type neuroblasts. Green balls represent unconverted Polo::mDendra2 molecules localized to astral MTs (grey lines) or in the cytoplasm (white background). The red crosshair indicates the target area. **(B)** Representative image sequence of a wild type neuroblast expressing the microtubule marker G147 (MTs; top row; white) and Polo::mDendra2 (photoconverted in bottom row (white)). Red crosshairs represent the target area that was photoconverted. For this control experiment, the cytoplasm was targeted. Note that essentially no photoconverted Polo is detectable. **(C)** Cartoon illustrating a control photoactivation experiment in colcemid treated wild type neuroblasts. **(D)** Representative image sequence of a wild type, colcemid treated neuroblast expressing the microtubule marker G147 (MTs; top row; white) and Polo::mDendra2 (photoconverted in bottom row (white)). Note that MTs were not completely depolymerized. Yellow crosses represent the center of the centrosome. Time in h:min; Scale bar is 5 µm.

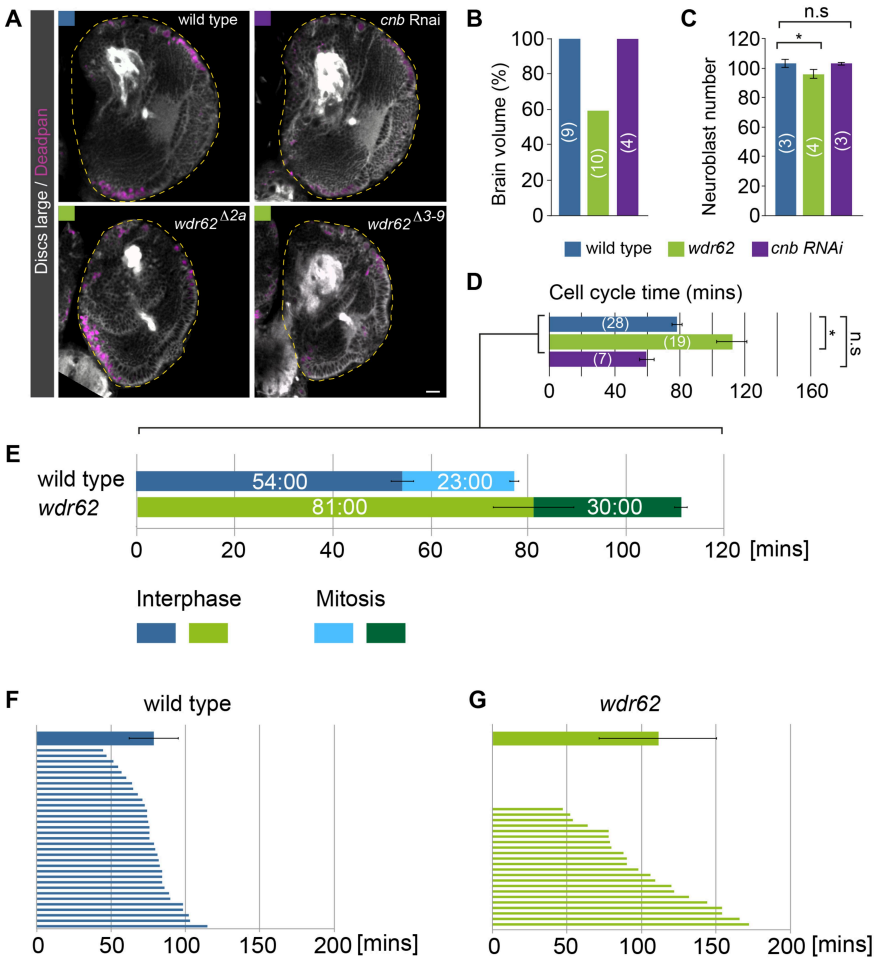


**Figure S7: *wdr62* mutant brains are decreased in size due to cell cycle defects, related to Figure 7**
**(A)** Sections of representative third instar brain lobes for the indicated genotypes and labeled with the cell membrane marker discs large (Dlg; white) and the neuroblast marker Deadpan (Dpn; magenta). **(B)** Brain volumes of wild type, *wdr62* and *cnb* RNAi are displayed as a percentage. **(C)** Neuroblast number and **(D)** cell cycle times are shown for the indicated genotypes (*wdr62*$^{\Delta 3\text{-}9}$*/Df(2L)Exel8005)*. **(E)** Cell cycle time was split up into interphase and mitosis for wild type (dark and light blue bars) and *wdr62* mutant (*wdr62*$^{\Delta 3\text{-}9}$*/Df(2L)Exel8005;* dark and light green bars) neuroblasts. **(F)** Cell cycle length (interphase and mitosis) measured for wild type **(F)** and **(G)** *wdr62* (*wdr62*$^{\Delta 3\text{-}9}$*/Df(2L)Exel8005*) mutant neuroblasts, all of which showing the centrosome asymmetry phenotype. Thin lines represent individual neuroblasts (blue; wild type, green; *wdr62* mutants) and the thicker bar on top denotes the average cell cycle time. For all panels, number of scored neuroblasts is indicated in brackets (n's). Error bars correspond to standard error of the mean (SEM). ***; $p < 0.0001$. **; $p < 0.001$, *; $p < 0.05$. n.s; not significant. Scale bar is 20 μm.

## Supplemental movies

**Movie 1: wild type neuroblasts maintain an active MTOC tethered to the apical cortex, related to Figure 1**
Wild type larval neuroblast expressing the centriolar marker DSas4::GFP (green) and the MTOC marker Cherry::Jupiter (white). Note that after centrioles separate (starting at 0:02:57), one centriole remains tethered to the apical cortex, maintaining an active MTOC. The mother centriole-containing centrosome downregulates MTOC activity, regaining it only at prophase (starting at 0:17:42). The neuroblast was imaged every 59s. Time scale is h:mm:ss:ms. The scale bar is 3 μm.

**Movie 2: *wdr62* mutants downregulate MTOC activity on the apical centrosome, related to Figure 1**
*wdr62* mutant larval neuroblast expressing the centriolar marker DSas4::GFP (green) and the MTOC marker Cherry::Jupiter (white). Note that the apical centriole loses the MTOC marker Cherry::Jupiter and moves away from the apical cortex. Maturation starts at 1:44:26. The neuroblast was imaged every 118s. Time scale is h:mm:ss:ms. The scale bar is 4 μm.

**Movie 3: Wild type centrosomes maintain γ-Tubulin on the active MTOC throughout the cell cycle, related to Figure 1**
Wild type larval neuroblast expressing the PCM marker γ-Tub::GFP (green in merged movie on the left; green in single channel movie on the right) and the MTOC marker Cherry::Jupiter (white; left movie). Note that the apical MTOC maintains γ-Tub::GFP throughout the cell cycle. The neuroblast was imaged every 57s. Time scale is h:mm:ss:ms. The scale bar is 2 μm.

**Movie 4: *wdr62* mutant neuroblasts downregulate γ-Tubulin on the active MTOC during interphase, related to Figure 1**
*wdr62* mutant larval neuroblast expressing the PCM marker γ-Tub::GFP (green in merged movie on the left; green in single channel movie on the right) and the MTOC marker Cherry::Jupiter (white; left movie). Note that the apical MTOC downregulates γ-Tub::GFP and Cherry::Jupiter significantly during interphase. Maturation starts simultaneously on both centrosomes (~2:36:29). The neuroblast was imaged every 89s. Time scale is h:mm:ss:ms. The scale bar is 2 μm.

**Movie 5: Wild type centrosomes maintain Polo on the active MTOC throughout the cell cycle, related to Figure 2**
Wild type larval neuroblast expressing Polo::GFP (green in merged movie on the left; green in single channel movie on the right) and the MTOC marker Cherry::Jupiter (white; left movie). Note that the apical MTOC maintains Polo::GFP throughout the cell cycle. The neuroblast was imaged every 47s. Time scale is h:mm:ss:ms. The scale bar is 2 μm.

**Movie 6: *wdr62* mutant neuroblasts downregulate Polo from the active MTOC, related to Figure 2**
*wdr62* larval neuroblast expressing Polo::GFP (green in merged movie on the left; green in single channel movie on the right) and the MTOC marker Cherry::Jupiter (white; left movie). Note that the apical MTOC downregulates Polo::GFP during interphase concomitantly with cherry::jupiter and loses its position on the apical cortex. The neuroblast was imaged every 90s. Time scale is h:mm:ss:ms. The scale bar is 2 μm.

**Movie 7: *polo*$^{1}$ mutant neuroblasts downregulate MTOC activity on apical centrosome, related to Figure 2**
*polo*$^{1}$ mutant larval neuroblast expressing the centriolar marker DSas4::GFP (green) and the MTOC marker Cherry::Jupiter (white). Note that the apical centriole loses the MTOC marker Cherry::Jupiter and moves away from the apical cortex. Maturation starts normally at 1:11:02. The neuroblast was imaged every 118s. Time scale is h:mm:ss:ms. The scale bar is 3 μm.

## Supplemental Experimental Procedures

**Fly strains and genetics:** All mutant chromosomes were balanced over CyO actin::GFP or TM6B, Tb. The following fly strains were used: Oregon-R (wild type), *Df(2L)Exel8005,* (a deficiency removing the entire *wdr62* locus and adjacent genes; Bloomington stock center), *polo*$^{1}$ (Sunkel and Glover, 1988), *cnb* RNAi (v28651; VDRC), *wdr62*$^{\Delta 2a}$, *wdr62*$^{\Delta 3\text{-}9}$ (this work), *zeste-white 10* (Bloomington stock center). Until otherwise noted, mutants were crossed over the corresponding deficiency and analyzed in a heteroallelic combination. Transgenes and fluorescent markers: *pUbq-DSas4::GFP* (Peel et al., 2007), *pUbq-Cnb::YFP* (Januschke et al., 2013), *pUASp-YFP-cnb::PACT* (Januschke et al., 2013), *worGal4, pUAST-cherry::Jupiter* (Cabernard and Doe, 2009), *ncd-γ-Tub::EGFP* (Hallen et al., 2008), *polo::GFP*$^{CC01326}$ (protein trap line; (Buszczak et al., 2007)).

**Generation of *wdr62* alleles:** *wdr62*$^{\Delta 2a}$: the piggyBac insertion line *PBac{PB}CG7337(c04508)* and *PBac{PB}CG7337(c04728)* (Exelixis) were crossed to *hsFlp* and the resulting progeny was heat shocked at 37°C to induce Flipase activity according to previously published protocols (Thibault et al., 2004). *wdr62*$^{\Delta 3\text{-}9}$*:* Target-specific sequences with high efficiency were chosen using the CRISPR optimal target finder (http://tools.flycrispr.molbio.wisc.edu/targetFinder/) and DRSC CRISPR Efficiency Predictor web tools (http://www.flyrnai.org/evaluateCrispr/). These sequences were then cloned into pU6-BbsI-chiRNA (Gratz et al., 2013). To generate the replacement donor, 1kb homology arms flanking the target sequences at 5' and 3' ends were cloned into pHD-DsRed-attP. Flies expressing *nos-Cas9* (Ren et al., 2013) were injected with 5' and 3' specific target chiRNA and the replacement donor vector. Successful mutagenesis was detected by screening for DsRed+ eyes. Constitutively active Cre (Bloomington stock center) was crossed in to remove the DsRed marker.

**Generation of *wdr62::GFP* and *cnn::mCherry* MiMIC lines:** *Mi{MIC}-CG7337(MI0770)* and *Mi{MIC}-cnn(MI08383)* (Venken et al., 2011) was crossed to phiC31 integrase (expressed under the vasa promotor; Bloomington stock center) and the resulting progeny were injected with GFP and mCherry exchange cassettes, respectively (Venken et al., 2011). Positive lines were initially screened for loss of yellow body marker and the orientation of the insert was checked by PCR.

**Generation of transgenic lines:** Generation of *pUASt-wdr62RA::mDendra2*: *wdr62-RA* was PCR amplified from the full length cDNA (DGRC clone LD01189) and cloned into *pUASt-attB* using Kpn1 and Not1. The construct was injected into attP(VK00033) (Venken et al., 2006) flies. *pUbq-Cnb::YFP* and *cnn::mCherry* were recombined onto *wdr62*$^{\Delta 2a}$ using standard genetic procedures. All UAS transgenes were expressed using *worGal4* (Albertson and Doe, 2003).
Generation of *polo::mDendra2: Polo::mDendra2* was cloned into *pattB* vector using In-Fusion Multiple fragment cloning (Clontech). *Polo 5'UTR* and *mDendra2* were PCR amplified and inserted between XhoI and NdeI restriction site, followed by inserting PCR amplified *Polo* coding and *Polo 3'UTR* between NdeI and BamHI restriction sites. *pattB-polo::mDendra* was injected into attP40 and attP(VK00027) landing sites (Genetic Services).

**Antibodies used:** The following primary antibodies were used: rabbit anti-aPKC (1:1000; Santa Cruz Biotechnology), mouse anti-γ-tub (Sigma; 1:500), guinea pig anti-Deadpan (1:1000, gift from J. Skeath), rat anti-α-Tub (Serotec; 1:1000), mouse anti-Discs large (1:100; Developmental Study Hybridoma Bank (DSHB)), mouse anti-α-Tub (DM1A, Sigma; 1:2500), guinea-pig anti-Bazooka (1:1000), rat anti-Pins (1:400) (gift from Fumio Matsuzaki), mouse anti-Pros (1:1000), rat and guinea-pig anti-Mira (1:500) (gifts from Chris Doe), rabbit anti-Numb (1:100; gift from J. Knoblich), rabbit anti-Asl (1:500), rabbit anti-Plp (1:1000; gift from N. Rusan), rabbit anti-Sas4 (1:250), rabbit anti-Cnn (1:1000) (gifts from J. Raff). Secondary antibodies were from Molecular Probes and the Jackson Immuno laboratory.

**Immunostainings**: 96-120h (AEL; after egg laying) larval brains were dissected in Schneider's medium (Sigma) and fixed for 20 min in 4% paraformaldehyde in PEM (100mM PIPES pH 6.9, 1mM EGTA and 1mM $MgSO_4$). After fixing, the brains were washed with PBSBT (1X PBS, 0.1% Triton-X-100 and 1% BSA) and then blocked with 1X PBSBT for 1h. Primary antibody dilution was prepared in 1X PBSBT and brains were incubated overnight at 4 °C. Brains were washed with 1X PBSBT four times for 20 minutes each and then incubated with secondary antibodies diluted in 1X PBSBT at 4 °C overnight. The next day, brains were washed with 1X PBST (1x PBS, 0.1% Triton-X-100) four times for 20 minutes each and kept in Vectashield (Vector laboratories) mounting media at 4 °C. For brain size stainings, embryo collections were done every 4 hours and the larvae were incubated at 25°C until 120h AEL.
**Image Acquisition**: Fixed samples were imaged using an inverted Leica TSC SPE confocal microscope. For representative images a 60X/1.40NA oil immersion objective was used. For 4X scans a z-step size of 0.3 µm and

for 1X scans a z-step size of 1.0 µm was used. Live samples were imaged with an Andor revolution spinning disc confocal system, consisting of a Yokogawa CSU-X1 spinning disk unit and two Andor iXon3 DU-897-BV EMCCD cameras. A 60X/1.4NA oil immersion objective mounted on a Nikon Eclipse Ti microscope was used for most images. Live imaging voxels sizes are 0.22 X 0.22 X 0.5µm (60x/1.4NA spinning disc).

**Live imaging sample preparation**: 5ml Schneider's insect medium (Sigma-Aldrich S0146) was mixed with 5µL of 0.5M ascorbic acid (Sigma-Aldrich A4034) and 50µL of HyClone bovine growth serum (Thermo Scientific SH3054102) immediately before use and warmed up to room temperature. This imaging medium was supplemented with fat bodies of ~ 10 *yw* third instar larvae. 96-120hr AEL old mutant or wild type larval brains were dissected in imaging medium. The dissected brains, along with fat bodies, were transferred onto a gas-permeable membrane (YSI Life Sciences 5793), fitted on a metallic slide. Brains were oriented with the brain lobes facing the coverslip. Excess media was removed until the brain lobes were in contact with the coverslip. The sample was sealed with Vaseline (Cabernard and Doe, 2013).

**Super–Resolution 3D Structured Illumination Microscopy (3D-SIM):** 3D-SIM was performed on fixed brain samples using a DeltaVision OMX-Blaze system (version 4; Applied Precision, Issaquah, WA), equipped with 405, 445, 488, 514, 568 and 642 nm solid-state lasers. Images were acquired using a Plan Apo N 60x, 1.42 NA oil immersion objective lens (Olympus) and 4 liquid-cooled sCMOs cameras (pco Edge, full frame 2560 x 2160; Photometrics). Exciting light was directed through a movable optical grating to generate a fine-striped interference pattern on the sample plane. The pattern was shifted laterally through five phases and three angular rotations of 60° for each z section. Optical z-sections were separated by 0.125 µm. The laser lines 488, 568 and 642 nm were used for 3D-SIM acquisition. Exposure times were typically between 3 and 100 ms, and the power of each laser was adjusted to achieve optimal intensities of between 5,000 and 8,000 counts in a raw image of 15-bit dynamic range at the lowest laser power possible to minimize photobleaching. Multichannel imaging was achieved through sequential acquisition of wavelengths by separate cameras.

**Definition of interphase and mitosis time and calculation of cell cycle length:**
Interphase was defined as the time window from the end of telophase until prophase, when centrosome maturation set in, manifested in the appearance of the basal MTOC. Mitosis was defined as the window from prophase until the end of telophase. The spindle/MTOC marker Cherry::Jupiter was used to determine the different cell cycle stages. Whenever possible, neuroblasts were also considered undergoing two divisions within the time span of the movie recordings. In these instances, cell cycle times were measured from two repeating and recognizable cell cycle stages (e.g metaphase 1 – metaphase 2).

**Detection and counting of neuroblasts:** We dissected carefully staged wild type, *cnb* RNAi expressing (v28651; VDRC) and $wdr62^{\Delta 2a}$ mutant third instar larvae (120h after egg laying) and stained with the neuroblast markers Deadpan (Dpn) and Discs large 1 (Dlg1). $Dpn^{+}$ neuroblasts were counted in 3D reconstructions using Imaris imaging software (spot function).
*cnb* was knocked-down by crossing the neuroblast specific worniu-Gal4 (worGal4) driver (Albertson and Doe, 2003) to v28651. WorGal4 turns on in the embryonic CNS and is also active in all larval stages.

**3D-SIM Image Reconstruction:** Raw 3D-SIM images were processed and reconstructed using the DeltaVision OMX SoftWoRx software package (Applied Precision; (Gustafsson, 2000)). The resulting size of the reconstructed images was of 512 x 512 px from an initial set of 256 x 256 raw images. The channels were aligned in the image plane and around the optical axis using predetermined shifts as measured using a target lens and the SoftWoRx alignment tool. The channels were then carefully aligned using alignment parameter from control measurements with 0.5 µm diameter multi-spectral fluorescent beads (Invitrogen, Molecular Probes).

**Image processing and calculations**: Images were processed using Imaris x64 7.5.2 and Fiji. Andor IQ2 files were converted into Imaris files using a custom-made Matlab code. Centrosomes were tracked in live and fixed samples using the spot tool in Imaris, which calculated the mean intensities specific to where the spot was placed. Asymmetry indices were calculated by dividing the apical centrosome to the basal centrosome. To calculate the position of each centrosome during maturation in live samples, the angle of each maturing centrosome, using the cell center as the reference point in relation to the future division axis, was calculated. Spindle orientation in fixed samples was measured by determining the coordinates of the center of maximum intensity of apical and basal crescents, respectively. These coordinates were used to calculate a polarity axis vector. Spindle axis vector were calculated using similar methods. Custom-made Matlab codes were used to calculate the angle between polarity and spindle vectors in 3D. The spindle orientation correction factor was determined from live imaging experiments by calculating the angle between two spindle vectors: (1) a spindle vector at the beginning of metaphase and (2) the spindle vector at the end of metaphase, respectively. Brain volumes were calculated in fixed samples by manually

generating a surface on the brain lobe using the surface tool in Imaris. Intensity profiles of centrosomes and MTs were generated in Fiji. Maximum intensity projections were generated and a line was used to measure the intensity at the centriole position. Using a Macro, this line was duplicated onto the channel to be measured. Pictures were assembled in Adobe Illustrator CS6. Quantifications and graphical representations were generated in Microsoft Excel.
3D SIM Image Analysis: The reconstructed images were converted to OME-TIFF files and 3D heat plots were generated using a custom made MATLAB code. Representative images were taken in Imaris after interpolation.

**Definition of apical and basal centrosome**
Apical and basal centrosomes are distinguished based on two criteria: (1) we experimentally determined in *wdr62* mutants that the $Cnb^{+}$ centriole maintains MTOC activity longer than the $Cnb^{-}$ centrosome. Since the apical centrosome contains the $Cnb^{+}$ centriole in wild type neuroblasts, we therefore consider the centrosome maintaining MTOC for a longer time to be the apical centrosome. (2) We experimentally determined that apical centrosomes in interphase neuroblasts contain more Polo in both wild type and *wdr62* mutants.

**Supplemental References**

Albertson, R., and Doe, C.Q. (2003). Dlg, Scrib and Lgl regulate neuroblast cell size and mitotic spindle asymmetry. Nat. Cell Biol. *5*, 166–170.

Buszczak, M., Paterno, S., Lighthouse, D., Bachman, J., Planck, J., Owen, S., Skora, A.D., Nystul, T.G., Ohlstein, B., Allen, A., et al. (2007). The carnegie protein trap library: a versatile tool for Drosophila developmental studies. Genetics *175*, 1505–1531.

Cabernard, C., and Doe, C.Q. (2013). Live Imaging of Neuroblast Lineages within Intact Larval Brains in Drosophila. Cold Spring Harbor Protocols *2013*, 970–977.

Cabernard, C., and Doe, C.Q. (2009). Apical/basal spindle orientation is required for neuroblast homeostasis and neuronal differentiation in Drosophila. Dev. Cell *17*, 134–141.

Gratz, S.J., Cummings, A.M., Nguyen, J.N., Hamm, D.C., Donohue, L.K., Harrison, M.M., Wildonger, J., and O'Connor-Giles, K.M. (2013). Genome engineering of Drosophila with the CRISPR RNA-guided Cas9 nuclease. Genetics *194*, 1029–1035.

Gustafsson, M.G.L. (2000). Surpassing the lateral resolution limit by a factor of two using structured illumination microscopy. J Microsc *198*, 82–87.

Hallen, M.A., Ho, J., Yankel, C.D., and Endow, S.A. (2008). Fluorescence recovery kinetic analysis of gamma-tubulin binding to the mitotic spindle. Biophys. J. *95*, 3048–3058.

Januschke, J., Reina, J., Llamazares, S., Bertran, T., Rossi, F., Roig, J., and Gonzalez, C. (2013). Centrobin controls mother–daughter centriole asymmetry in Drosophila neuroblasts. Nat. Cell Biol. *15*, 241–248.

Peel, N., Stevens, N.R., Basto, R., and Raff, J.W. (2007). Overexpressing centriole-replication proteins in vivo induces centriole overduplication and de novo formation. Curr. Biol. *17*, 834–843.

Ren, X., Sun, J., Housden, B.E., Hu, Y., Roesel, C., Lin, S., Liu, L.-P., Yang, Z., Mao, D., Sun, L., et al. (2013). Optimized gene editing technology for Drosophila melanogaster using germ line-specific Cas9. Proceedings of the National Academy of Sciences *110*, 19012–19017.

Sunkel, C.E., and Glover, D.M. (1988). polo, a mitotic mutant of Drosophila displaying abnormal spindle poles. Journal of Cell Science *89 ( Pt 1)*, 25–38.

Thibault, S.T., Singer, M.A., Miyazaki, W.Y., Milash, B., Dompe, N.A., Singh, C.M., Buchholz, R., Demsky, M., Fawcett, R., Francis-Lang, H.L., et al. (2004). A complementary transposon tool kit for Drosophila melanogaster using P and piggyBac. Nat Genet *36*, 283–287.

Venken, K.J.T., He, Y., Hoskins, R.A., and Bellen, H.J. (2006). P[acman]: a BAC transgenic platform for targeted insertion of large DNA fragments in D. melanogaster. Science *314*, 1747–1751.

Venken, K.J.T., Schulze, K.L., Haelterman, N.A., Pan, H., He, Y., Evans-Holm, M., Carlson, J.W., Levis, R.W., Spradling, A.C., Hoskins, R.A., et al. (2011). MiMIC: a highly versatile transposon insertion resource for engineering Drosophila melanogaster genes. Nat. Methods *8*, 737–743.

# Manuscript III

## 4.3 3D-structured illumination microscopy of Centriolar and Centrosomal proteins in *Drosophila melanogaster* neuroblasts

Anjana Ramdas Nair[1], Priyanka Singh[1,2], Emmanuel Gallaud[1], Alexia Isabelle Loynton-Ferrand[1] and Clemens Cabernard[1]

[1] Biozentrum, University of Basel
Klingelbergstrasse 50-70
CH-4056 Basel, Switzerland

[2] Present address:
Max-Planck Institute of Molecular Physiology
Department of Mechanistic Cell Biology
Otto-Hahn-Str. 11
D-44227 Dortmund, Germany

**Unpublished Data**

## Summary

Centrosomes are the microtubule organizing centers (MTOCs) of eukaryotic cells, consisting of a pair of centrioles, surrounded by a matrix of pericentriolar proteins. *Drosophila* neuroblasts consist of physical and molecular asymmetric centrosomes (Conduit and Raff, 2010; Januschke et al., 2011). This asymmetry is necessary for correct centrosome positioning, spindle orientation and centrosome segregation (Rebello et al., 2007; Rusan and Peifer , 2007). However, the mechanisms underlying the establishment of centrosome asymmetry are incompletely understood. Here, we have used super-resolution 3D-structured illumination microscopy (3D-SIM) to better understand the spatial relationship of key pericentriolar proteins and centriolar components of *Drosophila* neuroblast centrosomes at different cell cycle stages.

We found that centriolar proteins localize either as a dot at the center of the centriole or in a ring-like structure along the centriolar wall. For instance, Sas-6 was detectable as a dot at the core of the centriole, consistent with its role in cartwheel formation. Interestingly, Sas-6 formed a dot next to the older centriole soon after centriole separation at interphase, indicating that Sas-6 is an early marker for the site of nascent centriole formation. The other centriolar wall proteins including Bld10 and Sas-4 start localizing to the walls of the nascent centriole by prometaphase. Pericentrin-like protein (PLP) and Polo asymmetrically localize on centrioles as has been previously reported with confocal imaging. This asymmetric localization was observed after centrosomes separated during interphase. Remarkably, our data suggests that Polo starts to localize on the nascent centriole from metaphase onwards while Plp remains on the older centriole. These results suggest that molecular markers involved in establishing centrosome asymmetry have a very precise segregation pattern based on the age of the centrioles and using 3D-SIM, we are able to define the time points of the

occurrence of these events.

## Introduction

Recent reports have already established the use of 3D-SIM to better understand centrosome architecture in different model systems (Sillibourne et al. 2011; Fu and Glover 2012; Lau et al. 2012; Lawo et al. 2012; Mennella et al. 2012; Sonnen et al. 2012). Our understanding of the *Drosophila* neuroblasts' centrosome architecture is limited and this would be the first attempt to investigate these centrosomes in higher resolution. This is interesting as it contributes to our knowledge of centrosome structure conservation among species and secondly, in understanding centrosome asymmetry. A mammalian centrosome consists of two centrioles, called a diplosome; the older mother centriole and the younger daughter centriole. Centrosome duplication is a tightly regulated process and usually begins with the formation of the cartwheel at an orthogonal position to each of the existing centrioles within the centrosome during interphase (Azimzadeh and Bornens, 2007; Strnad and Gönczy, 2008; Gönczy, 2012; Pelletier et al., 2006). Soon after cartwheel formation, the centriole wall begins to form and elongate (Mahjoub et al. 2010; Comartin et al. 2013; Lin et al. 2013b). In *Drosophila* neuroblasts, it was not clear for a very long time whether separating centrosomes already contain a full diplosome or a single centriole instead. Furthermore, the time point of centriole duplication was also not known. In 2011, it was proposed that in neuroblasts, centriole duplication occurred after centrosomes separated (Januschke et al. 2011). It was also confirmed that neuroblast centrosomes contain only a single centriole instead of two centrioles. However, the exact time point of centriole duplication was still not defined.

Asymmetric centrosome behavior has been documented in various model systems including flies and mice. The correlation between unequal centrosomes and cell fate has been an area of keen interest. Drosophila centrosomes are asymmetric in terms of age, molecular composition and its ability to maintain PCM proteins. Key centrosomal proteins involved in establishing centrosome asymmetry are Cnb, Plp and Polo.

## Results and Discussion

### Spatial organization of key centriolar and centrosomal proteins in Drosophila neuroblasts

Using 3D-SIM, we proceeded to examine the spatial relationship between eight centriolar/PCM components at different cell cycle stages in fixed *Drosophila* neuroblasts. For this purpose, we used an assortment of well-characterized antibodies and transgenic lines expressing centriolar and centrosomal proteins tagged with GFP (see methods). Neuroblasts at interphase after centrosome separation revealed that centriolar proteins localized in either a dot or ring-like structure. For instance, the cartwheel proteins Sas-6 and Ana-2 localized as compact dots whereas Bld10 and Sas4 localized as ring-like structures of varying diameters corresponding to their localization on the centriolar wall (Figure 1(A)). The analysis of PCM components revealed two separate overlapping domains. Plp and Asl localize as rings of much larger diameter compared to centriolar wall components. Cnn on the other hand formed a scaffold-like structure with a hollow center farther away from the centriole walls. Polo kinase (Plk1 in humans) was the only protein to localize both to the centriolar wall and in the PCM, supporting its function as a key regulator of the centrosome cycle in *Drosophila* neuroblasts. Maximum intensity projections of interphase neuroblasts were used to do diameter measurements. Based on these

measurements, we were able to divide the neuroblast centrosome into four sections: Cartwheel, Centriole wall, Centriole-PCM interface and PCM (Figure 1(B)). However, the boundaries of these sections are hard to define as large centrosomal proteins may overlap with other sections especially in cases where proteins comprise of extended coiled-coil domains. For example, Asl and Plp have been reported to localize with their carboxy terminal towards the centriole wall and amino terminal stretched outwards into the PCM (Sonnen et al 2012; Menella et al. 2012) and hence they are referred to here as Centriole-PCM interface proteins.

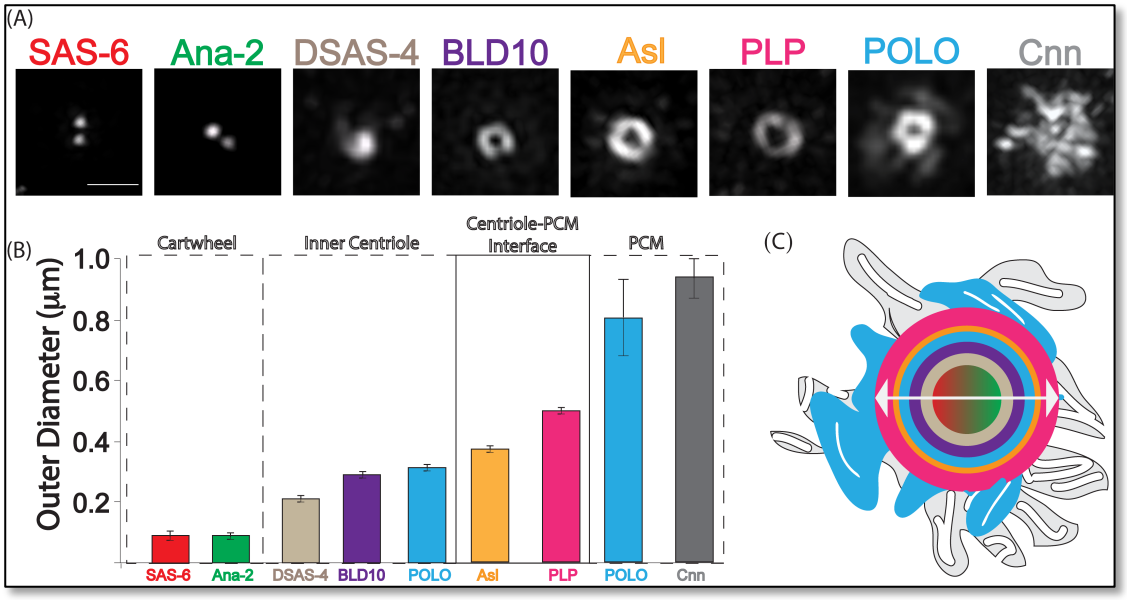


**Figure1. 3D SIM of centrosomal proteins revealed four distinct structural domains within the neuroblast centrosome:** A) Representative images of interphase neuroblasts stained for the indicated markers (scale bar 0.5um) (B) shows the average diameter of each protein. Please note that Polo appears as a centriolar and dispersed PCM pool. (C) Graphical representation of centriolar/centrosomal protein arrangement in interphase fly neuroblasts. Colours correspond to indicated markers in (A) and (B)

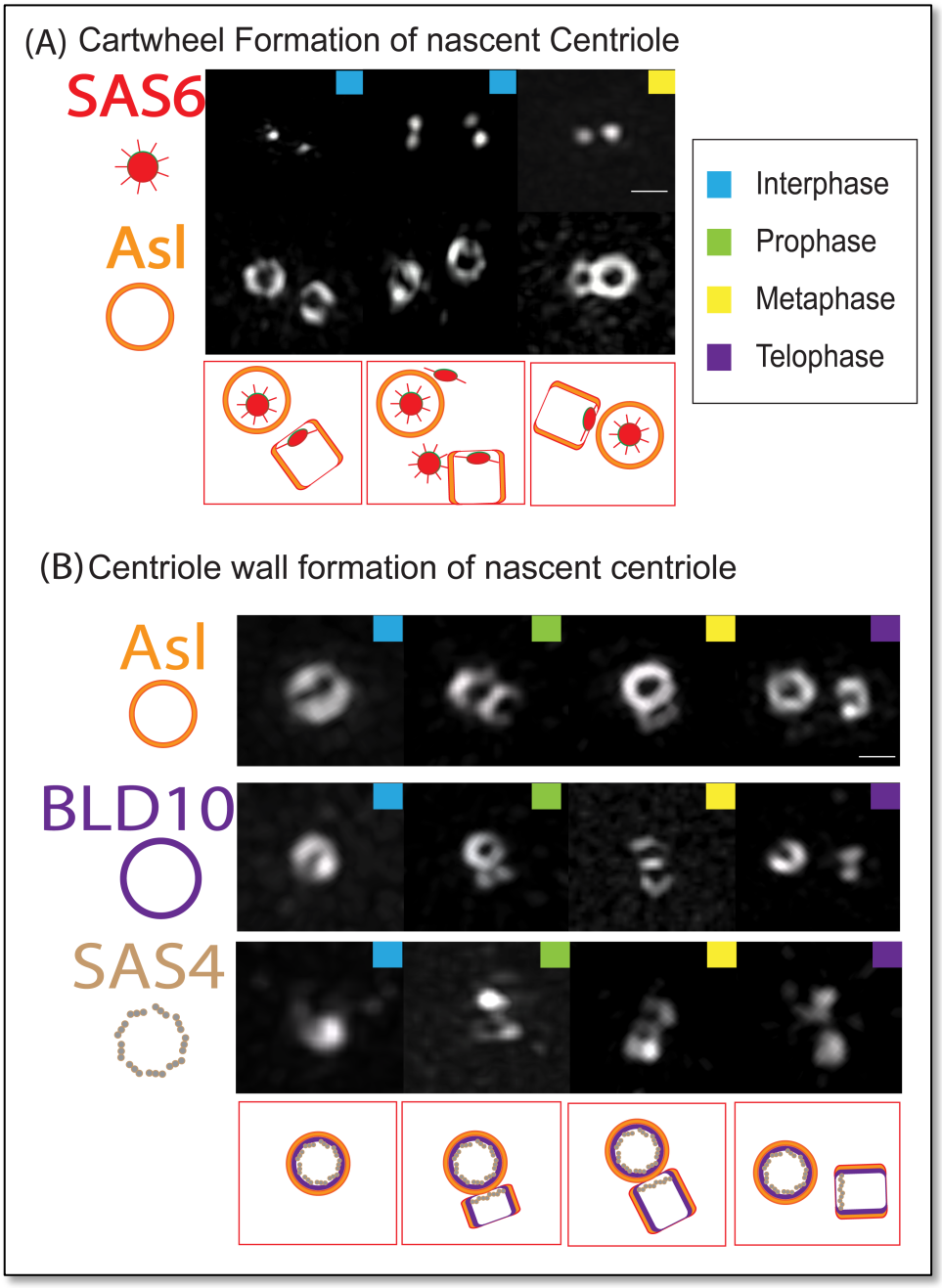


**Figure 2. Centriole duplication begins during interphase soon after centriole separate**: (A) Centrioles stained with Asl (Centriole Wall) and expressing SAS-6::GFP (cartwheel) indicate that cartwheel formation of the nascent centriole starts soon after centrioles separate. (B) Inner centriolar and centriolar wall components such as SAS-4, Bld10 begins to localize to the nascent centriole wall during Prophase. .

(A)&(B) bottom row are representations of centriole duplication process (Asl:Orange, Sas-6: Red, Bld10: Purple, Sas-4: Beige) Scale bar 0.5um

**Temporal regulation of Centriole duplication**

We performed 3D-Structured illumination microscopy (SIM) imaging using Sas6::GFP, Asl and Mira in fixed neuroblasts. Neuroblasts were imaged at various cell cycle stages to determine the time point of centriole duplication. We found that as long as the centrioles were still close together, the centrioles are unable to initiate cartwheel formation (Figure 2A). Cartwheel formation starts as soon as the centrioles have separated a certain distance indicated by the presence of another Sas-6 dot orthogonal to the existing centriole. Hence, it can be concluded that soon after centriole separation, cartwheel formation occurs and later both centrosomes separate. Moreover, 3D-SIM of fixed neuroblasts from interphase to telophase expressing Bld10::GFP and stained for Asl revealed that centriole wall formation starts at prophase and is complete by metaphase (Figure 2B). However, 3D-SIM live imaging is necessary to better understand the temporal regulation of centriole duplication and protein localization onto the nascent centriole.

**Timing of centrosome asymmetry establishment on apical centrosome**

Since we were able to follow nascent centriole formation and protein localization, we questioned when exactly does the nascent centriole start to recruit centrosome asymmetry markers such as Polo and Plp. To understand how centrosome asymmetry is established we analysed fixed neuroblasts expressing Polo::GFP (protein trap) stained with Plp using 3D-SIM through different stages of the neuroblast cell cycle. Since Polo is maintained in robust amounts on the apical daughter centrosome, and Plp

is upregulated on the mother centrosome, we used these markers in order to differentiate between the older and the younger centriole (Figure 3A). We found that during metaphase both centrosomes already display centrosome asymmetry. The newly formed centriole starts to accumulate more Polo compared to the older one. Plp on the other hand remains on the older centriole (Figure 3B&C). Hence, during metaphase, centrioles are already asymmetric before they disengage and separate in the next cell cycle and thus, the centrosome cycle is always one cycle ahead of the cell cycle(Figure 4).

The key to understanding centrosome asymmetry would be to understand what controls the transfer of Polo to the younger nascent centriole and blocks Plp on the older centriole. This could be because Centrobin starts to be expressed on the nascent centriole. Centrobin undergoes Polo phosphorylation and hence Polo starts to accumulate on the younger centriole. There is very little evidence to conclude whether the presence of Cnb is sufficient to prevent Plp localization on the new centriole but this could be a possibility (Lerit and Rusan, 2013). The other possibility is that an identified factor is responsible for anchoring Plp to the mother centriole. Further studies are necessary to conclude what interactions are involved in this elaborate process of centrosome asymmetry establishment. Further imaging involving *Cnb* and *bld10* mutants, where centrosome asymmetry is compromised, would be clear indicators of how this process is regulated.

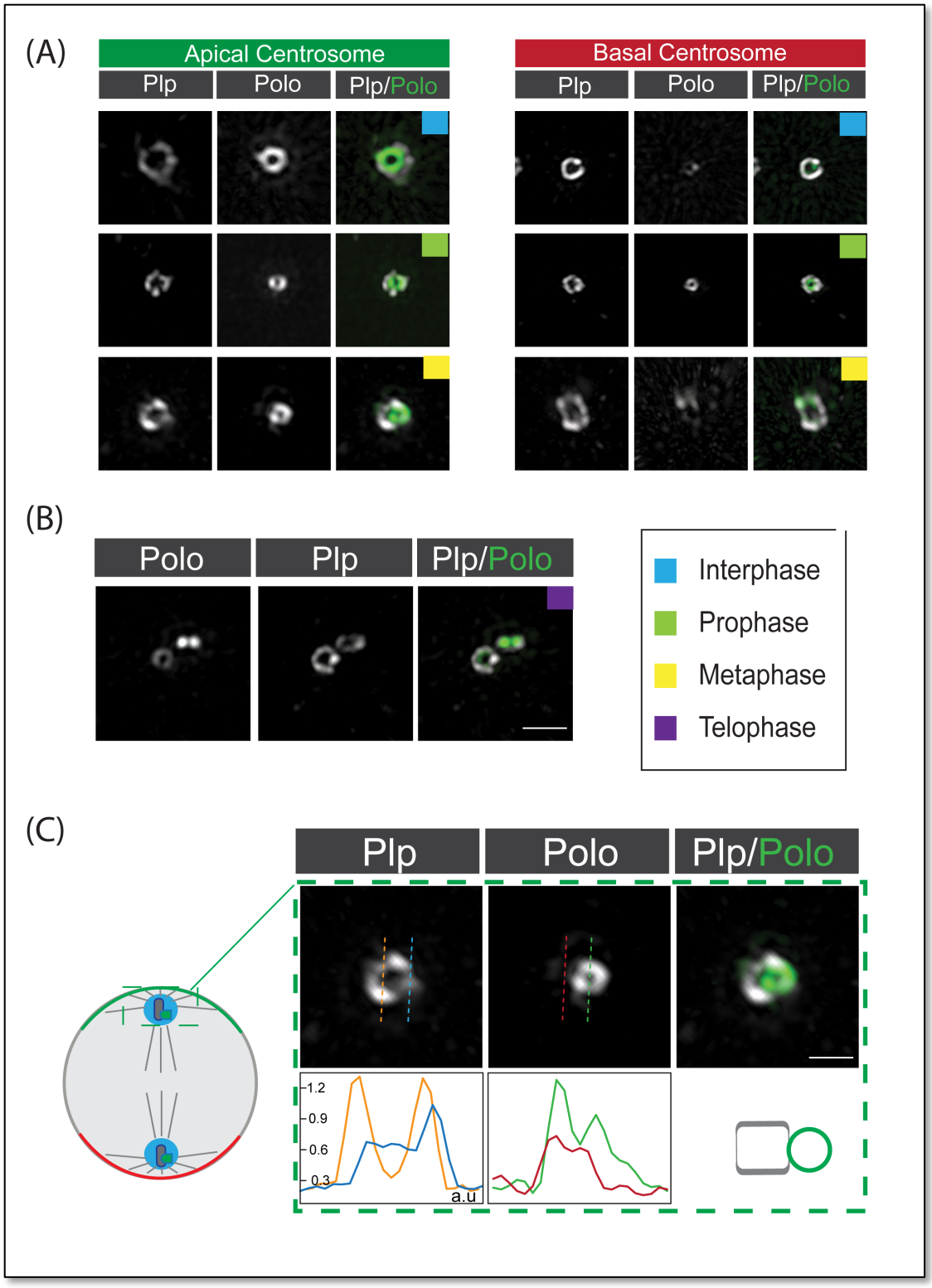


**Figure 3 Polo and Plp are asymmetric at metaphase** (A) Representative images of Polo and Plp on apical and basal centrosome from Interphase to Metaphase (B) Representative images of Polo and Plp showing clear asymmetry at telophase as has

been published. (C) Representative image of the apical centrosome at metaphase. Bottom row shows intensity plots corresponding to dotted line in the images above. Blue and orange lines correspond to Plp. Green and Red lines to Polo. Scale bar 0.5um

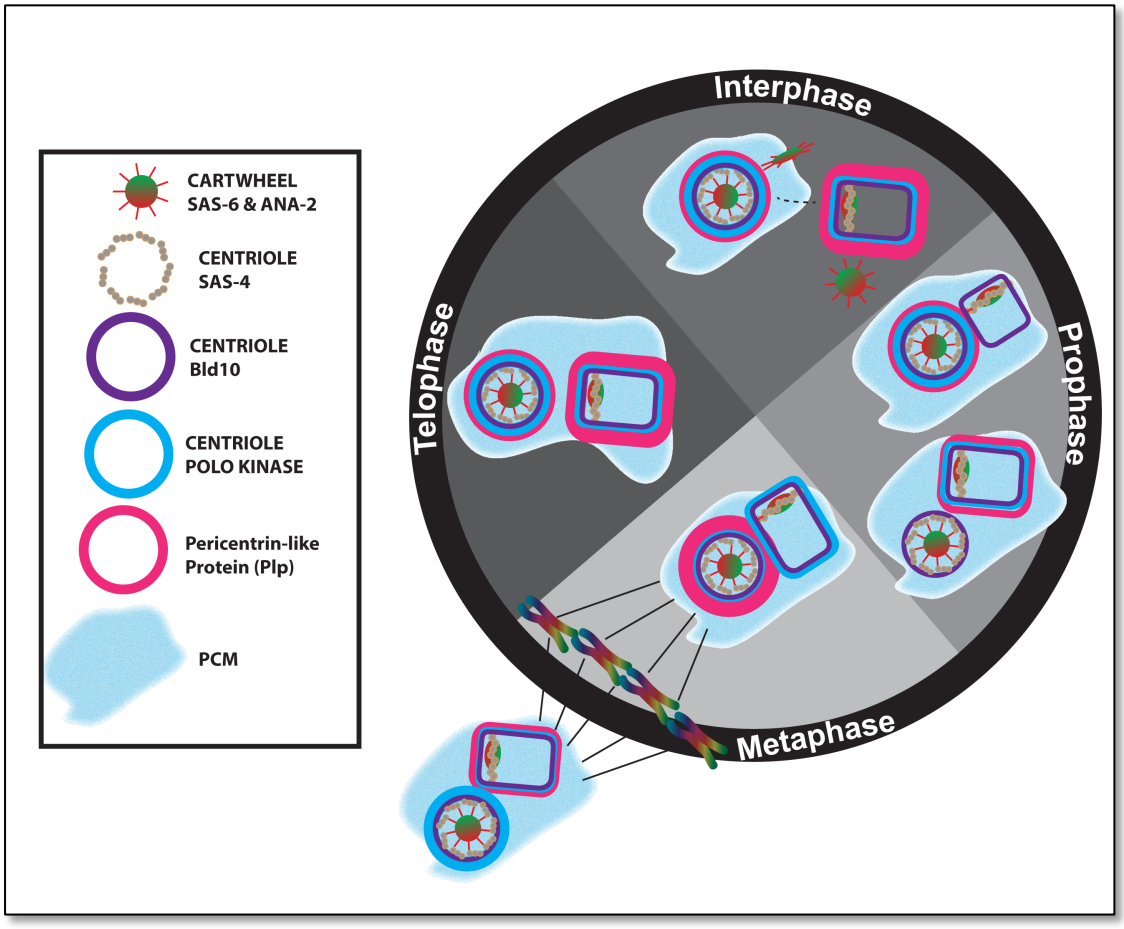


**Figure 4. Centrosome Cycle in *Drosophila* Neuroblasts .** At telophase, the centrosome consists of two centrioles, one centriole displays robust amounts of Polo kinase (Blue) and the other centriole maintains high level of Plp (Pink). Shortly after cytokinesis, in interphase, the centrioles begin to separate (indicated by dotted line) and begin cartwheel formation for procentriole assembly. By prophase, when both centrosomes mature, the centriolar markers such as bld10 (Purple) start to localise to

the wall of the procentrioles. At metaphase, Polo starts localizing on the procentriole and Plp remains on the older centriole and hence the centrioles are already asymmetric.

## Methods

Fly strains and genetics: The following transgenes and fluorescent markers were used: pUbq-DSas4::GFP, pUbq-GFP::DSas6, pUbq-Ana2::GFP, (from Raff group), polo::GFPCC01326 (protein trap line; Buszczak et al. 2007), bld10::GFP expressing bld10 under the endogenous promoter (Blachon et al. 2008).

Antibodies: The following primary antibodies were used: rat anti-α-Tub (Serotec; 1:1000) , mouse anti-α-Tub (DM1A, Sigma; 1:2500), rat and guinea-pig anti-Mira (1:500) (gifts from Chris Doe), rabbit anti-Asl (1:500), rabbit anti-Plp (1:1000; gift from N. Rusan), rabbit anti-Sas4 (1:250), rabbit anti-Cnn (1:1000) (gifts from J. Raff). Secondary antibodies were from Molecular Probes and the Jackson Immuno laboratory.

Immunostaining: 96-120h (AEL; after egg laying) larval brains were dissected in Schneider's medium (Sigma) and fixed for 20 min in 4% paraformaldehyde in PEM (100mM PIPES pH 6.9, 1mM EGTA and 1mM MgSO4). After fixing, the brains were washed with PBSBT (1X PBS, 0.1% Triton-X-100 and 1% BSA) and then blocked with 1X PBSBT for 1h. Primary antibody dilution was prepared in 1X PBSBT and brains were incubated overnight at 4 °C. Brains were washed with 1X PBSBT four times for 20 minutes each and then incubated with secondary antibodies diluted in 1X PBSBT at 4 °C, overnight. The next day, brains were washed with 1X PBST (1x PBS, 0.1% Triton-X-100) four times for 20 minutes each and kept in Vectashield (Vector laboratories) mounting media at 4 °C.

Super–Resolution 3D Structured Illumination Microscopy (3D-SIM): 3D-SIM was performed on fixed brain samples using a DeltaVision OMX-Blaze system (version 4; Applied Precision, Issaquah, WA), equipped with 405, 445, 488, 514, 568 and 642 nm solid-state lasers. Images were acquired using a Plan Apo N 60x, 1.42 NA oil immersion objective lens (Olympus) and 4 liquid-cooled sCMOs cameras (pco Edge, full frame 2560 x 2160; Photometrics). Exciting light was directed through a movable optical grating to generate a fine-striped interference pattern on the sample plane. The pattern was shifted laterally through five phases and three angular rotations of 60° for each z section. Optical z-sections were separated by 0.125 µm. The laser lines 405, 488, 568 and 642 nm were used for 3D-SIM acquisition. Exposure times were typically between 3 and 100 ms, and the power of each laser was adjusted to achieve optimal intensities of between 5,000 and 8,000 counts in a raw image of 15-bit dynamic range at the lowest laser power possible to minimize photobleaching. Multichannel imaging was achieved through sequential acquisition of wavelengths by separate cameras.

3D-SIM Image Reconstruction: Raw 3D-SIM images were processed and reconstructed using the DeltaVision OMX SoftWoRx software package (Applied Precision; Gustafsson, M. G. L. 2000). The resulting size of the reconstructed images was of 512 x 512 px from an initial set of 256 x 256 raw images. The channels were aligned in the image plane and around the optical axis using predetermined shifts as measured using a target lens and the SoftWoRx alignment tool. The channels were then carefully aligned using alignment parameter from control measurements with 0.5 µm diameter multi-spectral fluorescent beads (Invitrogen, Molecular Probes).

# 5. DISCUSSION

Unequal centrosomes arise due to differences in age, size and/or molecular composition between the two centrosomes and this has been referred to as 'centrosome asymmetry'. It has been implied that this asymmetry is not only necessary to form a normal bipolar spindle, it also seems to affect centrosome segregation a variety of cells (Januschke and Nathke , 2014). Recent reports have hypothesized that cell specific centrosome segregation pattern may have a role in cell fate in asymmetrically dividing cells (Yamashita et al., 2007; Cheng et al., 2008). In support of this hypothesis, in mouse neuroprogenitor cells missegregation of the younger centrosome into the stem cell causes loss of stem cell identity. (Wang et al. 2009) This leads to a scenario where the cell switches into differentiation mode and hence reducing the number of neuroprogenitor cells. Hence, I am interested in understanding the role of centrosome asymmetry in *Drosophila* neuroblasts' cell cycle progression, cell fate and overall development of the fly brain.

*Drosophila* neuroblast centrosomes are intrinsically asymmetric; the daughter centrosome maintains PCM and MTOC activity and the mother centrosome downregulates MTOC activity. In a gene candidate approach we decided to study Bld10 (Cep135 in humans) and CG7337 (WDR62 in humans) since its vertebrate orthologs have been implicated in centrosome regulation as well as Microcephaly. Furthermore, we used super resolution microscopy to understand localization of various centrosomal proteins, which gave us insight into how the centrosome cycle is regulated in neuroblasts as well as when centrosome asymmetry is established.

## 5.1 The centriolar proteins Bld10 and Plp work together to downregulate Polo kinase on the mother centrosome

Bld10, the ortholog of human Cep135, has been implicated in cartwheel formation and centriole duplication in *Chlamydomonas* and *Paramecium* (Hiraki et al, 2007; Jerka-Dziadosz et al, 2010). However, in *Drosophila*, its been established that while bld10 is not necessary for cartwheel formation, it plays an integral role in stabilizing the connection of the centriole wall to outer centriolar wall components (Roque et al. 2012). Bld10 has also been known to assemble and stabilize central microtubule pair formation in flagella biogenesis during *Drosophila* spermatogenesis (Mottie-Pavie and Megraw, 2009; Carvalho-Santos et al., 2012). In *Drosophila* neuroblasts, we observed that *bld10* mutant neuroblasts failed to downregulate PCM proteins and MTOC activity on the mother centrosome. In wild type neuroblasts, we show that the mother centrosome after separation sheds PCM proteins such as Cnn, γ-Tub and Msps in order to establish unequal centrosomes. Our live imaging experiments in mutant neuroblasts suggest that the two active MTOCs are maintained because Polo is not downregulated from the mother centriole-containing centrosome. Another protein that seems to be implicated in downregulating Polo on the mother centrosome is Plp (Lerit and Rusan, 2013). Consistent with the role of Plp in blocking Polo on the mother centrosome, Plp is upregulated on the mother centriole compared to the daughter during interphase. Loss of Plp shows a phenotype similar to *bld10* mutants. However Bld10 and Plp do not interact directly based on our yeast two hybrid data. Therefore, based on these results, we concluded that Bld10 and Plp work in parallel pathways, required to shed Polo mother centrosome. As a consequence of perturbed centrosome asymmetry, mutant neuroblasts displayed misaligned spindles that were rescued by anaphase onset. The prominent defect of centrosome asymmetry we observed was

missegragation of centrosomes. In wild type neuroblasts, the daughter centrosome normally remains in the neuroblasts (Conduit and Raff, 2010; Januschke et al., 2011). In *bld10* mutants, the mother centrosome was retained in approximately 50% of neuroblasts. However, the consequence of missegregation of centrosomes is still unknown. Hence, we were able to report the novel role of Bld10 in establishing centrosome asymmetry in *Drosophila* neuroblasts.

## 5.2 The Microtubule binding protein Wdr62 is required for microtubule stability and timely mitotic entry

WDR62 is a spindle pole protein required for normal mitotic progression and brain development in humans (Nicholas et al., 2010; Yu et al., 2010; 21. Bilgüvar et al., 2010; Chen et al., 2014). Due to the conservation between human WDR62 and *Drosophila* CG7337, henceforth we will refer to CG7337 as Wdr62. In *Drosophila* neuroblasts, I was able to show that Wdr62 co-localizes with microtubules during the cell cycle, consistent with its human ortholog. I also observed by live imaging that *wdr62* mutant neuroblasts tend to lose MTOC activity on the apical centrosome during interphase giving rise to cells with naked centrioles. Moreover, when these mutant neuroblasts were subjected to cold treatment, the majority of cells displayed reduced MTOC activity while wild type cells still maintained MTOC activity. In addition, cold treatment of neuroblasts overexpressing Wdr62 in wild type background was sufficient for stabilization of microtubules and displayed longer microtubules. Taken together, these findings support the conclusion that Wdr62 is necessary for microtubule stability in general. However, the exact molecular mechanism remains to be identified. Since Wdr62 expression in other mutants such as Cnb and Pins does not rescue the loss of MTOC activity phenotype, its fair to

consider that there are still other molecular players involved that are upstream of Wdr62. I also observed that *wdr62* mutant neuroblasts show a significant amount of cell cycle delay in comparison to wild type. This cell cycle delay could affect the development of the fly brain as the cells proliferate at a much slower rate. When we compared brain size of *wdr62* to wild type, we observed a 40% decrease in brain volume owing to developmental delay. The role of Wdr62 in stabilizing microtubules and regulating mitotic entry are consistent with earlier publications in mice (Chen et al. 2014).

### 5.3 The role of microtubules in maintaining Polo kinase on the daughter centrosome

An important regulator of establishing centrosome asymmetry is Polo. Polo kinase ensures that centriolar and PCM proteins such as Cnb, Cnn, Asp and γ-Tubulin complexes are activated by phosphorylation and recruited to the centrosome in order to establish and maintain its microtubule activity (Conduit et al., 2014; Lane and Nigg, 1996; Lee and Rhee, 2011; Sunkel and Glover, 1988). We observed that during interphase in wild type neuroblasts, Polo is maintained in robust amounts on the apical daughter centrosome due to phosphorylation of Cnb and downregulation of Plp (Januschke et al. 2013;Lerit and Rusan 2013). The mother centrosome sheds Polo due to Plp upregulation and Bld10. As mentioned earlier, *wdr62* mutant neuroblasts displayed complete loss of MTOC activity on the daughter centrosome. Live imaging of Polo in mutant neuroblasts revealed that the apical centrosome have drastically low levels of Polo.

To further examine this defect, we used 3D-SIM (Structured Illumination Microscopy) to visualize the interphase apical centrosome in higher resolution. In

wild type the apical centrosome have two separate pools of Polo; a centriolar pool and an outer PCM pool. Two separate pools of Polo have been observed before during mitosis in Drosophila S2 cells and reported in Fu and Glover, 2012. In *wdr62* mutant neuroblasts, the PCM pool of Polo was completely lost. Moreover, we observed that the apical centrosome maintained high amounts of Plp unlike in wild type. Similar observations were made when microtubules were depolymerized using colcemid drug treatment. This led to the hypothesis that Polo recruitment to the centrosome and maintenance of PCM polo depends on stable microtubules. We confirmed this by using photoconversion and observed cytoplasmic photoconverted Polo molecules travel through microtubules to accumulate on the centrosome. Moreover photoconverted Polo failed to accumulate at the centrosome in colcemid treated neuroblasts. Hence, we were able to conclusively show the role of stable microtubules in Polo recruitment and maintenance during Interphase. We were able to further confirm based on live imaging of colcemid-treated neuroblasts that PCM proteins such as Cnn also require microtubules for their constant turnover.

## 5.4 Novel insight into centriole duplication and centrosome asymmetry establishment

Our knowledge of centrosome organization in *Drosophila* was for a very long time limited to data from electron microscopy. More recently, with the application of 3D-SIM, there have been reports about centrosome organization in *Drosophila* S2 cells and spermatocytes (Fu and Glover, 2012; Mennella et al., 2012). This revealed that centrosome organization between different populations of cells from the same animal could be different. Hence, our curiosity led us to investigate the spatial and temporal regulation of centrosomal and centriolar proteins using 3D-SIM. Our initial analysis

revealed that the neuroblasts centrosome could be divided into four structural domains: Cartwheel (a compact dot like structure); Centriole wall (a ring–like structure); Centriole-PCM interface proteins (a ring-like structure of much greater diameter than the centriole) and PCM (scaffold). Imaging of Sas6 and Asl at different cell cycle stages revealed that centriole duplication begins as soon as centrioles separate and Bld10 starts to localize to the centriole wall by Prophase. Hence, for the first time, we are able to describe the centrosome cycle with such in depth details in *Drosophila* neuroblasts. Based on this result, we questioned when exactly is centrosome asymmetry established. Existing reports based on conventional confocal microscopy suggests that asymmetry is established after centrosomes separate when proteins like Polo and Plp show asymmetric localization (Conduit and Raff, 2010; Januschke et al., 2013). We confirmed the asymmetric localization of Polo and Plp on the daughter and mother centrosome, respectively. Interestingly, in metaphase, when the nascent centriole is already present, Polo remains on one centriole while Plp remains on the other. Based on the literature, Plp stays on the older centriole (Lerit and Rusan, 2013). Therefore we can predict Polo stays on the nascent centriole. Although ideally, this would needs to be further verified using Cnb as a daughter centriole specific marker. Based on these results, we can conclude that centrioles duplicate soon after centriole separation and newly formed centrioles localize Polo and Plp asymmetrically by metaphase. This asymmetric localization ensures that in the next cell cycle the mother centrosome loses MTOC activity and the daughter centrosome maintains MTOC activity. Hence, centrosome cycle is always ahead of the cell cycle in *Drosophila* neuroblasts.

## 5.5 New players and methods redefine the centrosome asymmetry model in *Drosophila* neuroblasts

Centrosome asymmetry in neuroblasts is key to accurate spindle orientation and faithful centrosome segregation. Hence there has been growing interest in discovering the molecular players that control centrosome asymmetry. Polo, Cnb and Plp are the known players involved in establishing centrosome asymmetry. These three proteins were combined in a very simplistic model describing how Polo-phosphorylated Cnb is necessary for maintenance of MTOC activity on the daughter centrosome and Plp blocks Polo recruitment on mother centrosome (Lerit and Rusan, 2013; Januschke et al., 2013). Based on our findings, we are able to add to the existing model of centrosome asymmetry establishment and maintenance.

The centriolar protein Bld10 works with Plp in ensuring that the mother centrosome sheds PCM proteins and downregulates MTOC activity. However, Plp localizes normally in *bld10* mutants indicating that Plp localization is independent of Bld10. This leads us to the hypothesis that they could be part of parallel pathways involved in downregulating Polo on the mother centrosome. Moreover, we were not able to conclusively prove that Bld10 is involved in the same pathway described before. Hence, there should be other molecular players involved that interact with Bld10 to ensure that mother centriole remains naked.

Another uncharacterized protein involved in maintaining centrosome asymmetry is Wdr62. Although, its human counter part has been implicated in mitotic progression and spindle formation, WDR62's role in centrosome asymmetry is unknown. Wdr62 controls the maintenance of centrosome asymmetry by maintaining stable microtubule array ensuring proper recruitment of Polo and PCM proteins. This turnover of Polo is impaired in the scenario where microtubules are unstable and have tendency to

depolymerize. If Polo molecules were not available freely in the PCM for phosphorylating and activating proteins Cnn involved in PCM retention and microtubule nucleation, this would further reduce its capability to nucleate microtubules. Hence, the maintenance of MTOC activity on the daughter centrosome can be described as a feedback loop. Decrease in the amount of Polo on the daughter centrosome could also affect the phosphorylation of Cnb. It is hypothesized that Polo phosphorylated Cnb blocks Plp upregulation on the apical centrosome (Lerit and Rusan, 2013). Hence, reduced Polo phosphorylation of Cnb could lead to Plp being upregulated. Therefore in parallel to the feedback loop involving PCM proteins for microtubule maintenance, there is a negative feedback loop ensuring that Plp levels are correctly maintained.

To clearly understand how centrosome asymmetry is regulated, we need to understand when centrosomes become asymmetric. Recent reports have proposed that this asymmetry is established at Interphase once the centrioles separate (Rebello et al., 2007; Rusan and Peifer, 2007; Januschke and Gonzalez, 2010; Januschke et al., 2013; Lerit and Rusan, 2013). 3D-SIM imaging of neuroblasts, however, revealed that centrioles were already asymmetric before separation. In fact, they became asymmetric by metaphase when the nascent centriole was formed. Polo transfers to the younger nascent centriole and Plp remains on the older centriole. This is could Cnb dependent as Cnb undergoes Polo phosphorylation and hence Polo starts to accumulate on the younger centriole. There is very little evidence to conclude whether the presence of Cnb is sufficient to prevent Plp localization on the new centriole but this could be a possibility (Lerit and Rusan, 2013). The other possibility is that an identified factor is responsible for anchoring Plp to the mother centriole. A recently published report from Rusan group has confirmed that Plp interaction with

Calmodulin is necessary for its localization to the centrosome (Galleta et al., 2014). This interaction is key for Plp recruitment and maintenance of Plp levels on the centrosome. Calmodulin is a calcium binding messenger protein known in *C.elegans* to play in promoting meiotic spindle formation (van der Voet et al., 2009). Hence, Calmodulin could be the factor locking Plp on the older centriole, preventing it form moving to the new centriole. Further studies are necessary discover other proteins involved this elaborate process of centrosome asymmetry establishment.

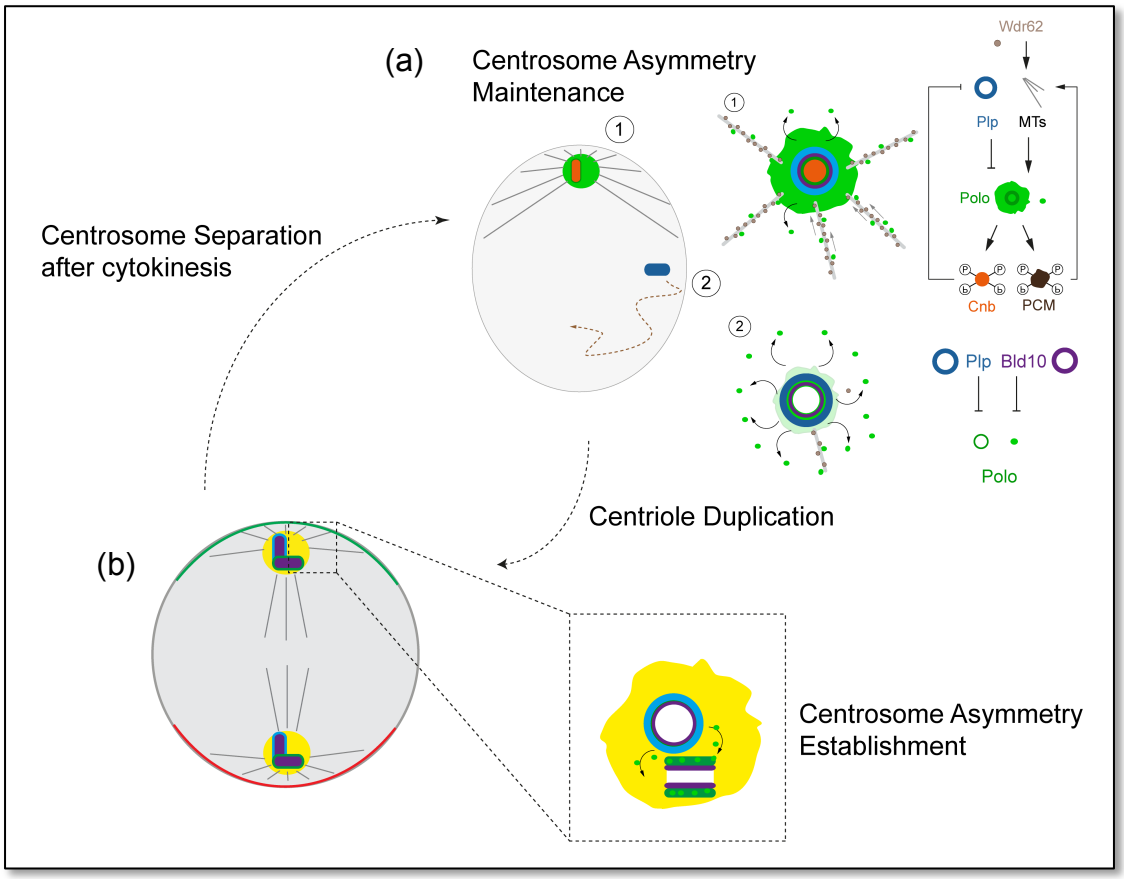


**Figure 1. Centrosome asymmetry establishment and maintenance during the *Drosophila* neuroblast cell cycle**. (a) Centrosome asymmetry maintenance: 1. After centriole separation, the daughter centriole maintains PCM and microtubules.This is primarily due to the presence of Polo (Green) which phosphorylates Cnb (Orange) to

keep Plp (blue) levels low and maintain MTOC activity. However, Polo is constantly turned over during interphase and Polo requires stable microtubules for its turnover. Wdr62 is necessary for stabilization of microtubules and ensuring maintenance of MTOC activity by active recruitment of Polo. 2.On the mother centrosome, Plp is maintained at high levels and along with Bld10 (Purple), it blocks Polo from being recruited on the mother centrosome. Hence the mother centrosome sheds PCM and loses MTOC activity. (b) Centrosome asymmetry establishment: During metaphase, the older centriole retains Plp and Polo relocates to the the newly formed procentriole (indicated by green dots and arrows). This asymmetry gives the centrioles identity in order that the daughter centriole maintains MTOC activity and the mother centriole becomes naked.

**5.6 Is perturbed centrosome asymmetry a cause for microcephaly?**

Mutations in Cep135 and Wdr62 are known to cause microcephaly in humans. In *Drosophila* neuroblasts, loss of Cep135/Bld10 and Wdr62 causes defects in centrosome asymmetry during interphase. This leads to spindle misalignment and wrongful centrosome segregation. Moreover, both mutants tend to show a reduced brain size phenotype compared to wildtype. The spindle misalignment is rescued by unknown rescue mechanisms by anaphase onset and cells continue to divide asymmetrically and hence cannot contribute to the brain size phenotype.

In mouse neuroprogenitor cells, the mother centrosome is retained by the stem cell in order to maintain stemness. We are yet to rule out whether the missegregation of the centrosomes affects cell fate in neuroblasts. It could be interesting to verify whether this has any affect on the neuroblast's ability to continue dividing or on the ability of the GMC to differentiate into neuron/glia.

WDR62 is responsible for activating the c-Jun N-terminal protein kinases (JNK) pathway required for proper neurogenesis during mitosis. (Xu et al., 2014; Bogoyevitch et al., 2012). JNK activity is known to regulate apoptosis, neurodegeneration, cell differentiation and proliferation, etc. It has also been recently reported that Aurora Kinase A (AurA) is responsible for accumulation of WDR62 on spindle microtubules while JNK phosphorylation antagonizes WDR62 microtubule localization during mitosis (Lim et al. 2014). In the developing mouse brain widespread expression of Wdr62 was observed. Expression was seen in the ventricular zone and cortical plate, consistent with roles in progenitor cells and postmitotic neurons (Yu et al. 2010). Wdr62 mutant mice show an overall developmental delay and reduced brain size. Wdr62 interacts with Aur A during spindle formation and loss of Wdr62 cause cell cycle delays and cell death of neuroprogenitor cells (Chen et al. 2014). Wdr62 mutants also displayed significant cell cycle delay resulting in reduced brain size. *Wdr62* mutant neuroblasts also show a significant amount of cell cycle delay in comparison to wild type. As in the mouse model, the cell cycle delay could be AurA dependent. The other possibility is that due to loss of microtubule activity, the centrosome is no longer able to function as a signaling center. This cell cycle delay could affect the development of the fly brain as the cells proliferate at a much slower rate. In vertebrate model systems, Cdk/Cyclin complexes localize to centrosomes and their activity levels ensure timely transition through cell cycle phases (Arquint et al., 2014). However, further conclusive data is necessary to contemplate the role of Cdk/Cyclin complexes in *wdr62* mutant neuroblasts' timely mitotic entry.

### 5.7 Future direction and concluding remarks

This thesis, as the title suggests, a humble attempt in understanding a very precise tightly regulated structure known as the centrosome and how mitotic stem cells strive to make them clearly distinguishable. As Albert Einstein said, " To raise new questions, new possibilities, to regard old problems from a new angle, requires creative imagination and marks real advance in science". Our findings have not only added to the existing model of centrosome asymmetry but at the same time, brought new questions and ideas for the further understanding of the regulation of this tiny organelle.

Our work has convincingly established the role of Bld10 and Wdr62 in centrosome asymmetry. The consequences of disrupted centrosome asymmetry include spindle misalignment and centrosome missegregation. The impact of centrosome missegregation in neuroblasts is however unknown. Hence, further studies are necessary to understand the effect of disturbed centrosome asymmetry in development of the fly brain. For example, analyzing the mutants for defects in neuronal lineages, the development of the optic lobe and verifying that cell fate markers are correctly expressed in different cell types present in the brain. In addition, analyze if cells displaying centrosome asymmetry phenotype display apoptotic markers.

We described Polo regulation during interphase in avid detail for the first time. Since we were able to show that Polo and Cnn recruitment is dependent on microtubules, this would indicate that microtubule motor proteins are involved in transporting them. Kinesin and Dynein are microtubule motor proteins that travel along microtubules in opposite directions; Kinesin moves towards the plus end and Dynein moves towards the minus end. These proteins could be involved in regulating PCM protein

recruitment and turnover. In *Drosophila*, Lis1 binds to dynactin and dynein motor complex to ensure accurate metaphase spindle orientation (Siller and Doe, 2008). The study of microtubule motor proteins will give us further insight into how Polo molecules move from the centrosome to the kinetochores and back to centrosome once again.

Last but not least, we were able to follow centriole duplication and centrosome asymmetry establishment using 3D- SIM that has never before been done in *Drosophila* neuroblasts. Although we were able to precisely time the events with help of cell cycle and centrosomal markers, it would be interesting to develop a method to perform live imaging using 3D-SIM. Live imaging opens a wide field of potential experiments including Fluorescence recovery after photobleaching (FRAP) and Photoactivation that could help us better understand protein dynamics.

# 6. ABBREVIATIONS

3D-SIM: Three Dimensional Structured Illumination Microscopy
ACD: asymmetric cell division
Ana2: anastral spindle 2
aPKC: atypical protein kinase C
Asp: abnormal spindle protein
Aur A: aurora A kinase
Baz: bazooka
Bld10: basal body protein 10
CASC5: cancer susceptibility candidate 5
Cdk: cyclin-dependent kinase
Cdk5rap2: CDK5 regulatory subunit-associated protein 2
Cep/CP: centrosomal protein
Cnb:centrobin
Cnn: centrosomin
CNS: central nervous system
CPAP: centrosomal P4.1-associated protein
CTL: cytotoxic T lymphocytes
C-Nap: centrosomal Nek2-associated protein
Dlg: discs large
GSC: germline stem cell
INP: intermediate progenitor
Insc: inscuteable
GMC: gangalion mother cell
MCPH: autosomal recessive primary microcephaly
MTOC: microtubule organizing center
Mira: miranda
Nedd1: neural precursor cell expressed developmentally down-regulated protein 1
Nek2: never in mitosis A-related kinase 2
PCM: pericentriolar material/matrix
Pins: partner of inscuteable
Plk: polo-like kinase
PLP: pericentrin-like-protein
POC: protein of centriole
Pon: partner of numb
SAS: spindle assembly abnormal
SPB: spindle pole body
SPD-2: spindle-defective protein 2
TACC: Transforming acidic coiled-coil
VNC: ventral nerve cord
WDR62: WD repeat domain 62
ZYG-1: zygote defective protein 1
γ -TuRC: gamma tubulin ring complex
γ-TuSC: gamma tubulin small complex

# 7. REFERENCES

1. Anderson, C. T., & Stearns, T. (2009). Centriole Age Underlies Asynchronous Primary Cilium Growth in Mammalian Cells. *Current Biology*, *19*(17), 1498–1502. http://doi.org/10.1016/j.cub.2009.07.034
2. Arquint, C., Gabryjonczyk, A.-M., & Nigg, E. A. (2014). Centrosomes as signalling centres. *Philosophical Transactions of the Royal Society B-Biological Sciences*, *369*(1650), –20130464. http://doi.org/10.1098/rstb.2013.0464
3. Arquint, C., Sonnen, K. F., Stierhof, Y.-D., & Nigg, E. A. (2012). Cell-cycle-regulated expression of STIL controls centriole number in human cells. *Journal of Cell Science*, *125*(5), 1342–1352. http://doi.org/10.1242/jcs.099887
4. Atwood, S. X., & Prehoda, K. E. (2009). aPKC Phosphorylates Miranda to Polarize Fate Determinants during Neuroblast Asymmetric Cell Division. *Current Biology*, *19*(9), 723–729. http://doi.org/10.1016/j.cub.2009.03.056
5. Azimzadeh, J., & Bornens, M. (2007). Structure and duplication of the centrosome. *Journal of Cell Science*, *120*(13), 2139–2142. http://doi.org/10.1242/jcs.005231
6. Azimzadeh, J., & Marshall, W. F. (2010). Building the Centriole. *Current Biology*, *20*(18), R816–R825. http://doi.org/10.1016/j.cub.2010.08.010
7. Bass, P. W., Ahmad, F. J., & Yu, W. (2000). Critical features of neuronal polarity are established by antagonistic motor forces that regulate microtubule organization and distribution. *Journal of Neurochemistry*, *74*, S1–S1.
8. Basto, R., Brunk, K., Vinadogrova, T., Peel, N., Franz, A., Khodjakov, A., & Raff, J. W. (2008). Centrosome amplification can initiate tumorigenesis in flies. *Cell*, *133*(6), 1032–1042. http://doi.org/10.1016/j.cell.2008.05.039
9. Basto, R., Lau, J., Vinogradova, T., Gardiol, A., Woods, C. G., Khodjakov, A., & Raff, J. W. (2006). Flies without centrioles. *Cell*, *125*(7), 1375–1386. http://doi.org/10.1016/j.cell.2006.05.025
10. Berdnik, D., & Knoblich, J. A. (2002). Drosophila aurora-A is required for centrosome maturation and actin-dependent asymmetric protein localization during mitosis. *Current Biology*, *12*(8), 640–647.
11. Bertran, M. T., Sdelci, S., Regué, L., Avruch, J., Caelles, C., & Roig, J. (2011). Nek9 is a Plk1-activated kinase that controls early centrosome separation through Nek6/7 and Eg5. *The EMBO Journal*, *30*(13), 2634–2647. http://doi.org/10.1038/emboj.2011.179
12. Bettencourt-Dias, M., Hildebrandt, F., Pellman, D., Woods, G., & Godinho, S. A. (2011). Centrosomes and cilia in human disease. *Trends in Genetics*, *27*(8), 307–315. http://doi.org/10.1016/j.tig.2011.05.004
13. Bettencourt-Dias, M., Rodrigues-Martins, A., Carpenter, L., Riparbelli, M., Lehmann, L., Gatt, M. K., et al. (2005). SAK/PLK4 is required for centriole duplication and flagella development. *Current Biology*, *15*(24), 2199–2207. http://doi.org/10.1016/j.cub.2005.11.042
14. Bilguvar, K., Ozturk, A. K., Louvi, A., Kwan, K. Y., Choi, M., Tatli, B., et al. (2010). Whole-exome sequencing identifies recessive WDR62 mutations in severe brain malformations. *Nature*, *467*(7312), 207–U93. http://doi.org/10.1038/nature09327
15. BORNENS, M. (2002). Centrosome composition and microtubule anchoring mechanisms. *Current*

*Opinion in Cell Biology*, *14*(1), 25–34. http://doi.org/10.1016/S0955-0674(01)00290-3

16. BORNENS, M., PAINTRAND, M., BERGES, J., MARTY, M. C., & KARSENTI, E. (1987). Structural and Chemical Characterization of Isolated Centrosomes. *Cell Motility and the Cytoskeleton*, *8*(3), 238–249. http://doi.org/10.1002/cm.970080305
17. Bowman, S. K., Neumuller, R. A., Novatchkova, M., Du, Q. S., & Knoblich, J. A. (2006). The Drosophila NuMA homolog mud regulates spindle orientation in asymmetric cell division. *Developmental Cell*, *10*(6), 731–742. http://doi.org/10.1016/j.devcel.2006.05.005
18. Carvalho-Santos, Z., Machado, P., Alvarez-Martins, I., Gouveia, S. M., Jana, S. C., Duarte, P., et al. (2012). BLD10/CEP135 Is a Microtubule-Associated Protein that Controls the Formation of the Flagellum Central Microtubule Pair. *Developmental Cell*, *23*(2), 412–424. http://doi.org/10.1016/j.devcel.2012.06.001
19. Chavali, P. L., Puetz, M., & Gergely, F. (2014). Small organelle, big responsibility: the role of centrosomes in development and disease. *Philosophical Transactions of the Royal Society B-Biological Sciences*, *369*(1650), –20130468. http://doi.org/10.1098/rstb.2013.0468
20. Chen, J.-F., Zhang, Y., Wilde, J., Hansen, K. C., Lai, F., & Niswander, L. (2014). Microcephaly disease gene Wdr62 regulates mitotic progression of embryonic neural stem cells and brain size. *Nature Communications*, *5*. http://doi.org/10.1038/ncomms4885
21. Choksi, S. P., Southall, T. D., Bossing, T., Edoff, K., de Wit, E., Fischer, B. E., et al. (2006). Prospero acts as a binary switch between self-renewal and differentiation in Drosophila neural stem cells. *Developmental Cell*, *11*(6), 775–789. http://doi.org/10.1016/j.devcel.2006.09.015
22. Comartin, D., Gupta, G. D., Fussner, E., Coyaud, E., Hasegan, M., Archinti, M., et al. (2013). CEP120 and SPICE1 Cooperate with CPAP in Centriole Elongation. *Current Biology*, *23*(14), 1360–1366. http://doi.org/10.1016/j.cub.2013.06.002
23. Conduit, P. T., & Raff, J. W. (2010). Cnn Dynamics Drive Centrosome Size Asymmetry Ito Ensure Daughter Centriole Retention in Drosophila Neuroblasts. *Current Biology*, *20*(24), 2187–2192. http://doi.org/10.1016/j.cub.2010.11.055
24. Conduit, P. T., & Raff, J. W. (2015). Different Drosophila cell types exhibit differences in mitotic centrosome assembly dynamics. *Current Biology : CB*, *25*(15), R650–1. http://doi.org/10.1016/j.cub.2015.05.061
25. Conduit, P. T., Brunk, K., Dobbelaere, J., Dix, C. I., Lucas, E. P., & Raff, J. W. (2010). Centrioles Regulate Centrosome Size by Controlling the Rate of Cnn Incorporation into the PCM. *Current Biology*, *20*(24), 2178–2186. http://doi.org/10.1016/j.cub.2010.11.011
26. Conduit, P. T., Feng, Z., Richens, J. H., Baumbach, J., Wainman, A., Bakshi, S. D., et al. (2014a). The Centrosome-Specific Phosphorylation of Cnn by Polo/Plk1 Drives Cnn Scaffold Assembly and Centrosome Maturation. *Developmental Cell*, *28*(6), 659–669. http://doi.org/10.1016/j.devcel.2014.02.013
27. Conduit, P. T., Richens, J. H., Wainman, A., Holder, J., Vicente, C. C., Pratt, M. B., et al. (2014b). A molecular mechanism of mitotic centrosome assembly in Drosophila. *Elife*, *3*, e03399. http://doi.org/10.7554/eLife.03399
28. Cottee, M. A., Muschalik, N., Johnson, S., Leveson, J., Raff, J. W., & Lea, S. M. (2015). The

homo-oligomerisation of both Sas-6 and Ana2 is required for efficient centriole assembly in flies. *Elife*, *4*, e07236. http://doi.org/10.7554/eLife.07236

29. Cottee, M. A., Muschalik, N., Wong, Y. L., Johnson, C. M., Johnson, S., Andreeva, A., et al. (2013). Crystal structures of the CPAP/STIL complex reveal its role in centriole assembly and human microcephaly. *Elife*, *2*. http://doi.org/10.7554/eLife.01071
30. Cottee, M. A., Raff, J. W., Lea, S. M., & Roque, H. (2011). SAS-6 oligomerization: the key to the centriole? *Nature Chemical Biology*, *7*(10), 650–653. http://doi.org/10.1038/nchembio.660
31. de Carcer, G., Avides, M. D., Lallena, M. J., Glover, D. M., & Gonzalez, C. (2001). Requirement of Hsp90 for centrosomal function reflects its regulation of Polo kinase stability. *Embo Journal*, *20*(11), 2878–2884.
32. Delattre, M., Leidel, S., Wani, K., Baumer, K., Bamat, J., Schnabel, H., et al. (2004). Centriolar SAS-5 is required for centrosome duplication in C-elegans. *Nature Cell Biology*, *6*(7), 656–664. http://doi.org/10.1038/ncb1146
33. Delgehyr, N., Rangone, H., Fu, J., Mao, G., Tom, B., Riparbelli, M. G., et al. (2012). Klp10A, a Microtubule-Depolymerizing Kinesin-13, Cooperates with CP110 to Control Drosophila Centriole Length. *Current Biology*, *22*(6), 502–509. http://doi.org/10.1016/j.cub.2012.01.046
34. Dictenberg, J. B., Zimmerman, W., Sparks, C. A., Young, A., Vidair, C., Zheng, Y., et al. (1998). Pericentrin and gamma-tubulin form a protein complex and are organized into a novel lattice at the centrosome. *Journal of Cell Biology*, *141*(1), 163–174.
35. Dix, C. I., & Raff, J. W. (2007). Drosophila Spd-2 recruits PCM to the sperm centriole, but is dispensable for centriole duplication. *Current Biology*, *17*(20), 1759–1764. http://doi.org/10.1016/j.cub.2007.08.065
36. Dobbelaere, J., Josue, F., Suijkerbuijk, S., Baum, B., Tapon, N., & Raff, J. (2008). A genome-wide RNAi screen to dissect centriole duplication and centrosome maturation in Drosophila. *Plos Biology*, *6*(9), 1975–1990. http://doi.org/10.1371/journal.pbio.0060224
37. Doxsey, S. J. (2005). Molecular links between centrosome and midbody. *Molecular Cell*, *20*(2), 170–172. http://doi.org/10.1016/j.molcel.2005.10.010
38. Doxsey, S. J., Stein, P., Evans, L., Calarco, P. D., & KIRSCHNER, M. (1994). Pericentrin, a highly conserved centrosome protein involved in microtubule organization. *Cell*, *76*(4), 639–650.
39. Doxsey, S., McCollum, D., & Theurkauf, W. (2005a). Centrosomes in cellular regulation. *Annual Review of Cell and Developmental Biology*, *21*(1), 411–434. http://doi.org/10.1146/annurev.cellbio.21.122303.120418
40. Doxsey, S., Zimmerman, W., & Mikule, K. (2005b). Chromosome segregation and aneuploidy series: Centrosome control of the cell. *Trends in Cell Biology*, *15*(6), 303–311. http://doi.org/10.1016/j.tcb.2005.04.008
41. Dutcher, S. K. (2003). Elucidation of basal body and centriole functions in Chlamydomonas reinhardtii. *Traffic*, *4*(7), 443–451. http://doi.org/10.1034/j.1600-0854.2003.00104.x
42. Dzhindzhev, N. S., Tzolovsky, G., Lipinszki, Z., Schneider, S., Lattao, R., Fu, J., et al. (2014). Plk4 Phosphorylates Ana2 to Trigger Sas6 Recruitment and Procentriole Formation. *Current Biology*, *24*(21), 2526–2532. http://doi.org/10.1016/j.cub.2014.08.061

43. Egger, B., Boone, J. Q., Stevens, N. R., Brand, A. H., & Doe, C. Q. (2007). Regulation of spindle orientation and neural stem cell fate in the Drosophila optic lobe. *Neural Development*, *2*(1), 1. http://doi.org/10.1186/1749-8104-2-1
44. Egger, B., Gold, K. S., & Brand, A. H. (2010). Notch regulates the switch from symmetric to asymmetric neural stem cell division in the Drosophila optic lobe. *Development*, *137*(18), 2981–2987. http://doi.org/10.1242/dev.051250
45. Egger, B., Gold, K. S., & Brand, A. H. (2011). Regulating the balance between symmetric and asymmetric stem cell division in the developing brain. *Fly*, *5*(3), 237–241.
46. Enserink, J. M., & Kolodner, R. D. (2010). An overview of Cdk1-controlled targets and processes. *Cell Division*, *5*(1). http://doi.org/10.1186/1747-1028-5-11
47. FELIX, M. A., ANTONY, C., WRIGHT, M., & MARO, B. (1994). Centrosome Assembly in-Vitro - Role of Gamma-Tubulin Recruitment in Xenopus Sperm Aster Formation. *Journal of Cell Biology*, *124*(1-2), 19–31. http://doi.org/10.1083/jcb.124.1.19
48. Franz, A., Roque, H., Saurya, S., Dobbelaere, J., & Raff, J. W. (2013). CP110 exhibits novel regulatory activities during centriole assembly in Drosophila. *The Journal of Cell Biology*, *203*(5), 785–799. http://doi.org/10.1083/jcb.201305109
49. Fu, J., & Glover, D. M. (2012). Structured illumination of the interface between centriole and peri-centriolar material. *Open Biology*, *2*(8), –120104. http://doi.org/10.1098/rsob.120104
50. Fu, J., Hagan, I. M., & Glover, D. M. (2015). The Centrosome and Its Duplication Cycle. *Cold Spring Harbor Perspectives in Biology*, *7*(2), a015800. http://doi.org/10.1101/cshperspect.a015800
51. Gadde, S., & Heald, R. (2004). Mechanisms and molecules of the mitotic spindle. *Current Biology*, *14*(18), R797–R805. http://doi.org/10.1016/j.cub.2004.09.021
52. Galletta, B. J., Guillen, R. X., Fagerstrom, C. J., Brownlee, C. W., Lerit, D. A., Megraw, T. L., et al. (2014). Drosophila pericentrin requires interaction with calmodulin for its function at centrosomes and neuronal basal bodies but not at sperm basal bodies. *Molecular Biology of the Cell*, *25*(18), 2682–2694. http://doi.org/10.1091/mbc.E13-10-0617
53. Giet, R., McLean, D., Descamps, S., Lee, M. J., Raff, J. W., Prigent, C., & Glover, D. M. (2002). Drosophila Aurora A kinase is required to localize D-TACC to centrosomes and to regulate astral microtubules. *Journal of Cell Biology*, *156*(3), 437–451. http://doi.org/10.1083/jcb.200108135
54. Glover, D. M. (2005). Polo kinase and progression through M phase in Drosophila: a perspective from the spindle poles. *Oncogene*, *24*(2), 230–237. http://doi.org/10.1038/sj.onc.1208279
55. Glover, D. M., ALPHEY, L., AXTON, J. M., CHESHIRE, A., DALBY, B., FREEMAN, M., et al. (1989). Mitosis in Drosophila Development. *Journal of Cell Science*, 277–291.
56. Glover, D. M., Hagan, I. M., & Tavares, A. (1998). Polo-like kinases: a team that plays throughout mitosis. *Genes & Development*, *12*(24), 3777–3787. http://doi.org/10.1101/gad.12.24.3777
57. Goenczy, P. (2012). Towards a molecular architecture of centriole assembly. *Nature Reviews Molecular Cell Biology*, *13*(7), 425–435. http://doi.org/10.1038/nrm3373
58. Goetz, S. C., Liem, K. F. J., & Anderson, K. V. (2012). The Spinocerebellar Ataxia-Associated Gene Tau Tubulin Kinase 2 Controls the Initiation of Ciliogenesis. *Cell*, *151*(4), 847–858. http://doi.org/10.1016/j.cell.2012.10.010

59. GOLSTEYN, R. M., Lane, H. A., MUNDT, K. E., Arnaud, L., & Nigg, E. A. (1996). The family of polo-like kinases. *Progress in Cell Cycle Research*, *2*, 107–114.
60. GOLSTEYN, R. M., MUNDT, K. E., Fry, A. M., & Nigg, E. A. (1995). Cell-Cycle Regulation of the Activity and Subcellular-Localization of Plk1, a Human Protein-Kinase Implicated in Mitotic Spindle Function. *Journal of Cell Biology*, *129*(6), 1617–1628. http://doi.org/10.1083/jcb.129.6.1617
61. Gonzalez, C., Sunkel, C. E., & Glover, D. M. (1998a). Interactions between mgr, asp, and polo: asp function modulated by polo and needed to maintain the poles of monopolar and bipolar spindles. *Chromosoma*, *107*(6-7), 452–460.
62. Gonzalez, C., Tavosanis, G., & Mollinari, C. (1998b). Centrosomes and microtubule organisation during Drosophila development. *Journal of Cell Science*, *111*, 2697–2706.
63. Gratz, S. J., Cummings, A. M., Nguyen, J. N., Hamm, D. C., Donohue, L. K., Harrison, M. M., et al. (2013a). Genome engineering of Drosophila with the CRISPR RNA-guided Cas9 nuclease. *Genetics*, *194*(4), 1029–1035. http://doi.org/10.1534/genetics.113.152710
64. Gratz, S. J., Ukken, F. P., Rubinstein, C. D., Thiede, G., Donohue, L. K., Cummings, A. M., & O'Connor-Giles, K. M. (2014). Highly specific and efficient CRISPR/Cas9-catalyzed homology-directed repair in Drosophila. *Genetics*, *196*(4), 961–971. http://doi.org/10.1534/genetics.113.160713
65. Gratz, S. J., Wildonger, J., Harrison, M. M., & O'Connor-Giles, K. M. (2013b). CRISPR/Cas9-mediated genome engineering and the promise of designer flies on demand. *Fly*, *7*(4), 249–255. http://doi.org/10.4161/fly.26566
66. Gruss, O. J., & Vernos, I. (2004). The mechanism of spindle assembly: functions of Ran and its target TPX2. *Journal of Cell Biology*, *166*(7), 949–955. http://doi.org/10.1083/jch.200312112
67. Guichard, P., Desfosses, A., Maheshwari, A., Hachet, V., Dietrich, C., Brune, A., et al. (2012). Cartwheel Architecture of Trichonympha Basal Body. *Science*, *337*(6094), 553–553. http://doi.org/10.1126/science.1222789
68. Gunawardane, R. N., Lizarraga, S. B., Wiese, C., Wilde, A., & ZHENG, Y. X. (2000). gamma-tubulin complexes and their role in microtubule nucleation. *Centrosome in Cell Replication and Early Development*, *49*, 55–73.
69. Hannak, E., Kirkham, M., Hyman, A. A., & Oegema, K. (2001). Aurora-A kinase is required for centrosome maturation in Caenorhabditis elegans. *Journal of Cell Biology*, *155*(7), 1109–1115. http://doi.org/10.1083/jcb.200108051
70. Hatzopoulos, G. N., Erat, M. C., Cutts, E., Rogala, K. B., Slater, L. M., Stansfeld, P. J., & Vakonakis, I. (2013). Structural Analysis of the G-Box Domain of the Microcephaly Protein CPAP Suggests a Role in Centriole Architecture. *Structure*, *21*(11), 2069–2077. http://doi.org/10.1016/j.str.2013.08.019
71. Hilbert, M., Erat, M. C., Hachet, V., Guichard, P., Blank, I. D., Flueckiger, I., et al. (2013). Caenorhabditis elegans centriolar protein SAS-6 forms a spiral that is consistent with imparting a ninefold symmetry. *Proceedings of the National Academy of Sciences of the United States of America*, *110*(28), 11373–11378. http://doi.org/10.1073/pnas.1302721110

72. Hiraki, M., Nakazawa, Y., Kamiya, R., & Hirono, M. (2007). Bld10p constitutes the cartwheel-spoke tip and stabilizes the 9-fold symmetry of the centriole. *Current Biology*, *17*(20), 1778–1783. http://doi.org/10.1016/j.cub.2007.09.021
73. Homem, C. C. F., & Knoblich, J. A. (2012). Drosophila neuroblasts: a model for stem cell biology. *Development*, *139*(23), 4297–4310. http://doi.org/10.1242/dev.080515
74. Homem, C. C. F., Steinmann, V., Burkard, T. R., Jais, A., Esterbauer, H., & Knoblich, J. A. (2014). Ecdysone and mediator change energy metabolism to terminate proliferation in Drosophila neural stem cells. *Cell*, *158*(4), 874–888. http://doi.org/10.1016/j.cell.2014.06.024
75. Izumi, Y., Ohta, N., Hisata, K., Raabe, T., & Matsuzaki, F. (2006). Drosophila Pins-binding protein Mud regulates spindle-polarity coupling and centrosome organization. *Nature Cell Biology*, *8*(6), 586–593. http://doi.org/10.1038/ncb1409
76. Januschke, J., & Gonzalez, C. (2010). The interphase microtubule aster is a determinant of asymmetric division orientation in Drosophila neuroblasts. *The Journal of Cell Biology*, *188*(5), 693–706. http://doi.org/10.1083/jcb.200905024
77. Januschke, J., & Näthke, I. (2014). Stem cell decisions: a twist of fate or a niche market? *Seminars in Cell & Developmental Biology*, *34*, 116–123. http://doi.org/10.1016/j.semcdb.2014.02.014
78. Januschke, J., Llamazares, S., Reina, J., & Gonzalez, C. (2011). Drosophila neuroblasts retain the daughter centrosome. *Nature Communications*, *2*, 243. http://doi.org/10.1038/ncomms1245
79. Jaspersen, S. L., & Winey, M. (2004). The budding yeast spindle pole body: Structure, duplication, and function. *Annual Review of Cell and Developmental Biology*, *20*(1), 1–28. http://doi.org/10.1146/annurev.cellbio.20.022003.114106
80. Jerka-Dziadosz, M., Gogendeau, D., Klotz, C., Cohen, J., Beisson, J., & Koll, F. (2010). Basal Body Duplication in Paramecium: The Key Role of Bld10 in Assembly and Stability of the Cartwheel. *Cytoskeleton*, *67*(3), 161–171. http://doi.org/10.1002/cm.20433
81. Joo, K., Kim, C. G., Lee, M.-S., Moon, H.-Y., Lee, S.-H., Kim, M. J., et al. (2013). CCDC41 is required for ciliary vesicle docking to the mother centriole. *Proceedings of the National Academy of Sciences of the United States of America*, *110*(15), 5987–5992. http://doi.org/10.1073/pnas.1220927110
82. Kalt, A., & Schliwa, M. (1993). Molecular components of the centrosome. *Trends in Cell Biology*, *3*(4), 118–128.
83. Keller, L. C., Geimer, S., Romijn, E., Yates, J. I., Zamora, I., & Marshall, W. F. (2009). Molecular Architecture of the Centriole Proteome: The Conserved WD40 Domain Protein POC1 Is Required for Centriole Duplication and Length Control. *Molecular Biology of the Cell*, *20*(4), 1150–1166. http://doi.org/10.1091/mbc.E08-06-0619
84. Kemp, C. A., Kopish, K. R., Zipperlen, P., Ahringer, J., & O'Connell, K. F. (2004). Centrosome maturation and duplication in C. elegans require the coiled-coil protein SPD-2. *Developmental Cell*, *6*(4), 511–523.
85. Kiger, A. A., Jones, D. L., Schulz, C., Rogers, M. B., & Fuller, M. T. (2001). Stem cell self-renewal specified by JAK-STAT activation in response to a support cell cue. *Science*, *294*(5551), 2542–2545. http://doi.org/10.1126/science.1066707

86. Kirkham, M., Muller-Reichert, T., Oegema, K., Grill, S., & Hyman, A. A. (2003). SAS-4 is a C-elegans centriolar protein that controls centrosome size. *Cell*, *112*(4), 575–587. http://doi.org/10.1016/S0092-8674(03)00117-X
87. Kitagawa, D., Kohlmaier, G., Keller, D., Strnad, P., Balestra, F. R., Flückiger, I., & Gönczy, P. (2011). Spindle positioning in human cells relies on proper centriole formation and on the microcephaly proteins CPAP and STIL. *Journal of Cell Science*, *124*(Pt 22), 3884–3893. http://doi.org/10.1242/jcs.089888
88. Kleylein-Sohn, J., Westendorf, J., Le Clech, M., Habedanck, R., Stierhof, Y.-D., & Nigg, E. A. (2007). Plk4-induced centriole biogenesis in human cells. *Developmental Cell*, *13*(2), 190–202. http://doi.org/10.1016/j.devcel.2007.07.002
89. Kohlmaier, G., Loncarek, J., Meng, X., McEwen, B. F., Mogensen, M. M., Spektor, A., et al. (2009). Overly Lona Centrioles and Defective Cell Division upon Excess of the SAS-4-Related Protein CPAP. *Current Biology*, *19*(12), 1012–1018. http://doi.org/10.1016/j.cub.2009.05.018
90. Kotak, S., & Goenczy, P. (2013). Mechanisms of spindle positioning: cortical force generators in the limelight. *Current Opinion in Cell Biology*, *25*(6), 741–748. http://doi.org/10.1016/j.ceb.2013.07.008
91. Kotak, S., Busso, C., & Gönczy, P. (2013). NuMA phosphorylation by CDK1 couples mitotic progression with cortical dynein function. *Embo Journal*, *32*(18), 2517–2529. http://doi.org/10.1038/emboj.2013.172
92. KURIYAMA, R., & BORISY, G. G. (1981). Centriole Cycle in Chinese-Hamster Ovary Cells as Determined by Whole-Mount Electron-Microscopy. *Journal of Cell Biology*, *91*(3), 814–821.
93. Lacey, K. R., Jackson, P. K., & STEARNS, T. (1999). Cyclin-dependent kinase control of centrosome duplication. *Proceedings of the National Academy of Sciences of the United States of America*, *96*(6), 2817–2822.
94. Lane, H. A., & Nigg, E. A. (1996). Antibody microinjection reveals an essential role for human polo-like kinase 1 (Plk1) in the functional maturation of mitotic centrosomes. *Journal of Cell Biology*, *135*(6), 1701–1713.
95. LANGE, B., & GULL, K. (1995). A Molecular Marker for Centriole Maturation in the Mammalian-Cell Cycle. *Journal of Cell Biology*, *130*(4), 919–927.
96. Lau, L., Lee, Y. L., Sahl, S. J., Stearns, T., & Moerner, W. E. (2012). STED Microscopy with Optimized Labeling Density Reveals 9-Fold Arrangement of a Centriole Protein. *Biophysical Journal*, *102*(12), 2926–2935. http://doi.org/10.1016/j.bpj.2012.05.015
97. Lawo, S., Hasegan, M., Gupta, G. D., & Pelletier, L. (2012). Subdiffraction imaging of centrosomes reveals higher-order organizational features of pericentriolar material. *Nature Cell Biology*, *14*(11), 1148–. http://doi.org/10.1038/ncb2591
98. Leidel, S., & Gonczy, P. (2003). SAS-4 is essential for centrosome duplication in C-elegans and is recruited to daughter centrioles once per cell cycle. *Developmental Cell*, *4*(3), 431–439. http://doi.org/10.1016/S1534-5807(03)00062-5
99. Leidel, S., Delattre, M., Cerutti, L., Baumer, K., & Gonczy, P. (2005). SAS-6 defines a protein family required for centrosome duplication in C-elegans and in human cells. *Nature Cell Biology*,

*7*(2), 115–U19. http://doi.org/10.1038/ncb1220

100. Lerit, D. A., & Rusan, N. M. (2013). PLP inhibits the activity of interphase centrosomes to ensure their proper segregation in stem cells. *Journal of Cell Biology*, *202*(7), 1013–1022. http://doi.org/10.1083/jcb.201303141
101. Lerit, D. A., Poulton, J. S., Jordan, H. A., Peifer, M., & Rusan, N. M. (2014). PLP forms novel centriole satellites and is critical for embryonic development. *Molecular Biology of the Cell*, *25*.
102. Lerit, D. A., Poulton, J. S., Peifer, M., & Rusan, N. M. (2013). Novel Pericentrin structures orchestrate the PCM in rapidly dividing embryos. *Molecular Biology of the Cell*, *24*.
103. Lim, N. R., Yeap, Y. Y. C., Zhao, T. T., Yip, Y. Y., Wong, S. C., Xu, D., et al. (2015). Opposing roles for JNK and Aurora A in regulating the association of WDR62 with spindle microtubules. *Journal of Cell Science*, *128*(3), 527–540. http://doi.org/10.1242/jcs.157537
104. Lin, Y.-C., Chang, C.-W., Hsu, W.-B., Tang, C.-J. C., Lin, N., Chou, E.-J., et al. (2013a). Human microcephaly protein CEP135 binds to hSAS-6 and CPAP, and is required for centriole assembly. *Embo Journal*, *32*(8), 1141–1154. http://doi.org/10.1038/emboj.2013.56
105. Lin, Y.-N., Wu, C.-T., Lin, Y.-C., Hsu, W.-B., Tang, C.-J. C., Chang, C.-W., & Tang, T. K. (2013b). CEP120 interacts with CPAP and positively regulates centriole elongation. *Journal of Cell Biology*, *202*(2), 211–219. http://doi.org/10.1083/jcb.201212060
106. Lingle, W., Iturria, S., Negron, V., Gibson, C. E., Roche, P., Couch, F., et al. (2002). Genes associated with centrosome amplification in development and progression of breast cancer. *Molecular Biology of the Cell*, *13*, 105A–105A.
107. Mahjoub, M. R., Xie, Z., & Stearns, T. (2010). Cep120 is asymmetrically localized to the daughter centriole and is essential for centriole assembly. *The Journal of Cell Biology*, *191*(2), 331–346. http://doi.org/10.1083/jcb.201003009
108. Matsumoto, Y., Hayashi, K., & Nishida, E. (1999). Cyclin-dependent kinase 2 (Cdk2) is required for centrosome duplication in mammalian cells. *Current Biology*, *9*(8), 429–432.
109. Maurange, C., Cheng, L., & Gould, A. P. (2008). Temporal transcription factors and their targets schedule the end of neural proliferation in Drosophila. *Cell*, *133*(5), 891–902. http://doi.org/10.1016/j.cell.2008.03.034
110. Mayor, T., Meraldi, P., Stierhof, Y. D., Nigg, E. A., & Fry, A. M. (1999). Protein kinases in control of the centrosome cycle. *Febs Letters*, *452*(1-2), 92–95. http://doi.org/10.1016/S0014-5793(99)00534-7
111. Mennella, V., Keszthelyi, B., McDonald, K. L., Chhun, B., Kan, F., Rogers, G. C., et al. (2012). Subdiffraction-resolution fluorescence microscopy reveals a domain of the centrosome critical for pericentriolar material organization. *Nature Cell Biology*, *14*(11), 1159–1168. http://doi.org/10.1038/ncb2597
112. Moritz, M., Braunfeld, M. B., FUNG, J. C., SEDAT, J. W., ALBERTS, B. M., & Agard, D. A. (1995a). 3-Dimensional Structural Characterization of Centrosomes From Early Drosophila Embryos. *Journal of Cell Biology*, *130*(5), 1149–1159. http://doi.org/10.1083/jcb.130.5.1149
113. Moritz, M., Braunfeld, M. B., Guenebaut, V., Heuser, J., & Agard, D. A. (2000). Structure of the gamma-tubulin ring complex: a template for microtubule nucleation. *Nature Cell Biology*, *2*(6),

365–370. http://doi.org/10.1038/35014058

114. Moritz, M., Braunfeld, M. B., SEDAT, J. W., ALBERTS, B., & Agard, D. A. (1995b). Microtubule Nucleation by Gamma-Tubulin-Containing Rings in the Centrosome. *Nature*, *378*(6557), 638–640. http://doi.org/10.1038/378638a0

115. Mottier-Pavie, V., & Megraw, T. L. (2009). Drosophila bld10 is a centriolar protein that regulates centriole, basal body, and motile cilium assembly. *Molecular Biology of the Cell*, *20*(10), 2605–2614. http://doi.org/10.1091/mbc.E08-11-1115

116. Moutinho-Santos, T., Sampaio, P., Amorim, I., Costa, M., & Sunkel, C. E. (1999). In vivo localisation of the mitotic POLO kinase shows a highly dynamic association with the mitotic apparatus during early embryogenesis in Drosophila. *Biology of the Cell*, *91*(8), 585–596.

117. Myer, D. L., Bahassi, E. M., & Stambrook, P. J. (2005). The Plk3-Cdc25 circuit. *Oncogene*, *24*(2), 299–305. http://doi.org/10.1038/sj.onc.1208278

118. Nicholas, A. K., Khurshid, M., Desir, J., Carvalho, O. P., Cox, J. J., Thornton, G., et al. (2010). WDR62 is associated with the spindle pole and is mutated in human microcephaly. *Nature Genetics*, *42*(11), 1010–U138. http://doi.org/10.1038/ng.682

119. Nigg, E. A. (2006). Cell biology - A licence for duplication. *Nature*, *442*(7105), 874–875. http://doi.org/10.1038/442874a

120. Nigg, E. A., & Raff, J. W. (2009). Centrioles, Centrosomes, and Cilia in Health and Disease. *Cell*, *139*(4), 663–678. http://doi.org/10.1016/j.cell.2009.10.036

121. Nigg, E. A., & Stearns, T. (2011). The centrosome cycle: Centriole biogenesis, duplication and inherent asymmetries. *Nature Cell Biology*, *13*(10), 1154–1160. http://doi.org/10.1038/ncb2345

122. O'Connell, K. F., Caron, C., Kopish, K. R., Hurd, D. D., Kemphues, K. J., Li, Y., & White, J. G. (2001). The C. elegans zyg-1 gene encodes a regulator of centrosome duplication with distinct maternal and paternal roles in the embryo. *Cell*, *105*(4), 547–558.

123. O'Toole, E. T., Giddings, T. H., McIntosh, J. R., & Dutcher, S. K. (2003a). Three-dimensional organization of basal bodies from wild-type and delta-tubulin deletion strains of Chlamydomonas reinhardtii. *Molecular Biology of the Cell*, *14*(7), 2999–3012. http://doi.org/10.1091/mbc.E02-11-0755

124. O'Toole, E. T., McDonald, K. L., Mäntler, J., McIntosh, J. R., Hyman, A. A., & Müller-Reichert, T. (2003b). Morphologically distinct microtubule ends in the mitotic centrosome of Caenorhabditis elegans. *Journal of Cell Biology*, *163*(3), 451–456. http://doi.org/10.1083/jcb.200304035

125. OAKLEY, B. R., OAKLEY, C. E., YOON, Y. S., & JUNG, M. K. (1990). Gamma-Tubulin Is a Component of the Spindle Pole Body That Is Essential for Microtubule Function in Aspergillus-Nidulans. *Cell*, *61*(7), 1289–1301. http://doi.org/10.1016/0092-8674(90)90693-9

126. PAINTRAND, M., MOUDJOU, M., DELACROIX, H., & BORNENS, M. (1992). Centrosome Organization and Centriole Architecture - Their Sensitivity to Divalent-Cations. *Journal of Structural Biology*, *108*(2), 107–128.

127. Pelletier, L., O'Toole, E. T., Schwager, A., Hyman, A. A., & Muller-Reichert, T. (2006a). Centriole assembly in C. elegans. *European Journal of Cell Biology*, *85*, 122–123.

128. Pelletier, L., O'Toole, E., Schwager, A., Hyman, A. A., & Mueller-Reichert, T. (2006b). Centriole

assembly in Caenorhabditis elegans. *Nature*, *444*(7119), 619–623. http://doi.org/10.1038/nature05318

129. Pelletier, L., Ozlu, N., Hannak, E., Cowan, C., Habermann, B., Ruer, M., et al. (2006c). The Caenorhabditis elegans centrosomal protein SPD-2 is required for both pericentriolar material recruitment and centriole duplication (vol 14, pg 863, 2004). *Current Biology*, *16*(12), 1255–1255. http://doi.org/10.1016/j.cub.2006.06.021
130. Piel, M., Meyer, P., Khodjakov, A., Rieder, C. L., & BORNENS, M. (2000). The respective contributions of the mother and daughter centrioles to centrosome activity and behavior in vertebrate cells. *Journal of Cell Biology*, *149*(2), 317–329.
131. RAFF, J. W., & Glover, D. M. (1989). Centrosomes, and Not Nuclei, Initiate Pole Cell-Formation in Drosophila Embryos. *Cell*, *57*(4), 611–619. http://doi.org/10.1016/0092-8674(89)90130-X
132. Ren, X., Sun, J., Housden, B. E., Hu, Y., Roesel, C., Lin, S., et al. (2013). Optimized gene editing technology for Drosophila melanogaster using germ line-specific Cas9. *Proceedings of the National Academy of Sciences of the United States of America*, *110*(47), 19012–19017. http://doi.org/10.1073/pnas.1318481110
133. Reschen, R. F., Colombie, N., Wheatley, L., Dobbelaere, J., St Johnston, D., Ohkura, H., & Raff, J. W. (2012). Dgp71WD is required for the assembly of the acentrosomal Meiosis I spindle, and is not a general targeting factor for the γ-TuRC. *Biology Open*, *1*(5), 422–429. http://doi.org/10.1242/bio.2012596
134. Richens, J. H., Barros, T. P., Lucas, E. P., Peel, N., Pinto, D. M. S., Wainman, A., & Raff, J. W. (2015). The Drosophila Pericentrin-like-protein (PLP) cooperates with Cnn to maintain the integrity of the outer PCM. *Biology Open*, *4*(8), 1052–1061. http://doi.org/10.1242/bio.012914
135. Riparbelli, M. G., Callaini, G., & Megraw, T. L. (2012). Assembly and Persistence of Primary Cilia in Dividing Drosophila Spermatocytes. *Developmental Cell*, *23*(2), 425–432. http://doi.org/10.1016/j.devcel.2012.05.024
136. Roque, H., Wainman, A., Richens, J., Kozyrska, K., Franz, A., & Raff, J. W. (2012). Drosophila Cep135/Bld10 maintains proper centriole structure but is dispensable for cartwheel formation. *Journal of Cell Science*, *125*(Pt 23), 5881–5886. http://doi.org/10.1242/jcs.113506
137. ROUT, M. P., & KILMARTIN, J. V. (1990). Components of the Yeast Spindle and Spindle Pole Body. *Journal of Cell Biology*, *111*(5), 1913–1927.
138. Ruiz, F., de Loubresse, N. G., Klotz, C., Beisson, J., & Koll, F. (2005). Centrin deficiency in Paramecium affects the geometry of basal-body duplication. *Current Biology*, *15*(23), 2097–2106. http://doi.org/10.1016/j.cub.2005.11.038
139. Rusan, N. M., & Peifer, M. (2007). A role for a novel centrosome cycle in asymmetric cell division. *Journal of Cell Biology*, *177*(1), 13–20. http://doi.org/10.1083/jcb.200612140
140. Schaefer, M., & Knoblich, J. A. (2001). Protein localization during asymmetric cell division. *Experimental Cell Research*, *271*(1), 66–74. http://doi.org/10.1006/excr.2001.5371
141. Schaefer, M., Shevchenko, A., & Knoblich, J. A. (2000). A protein complex containing Inscuteable and the Galpha-binding protein Pins orients asymmetric cell divisions in Drosophila. *Current Biology*, *10*(7), 353–362.

142. Schmidt, T. I., Kleylein-Sohn, J., Westendorf, J., Le Clech, M., Lavoie, S. B., Stierhof, Y.-D., & Nigg, E. A. (2009). Control of Centriole Length by CPAP and CP110. *Current Biology*, *19*(12), 1005–1011. http://doi.org/10.1016/j.cub.2009.05.016

143. Schweisguth, F. (2004). Formation and remodeling of epithelial polarity. *Developmental Cell*, *6*(6), 749–755. http://doi.org/10.1016/j.devcel.2004.05.010

144. Sharma, N., Bryant, J., Wloga, D., Donaldson, R., Davis, R. C., Jerka-Dziadosz, M., & Gaertig, J. (2007). Katanin regulates dynamics of microtubules and biogenesis of motile cilia. *Journal of Cell Biology*, *178*(6), 1065–1079. http://doi.org/10.1083/jcb.200704021

145. Siegrist, S. E., & Doe, C. Q. (2005). Microtubule-induced Pins/G alpha i cortical polarity in Drosophila neuroblasts. *Cell*, *123*(7), 1323–1335. http://doi.org/10.1016/j.cell.2005.09.043

146. Siller, K. H., & Doe, C. Q. (2008). Lis1/dynactin regulates metaphase spindle orientation in Drosophila neuroblasts. *Developmental Biology*, *319*(1), 1–9. http://doi.org/10.1016/j.ydbio.2008.03.018

147. Siller, K. H., Cabernard, C., & Doe, C. Q. (2006). The NuMA-related Mud protein binds Pins and regulates spindle orientation in Drosophila neuroblasts. *Nature Cell Biology*, *8*(6), 594–600. http://doi.org/10.1038/ncb1412

148. Sillibourne, J. E., Specht, C. G., Izeddin, I., Hurbain, I., Tran, P., Triller, A., et al. (2011). Assessing the localization of centrosomal proteins by PALM/STORM nanoscopy. *Cytoskeleton*, *68*(11), 619–627. http://doi.org/10.1002/cm.20536

149. Singh, P., Ramdas Nair, A., & Cabernard, C. (2014). The centriolar protein Bld10/Cep135 is required to establish centrosome asymmetry in Drosophila neuroblasts. *Current Biology : CB*, *24*(13), 1548–1555. http://doi.org/10.1016/j.cub.2014.05.050

150. Smith, E., Hegarat, N., Vesely, C., Roseboom, I., Larch, C., Streicher, H., et al. (2011). Differential control of Eg5-dependent centrosome EMBO separation by Plk1 and Cdk1. *Embo Journal*, *30*(11), 2233–2245. http://doi.org/10.1038/emboj.2011.120

151. Smith, N. L., & Miskimins, W. K. (2011). Phosphorylation at serine 482 affects stability of NF90 and its functional role in mitosis. *Cell Proliferation*, *44*(2), 147–155. http://doi.org/10.1111/j.1365-2184.2011.00742.x

152. Sonnen, K. F., Schermelleh, L., Leonhardt, H., & Nigg, E. A. (2012). 3D-structured illumination microscopy provides novel insight into architecture of human centrosomes. *Biology Open*, *1*(10), 965–976. http://doi.org/10.1242/bio.20122337

153. Southall, T. D., & Brand, A. H. (2009). Neural stem cell transcriptional networks highlight genes essential for nervous system development. *Embo Journal*, *28*(24), 3799–3807. http://doi.org/10.1038/emboj.2009.309

154. STEARNS, T., & KIRSCHNER, M. (1994). In-Vitro Reconstitution of Centrosome Assembly and Function - the Central Role of Gamma-Tubulin. *Cell*, *76*(4), 623–637.

155. Stemm-Wolf, A. J., Morgan, G., Giddings, T. H., White, E. A., Marchione, R., McDonald, H. B., & Winey, M. (2005). Basal body duplication and maintenance require one member of the Tetrahymena thermophila centrin gene family. *Molecular Biology of the Cell*, *16*(8), 3606–3619. http://doi.org/10.1091/mbc.E04-10-0919

156. Stevens, N. R., Dobbelaere, J., Brunk, K., Franz, A., & Raff, J. W. (2010a). Drosophila Ana2 is a conserved centriole duplication factor. *Journal of Cell Biology*, *188*(3), 313–323. http://doi.org/10.1083/jcb.200910016

157. Stevens, N. R., Dobbelaere, J., Wainman, A., Gergely, F., & Raff, J. W. (2009). Ana3 is a conserved protein required for the structural integrity of centrioles and basal bodies. *The Journal of Cell Biology*, *187*(3), 355–363. http://doi.org/10.1083/jcb.200905031

158. Stevens, N. R., Raposo, A. A. S. F., Basto, R., St Johnston, D., & Raff, J. W. (2007). From stem cell to embryo without centrioles. *Current Biology*, *17*(17), 1498–1503. http://doi.org/10.1016/j.cub.2007.07.060

159. Stevens, N. R., Roque, H., & Raff, J. W. (2010b). DSas-6 and Ana2 Coassemble into Tubules to Promote Centriole Duplication and Engagement. *Developmental Cell*, *19*(6), 913–919. http://doi.org/10.1016/j.devcel.2010.11.010

160. Strnad, P., & Goenczy, P. (2008). Mechanisms of procentriole formation. *Trends in Cell Biology*, *18*(8), 389–396. http://doi.org/10.1016/j.tcb.2008.06.004

161. Sunkel, C. E., & Glover, D. M. (1988). Polo, a Mitotic Mutant of Drosophila Displaying Abnormal Spindle Poles. *Journal of Cell Science*, *89*, 25–38.

162. Tang, C.-J. C., Fu, R.-H., Wu, K.-S., Hsu, W.-B., & Tang, K. T. (2009). CPAP is a cell-cycle regulated protein that controls centriole length. *Nature Cell Biology*, *11*(7), 825–U103. http://doi.org/10.1038/ncb1889

163. Tanos, B. E., Yang, H.-J., Soni, R., Wang, W.-J., Macaluso, F. P., Asara, J. M., & Tsou, M.-F. B. (2013). Centriole distal appendages promote membrane docking, leading to cilia initiation. *Genes & Development*, *27*(2), 163–168. http://doi.org/10.1101/gad.207043.112

164. Thornton, G. K., & Woods, C. G. (2009). Primary microcephaly: do all roads lead to Rome? *Trends in Genetics*, *25*(11), 501–510. http://doi.org/10.1016/j.tig.2009.09.011

165. TRUMAN, J. W., & BATE, M. (1988). Spatial and Temporal Patterns of Neurogenesis in the Central Nervous-System of Drosophila-Melanogaster. *Developmental Biology*, *125*(1), 145–157. http://doi.org/10.1016/0012-1606(88)90067-X

166. Tsou, M.-F. B., & Stearns, T. (2006a). Controlling centrosome number: licenses and blocks. *Current Opinion in Cell Biology*, *18*(1), 74–78. http://doi.org/10.1016/j.ceb.2005.12.008

167. Tsou, M.-F. B., & Stearns, T. (2006b). Mechanism limiting centrosome duplication to once per cell cycle. *Nature*, *442*(7105), 947–951. http://doi.org/10.1038/nature04985

168. Tulina, N., & Matunis, E. (2001). Control of stem cell self-renewal in Drosophila spermatogenesis by JAK-STAT signaling. *Science*, *294*(5551), 2546–2549. http://doi.org/10.1126/science.1066700

169. van Breugel, M., Hirono, M., Andreeva, A., Yanagisawa, H.-A., Yamaguchi, S., Nakazawa, Y., et al. (2011). Structures of SAS-6 Suggest Its Organization in Centrioles. *Science*, *331*(6021), 1196–1199. http://doi.org/10.1126/science.1199325

170. van Breugel, M., Wilcken, R., McLaughlin, S. H., Rutherford, T. J., & Johnson, C. M. (2014). Structure of the SAS-6 cartwheel hub from Leishmania major. *Elife*, *3*. http://doi.org/10.7554/eLife.01812

171. van der Voet, M., Berends, C. W. H., Perreault, A., Nguyen-Ngoc, T., Goenczy, P., Vidal, M., et

al. (2009). NuMA-related LIN-5, ASPM-1, calmodulin and dynein promote meiotic spindle rotation independently of cortical LIN-5/GPR/G alpha. *Nature Cell Biology*, *11*(3), 269–U101. http://doi.org/10.1038/ncb1834

172. Wang, C., Li, S., Januschke, J., Rossi, F., Izumi, Y., Garcia-Alvarez, G., et al. (2011). An ana2/ctp/mud complex regulates spindle orientation in Drosophila neuroblasts. *Developmental Cell*, *21*(3), 520–533. http://doi.org/10.1016/j.devcel.2011.08.002
173. Wang, G., Krishnamurthy, K., & Bieberich, E. (2009a). Regulation of primary cilia formation by ceramide. *Journal of Lipid Research*, *50*(10), 2103–2110. http://doi.org/10.1194/jlr.M900097-JLR200
174. Wang, W.-J., Tay, H. G., Soni, R., Perumal, G. S., Goll, M. G., Macaluso, F. P., et al. (2013). CEP162 is an axoneme-recognition protein promoting ciliary transition zone assembly at the cilia base. *Nature Cell Biology*, *15*(6), 591–. http://doi.org/10.1038/ncb2739
175. Wang, X., Tsai, J.-W., Imai, J. H., Lian, W.-N., Vallee, R. B., & Shi, S.-H. (2009b). Asymmetric centrosome inheritance maintains neural progenitors in the neocortex. *Nature*, *461*(7266), 947–U206. http://doi.org/10.1038/nature08435
176. Wiese, C., & ZHENG, Y. X. (2000). A new function for the gamma-tubulin ring complex as a microtubule minus-end cap. *Nature Cell Biology*, *2*(6), 358–364. http://doi.org/10.1038/35014051
177. Wirtz-Peitz, F., Nishimura, T., & Knoblich, J. A. (2008). Linking cell cycle to asymmetric division: Aurora-A phosphorylates the par complex to regulate Numb localization. *Cell*, *135*(1), 161–173. http://doi.org/10.1016/j.cell.2008.07.049
178. Wodarz, A. (2005). Molecular control of cell polarity and asymmetric cell division in Drosophila neuroblasts. *Current Opinion in Cell Biology*, *17*(5), 475–481. http://doi.org/10.1016/j.ceb.2005.08.005
179. Wong, C., & Stearns, T. (2003). Centrosome number is controlled by a centrosome-intrinsic block to reduplication. *Nature Cell Biology*, *5*(6), 539–544. http://doi.org/10.1038/ncb993
180. Xiang, Y., Takeo, S., Florens, L., Hughes, S. E., Huo, L.-J., Gilliland, W. D., et al. (2007). The inhibition of polo kinase by matrimony maintains G2 arrest in the meiotic cell cycle. *Plos Biology*, *5*(12), 2831–2846. http://doi.org/10.1371/journal.pbio.0050323
181. Xu, D., Zhang, F., Wang, Y., Sun, Y., & Xu, Z. (2014). Microcephaly-Associated Protein WDR62 Regulates Neurogenesis through JNK1 in the Developing Neocortex (vol 6, pg 104, 2014). *Cell Reports*, *6*(6), 1176–1177. http://doi.org/10.1016/j.celrep.2014.03.021
182. Yamashita, Y. (2007). [Mechanisms of asymmetric stem cell division in the Drosophila male germ line]. *Tanpakushitsu Kakusan Koso. Protein, Nucleic Acid, Enzyme*, *52*(16 Suppl), 2130–2135.
183. Zhang, Y., Tian, Y., Yu, J.-J., He, J., Luo, J., Zhang, S., et al. (2013). Overexpression of WDR62 is associated with centrosome amplification in human ovarian cancer. *Journal of Ovarian Research*, *6*(1). http://doi.org/10.1186/1757-2215-6-55
184. ZHENG, Y. X., WONG, M. L., ALBERTS, B., & MITCHISON, T. (1995). Nucleation of Microtubule Assembly by a Gamma-Tubulin-Containing Ring Complex. *Nature*, *378*(6557), 578–583. http://doi.org/10.1038/378578a0

185. Zyss, D., & Gergely, F. (2009). Centrosome function in cancer: guilty or innocent? *Trends in Cell Biology*, *19*(7), 334–346. http://doi.org/10.1016/j.tcb.2009.04.001

# 8. CURRICULUM VITAE

# ANJANA RAMDAS NAIR

Strassburgeralle 93
4055 Basel
Switzerland
**Email** anjz87@gmail.com, a.nair@unibas.ch
**Mobile** +41786062342
**Skype** anjana.ramdas


## EDUCATION

| | |
|---|---|
| **2015-Present** | **Biozentrum, Universitat Basel, Basel, Switzerland**<br>**Postdoctoral Researcher Principle Investigator: Clemens Cabernard** |
| **2011-2015** | **Biozentrum, Universitat Basel, Basel, Switzerland**<br>**Ph.D Cell Biology Principle Investigator: Clemens Cabernard** |
| **2009-2010** | **University of Manchester, Manchester, UK**<br>**M.Sc. Biotechnology (School of Chemical Engineering and Analytical Sciences)**<br>Result: Merit |
| **2005 - 2009** | **Manipal Institute of Technology, Manipal (India)**<br>**B. E. Biotechnology**<br>CGPA: 7.39 |
| **1991 - 2005** | **The Indian High School, Dubai (UAE)**<br>**2005 - All India Senior School Certificate Examination**<br>Overall Percentage-84.4%<br>**2003 - All India Secondary School Examination**<br>Overall Percentage-88.2% |

## SKILLS

| | |
|---|---|
| Techniques | Cell Culture, Protein Biochemistry, Genetics, and Protein Purification |
| Microscope | Confocal Microscope, Spinning Disk Confocal Microscope, 3D-Superresolution Imaging Microscope (OMX V4) |
| Software | Image analysis software (Imaris and Image J), MATLAB, Adobe Illustrator, Adobe Photoshop, MS Office |

## RESEARCH EXPERIENCE

| | |
|---|---|
| **2011-Present** | **Biozentrum, Universitat Basel**<br>Ph.D Cell Biology<br>***'Investigating the cellular and molecular mechanisms involved in establishing and maintaining centrosome asymmetry in Drosophila neuroblasts'*** under the supervision of **Dr. Clemens Cabernard.** |
| **2010 April -** | **Manchester Interdisciplinary Biocentre, University of Manchester**<br>*Academic Research Intern* |

| | |
|---|---|
| **September** | *'**Quantification of effect of Azithromycin on E.Coli Proteome**'* under the supervision of **Dr. Jill Barber.** |
| **2009** | **Rajiv Gandhi Centre for Biotechnology** |
| **January - May** | *Internship in the Division of Molecular Reproduction* ***'Profiling of I121 at 'Window of Embryo Implantation' and its steroidal modifications***' under the supervision of **Dr. Malini Laloraya.** |

## TEACHING EXPERIENCE

| | | |
|---|---|---|
| **2014-2015** | **Biozentrum, Universität Basel** | |
| | Ph.D Cell Biology | |
| | ***Supervisor*** | *Master student* |
| **2010** | **University of Manchester** | |
| **April - September** | *M.Sc Biotechnology* | |
| | ***Academic Tutor*** | *Mathematics (A-level)* |

## PRESENTATIONS

| | |
|---|---|
| June 2015 | ***Biozentrum PhD Retreat****. Talk* |
| April 2015 | ***Swiss Fly Meeting****. Talk* |
| March 2015 | ***56$^{th}$ Annual Drosophila Genetics Research Conference****. Posters* |
| January 2015 | ***LS2 Annual Meeting 2015.*** *Poster* |
| September 2014 | ***Tri-Regional Stem Cell and Developmental Biology meeting****. Poster* |
| September 2014 | ***Basel Stem Cell Conference****. Poster* |
| August 2014 | ***Basel Fly Club****. Talk* |
| June 2014 | ***Swiss Fly Meeting****. Poster* |
| May 2012 | ***Biozentrum PhD Retreat****. Talk* |

## PUBLICATIONS

- **The Centriolar Protein Bld10/Cep135 Is Required to Establish Centrosome Asymmetry in *Drosophila* Neuroblasts. P. Singh, A. Ramdas Nair and C. Cabernard. *Current Biology* 24, 1548–1555, July 7, 2014**

- **The microcephaly protein WDR62/CG7337 is required to maintain centrosome asymmetry in *Drosophila* Neuroblasts. A. Ramdas Nair, P. Singh, D. R. Crespo, J. D. S. Garcia, B. Egger and C. Cabernard.**

- **Structured Illumination of Centriolar and Centrosomal proteins in *Drosophila melanogaster* neuroblasts.**
  **A. Ramdas Nair, E. Gallaud, P. Singh and C. Cabernard (in Progress)**

## REFERENCES

**Dr. Clemens Cabernard**
**Assistant Professor**
**Biozentrum, Universität Basel**
**clemens.cabernard@unibas.ch**
**Tel. No.: +41 61 267 21 88**

**Dr. Markus Affolter**
**Professor**
**Biozentrum, Universität Basel**
**markus.affolter@unibas.ch**
**Tel. No.: +41 61 267 20 72**

**Dr. Jill Barber**
**Senior Lecturer**
**Manchester Interdisciplinary Biocentre**
**jill.barber@manchester.ac.uk**
**Tel. No.: +44 (0)161 275 2369**